To the Graduate Council:

I am submitting herewith a dissertation written by Adana Ocak Muschelewicz entitled "Photolysis and Photooxidation of Nylon 66." I have examined the final copy of this dissertation for form and content and recommend that it be accepted in partial fulfillment of the requirements for the degree of Doctor of Philosophy, with a major in Home Economics.

Tyrone L. Vigo

Tyrone L. Vigo, Major Professor

We have read this dissertation
and recommend its acceptance:

James F. Kinstle

B C Clipson

Larry C. Wadsworth

Accepted for the Council:

Vice Provost
and Dean of The Graduate School

PHOTOLYSIS AND PHOTOOXIDATION

OF NYLON 66

A Dissertation

Presented for the

Doctor of Philosophy

Degree

The University of Tennessee, Knoxville

Adana Ocak Muschelewicz

June 1985

ACKNOWLEDGEMENTS

The author wishes to express her gratitude for the assistance, advice, encouragement and guidance given to her by Dr. James F. Kinstle, Dr. Tyrone L. Vigo, Dr. Bhuvenesh Goswami, and Dr. Larry Wadsworth during the course of this work.

Further appreciation is tendered to Dr. Kei Wei, Mr. James Irwin and Mr. Steve Smith for their assistance during the course of this research endeavor.

Financial assistance from the University of Tennessee and the United States Department of Agriculture, and support from the Department of Chemistry are gratefully acknowledged.

Thanks is also rendered to her husband, Ken, for his assistance, encouragement, love and support; to her parents, Mr. and Mrs. Mustafa Ocak, for their love and relentless faith; and to her daughter, Aliya, for her love and patience.

The author wishes to express her thanks to God for his love, guidance and assistance throughout her life.

ABSTRACT

Much research has been directed towards elucidating the UV degradation mechanism(s) of Nylon 66 by using various analytical methods, but until this study, mass spectrometry had not been used as an investigative technique. Nylon 66 films (with and without stabilizing additives), fibers, and nonwoven fabrics were photolyzed (at $\lambda \leq$ 300 nm) and photooxidized (at $\lambda \geq$ 300 nm) in a specially constructed UV apparatus, equipped with a high pressure mercury vapor lamp and a reattachable trap for collecting gaseous products formed during the UV exposures. After irradiation, the gas and solid samples were analyzed by mass spectrometry. Other techniques such as chemical analysis (for carboxyl end groups, imides, and pyrroles), and IR and UV-Vis spectrometry were also performed on the solid samples. Data generated from the samples photooxidized in the specially constructed UV apparatus were compared to data obtained from samples irradiated from a commonly used xenon arc source (Weatherometer). In order to demonstrate the loss in strength which occurs from irradiation, the tensile properties such as the energy-of-rupture, % elongation, and the breaking strength were also determined on the photooxidized Nylon 66 fabrics and fibers. The data produced in this study were combined with data from the literature, and mechanisms by which Nylon 66 degrades in sunlight are proposed.

TABLE OF CONTENTS

CHAPTER PAGE

LIST OF TABLES

TABLE PAGE

TABLE PAGE

LIST OF FIGURES

FIGURE PAGE

FIGURE PAGE

CHAPTER I

INTRODUCTION

Polyamides (nylons) were one of the new industrial materials of the late 1930's, and have since undergone steady, substantial and worldwide growth. Nylon fibers have good tensile strength, elasticity, and resiliency, and are used in the production of clothing, nonwoven fabrics, carpets, hosiery, rope, and tire cord (1). In the plastic form, nylons are used in the manufacture of brush bristles, zippers, gears, wire insulation, and piping (1). In spite of their many uses and desired properties, however, polyamides, especially the aliphatic type, have some deficiencies. Experience shows that for many applications, the environmental stability of aliphatic polyamides needs improvement against thermal and ultraviolet (UV) degradation. Under photolytic and/or thermal aging conditions, the nylons undergo undesirable changes in mechanical properties (become brittle) and in color (yellowing occurs). The behavior of aliphatic polyamides on exposure to heat and irradiation has therefore attracted much attention. A lot of research has been directed towards proposing UV and thermal degradation mechanisms of nylons by using various approaches. Electron spin resonance (ESR), chemical tests, infrared (IR) and ultraviolet-visible (UV-VIS) spectrometry, are among the analytical tools used in these studies to elucidate the degradation mechanisms. Another analytical tool, mass spectrometry, has been used to analyze polyamides degraded (a) by mechanical and thermal influences (2), and

(b) by pyrolysis at high temperatures (3), but this technique has not been used for the UV degradation studies of the nylons.

This research project deals with the UV degradation of Nylon 66 monitored by mass spectroscopic analysis of evolved gases and solid residues. With the use of the mass spectrometer and other analytical tools, the main objective of this research project is to combine data obtained from this study with other data from the literature, in order to elucidate the mechanism(s) by which Nylon 66 degrades in sunlight. Like much of the reported research on the UV degradation of polyamides this work concerns vacuum photolysis and photooxidation. Specifically, the objectives of this research project are as follows:

1. The photo- and photooxidative decomposition of Nylon 66 films, with and without photostabilizing additives, will be investigated. The UV degradation of a) bright Nylon 66 fibers, and b) spunbonded nonwoven fabrics (without additives), will also be studied in order to compare Nylon 66 in their fiber and textile form to the polymer as a film.
2. The photolysis and photooxidation of the Nylon 66 samples will be carried out in a specially constructed apparatus equipped with a high pressure mercury vapor lamp as the light source. Data generated from the photooxidation of the samples exposed to the mercury vapor lamp will be compared to data obtained from samples irradiated from a commonly used xenon arc source.
3. The exposed and unexposed nylon samples will be analyzed by gas and solid state mass spectrometry, and ultraviolet-visible and infrared spectrometry. Chemical tests, such as those which

determine the presence of pyrroles and imides, and the carboxy end group analysis, will also be carried out on the photooxidized and unexposed samples. A crosslinking study will also be performed on all of the films.

4. Several tensile properties, such as the energy-of-rupture, percent elongation at break, and the breaking strength, will be tested on the unexposed and photooxidized fibers and nonwoven fabrics, to correlate strength losses that occur with irradiation.
5. All data obtained from this study will be considered with data from the literature to elucidate the photo- and photooxidative degradation mechanism(s) of Nylon 66.

Before the literature is reviewed, an explanation of the photochemical process is necessary. The absorption of light by molecules, and the ways in which the absorbed energy is dissipated, will be discussed in the next chapter.

CHAPTER II

ABSORPTION AND EMISSION OF LIGHT

For a polymer to photodegrade, it must first absorb harmful incident radiation. The absorption of light by a molecule results in the promotion of an electron from a molecular orbital of lower energy to one of higher energy. Molecular orbitals are formed by a linear combination of the atomic orbitals of atoms within the molecule. The combination of two atomic orbitals give rise to two molecular orbitals; one a bonding orbital and the other an anti-bonding orbital. The electron forming the σ- or π-bond in the molecule, occupies the bonding orbital. In molecules containing heteroatoms like O or N, some of the electrons associated with the heteroatom are not involved in the molecular bonding system, but they occupy nonbonding molecular orbitals (n-orbitals). Figure 1 shows the molecular orbital diagram for the planar formaldehyde molecule (4); the formaldehyde structure contains all three types of molecular orbitals occurring in molecules. Figure 2 shows the relative energies of the different types of molecular orbitals of organic molecules (4). In general, the energy of a non-bonding orbital (n-orbital) is greater than that of a σ- or π-orbital, but less than that of the antibonding orbitals. In some molecules that have a high degree of conjugation, the energy of the π-orbital is greater than that of the n-orbital. The possible types of electronic transitions between the orbitals are σ-σ^*, π-π^*, n-π^* and the n-σ^*. But the electronic transitions of most concern for carbonyl compounds are the n -π^* and the π-π^*. In order

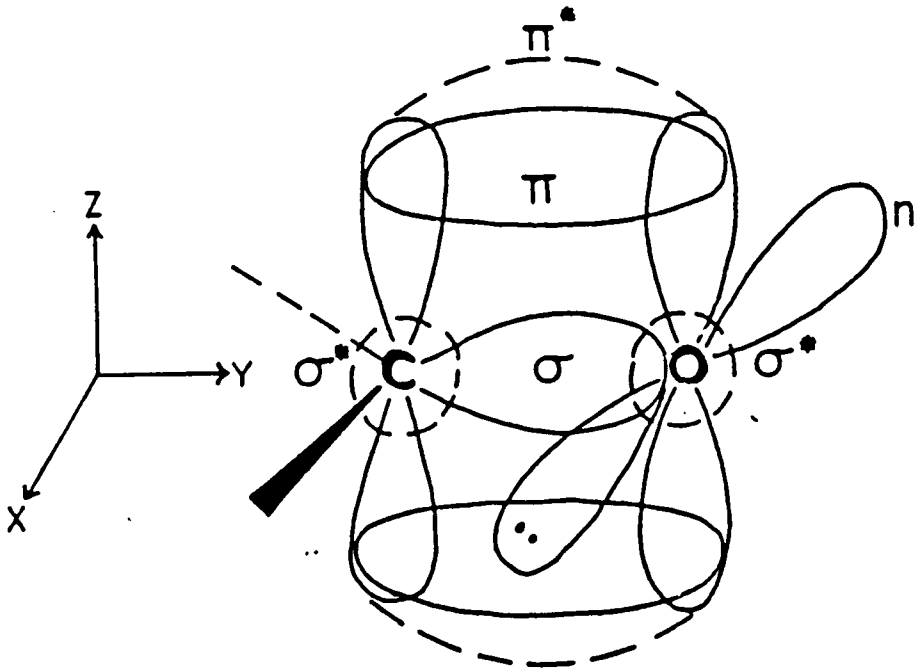

Figure 1. Molecular orbital diagram for the planar formaldehyde molecule.

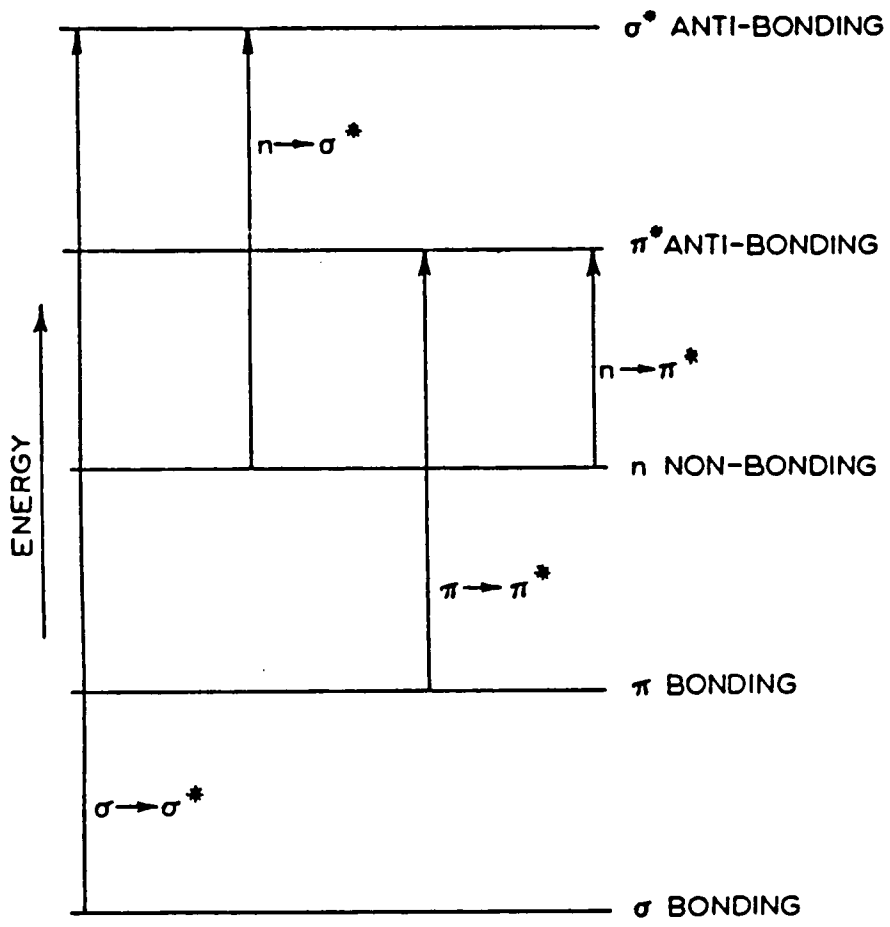

Figure 2. Relative energies of molecular orbitals and possible excitations between orbitals.

for an n - π* transition to occur, an electron from a lone pair on the oxygen moves to an unstable π * orbital; thus.

(1)

The π - π* transition on the other hand, occurs when an electron moves from a stable π orbital to an unstable π * orbital.

(2)

These transitions may be observed as absorption bands in the ultraviolet- visible absorption spectrum. A simple carbonyl compound undergoes an n - π * transition around 280 to 290 nm typical (ε =15) and a π- π* transition around 180 to 190 nm typical (ε = 900) (4). If groups such as $-NH_2$, -NH-, or -OR, are substituted in place of the hydrogen of the simple carbonyl, then an increase in the intensity, and a shift to shorter wavelengths is observed (4).

At room temperature, in the absence of light, the majority of molecules exist in their lowest energy level. The absorption of light (UV or Vis) by a molecule causes the excitation from a low energy orbital (initially occupied) to a high energy, and previously unoccupied orbital. The energy of the absorbed photon is used to energize an electron and cause it to "jump" to a higher energy orbital. There are two excited electronic states. In one state the electron spins are paired (antiparallel) and in the other state the electron spins are unpaired (parallel). The state with paired spins remains a singlet in the presence of a magnetic field and is called a

singlet state (S), whereas the state with unpaired spins interacts with a magnetic field and splits into three states and is therefore termed a triplet state (T). An energy diagram is a display of the relative energies of the singlet ground state (S_o), the excited singlet states (S_1 being the lowest energy excited, singlet state), and the excited triplet states of a molecule (T_1 is the lowest triplet state). An example of an energy diagram for simple carbonyl compounds can be seen in Figure 3 (5). Once the molecule absorbs light, the resultant absorbed energy may be dissipated by either photophysical (transitions which interconvert excited states with each other or excited states with the ground state) or photochemical processes (chemical reactions). The photophysical processes are classified as radiative and radiationless processes (6). These processes are illustrated in the energy diagram of the simple carbonyl compounds (Figure 3).

Radiative Processes:

1. Singlet-singlet absorption ($S_o + h\nu \longrightarrow S_1$)
2. "Forbidden" singlet-triplet absorption ($S_o + h\nu \longrightarrow T_1$)
3. Singlet-singlet called fluorescence ($S_1 \longrightarrow S_o + h\nu$)
4. "Forbidden" triplet-singlet called phosphorescence ($T_1 \longrightarrow S_o + h\nu$)

Radiationless Processes:

1. Transitions between states of the same spin, called internal conversion ($S_1 \longrightarrow S_o$ + heat)

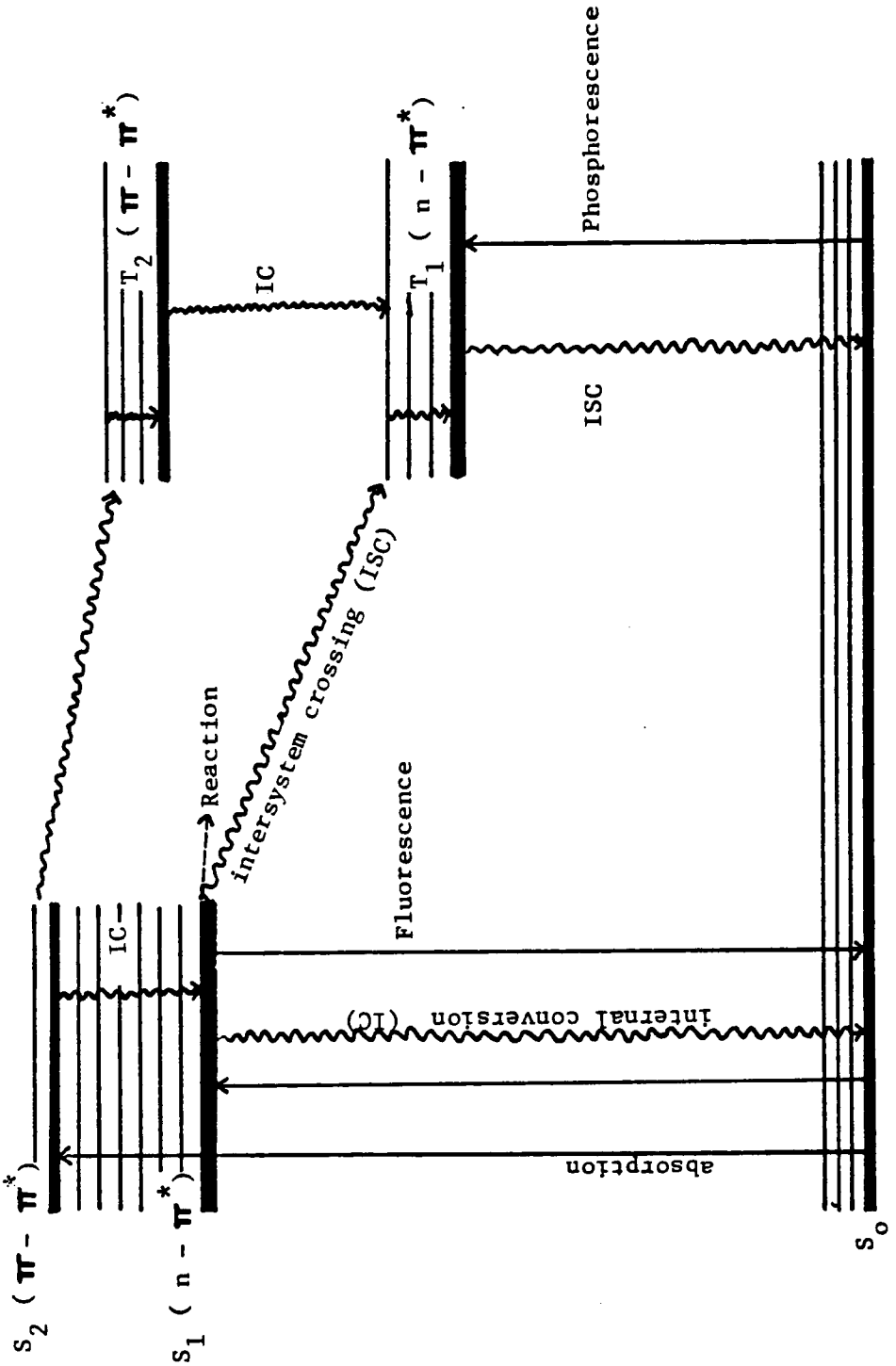

Figure 3. Energy diagram of a simple carbonyl compound.

2. "Forbidden" transitions between excited states of different spin called intersystem crossing ($S_1 \longrightarrow T_1$ + heat)
3. "Forbidden" transitions between triplet states and the ground state, also called intersystem crossing ($T_1 \longrightarrow S_o$ + heat)

In addition to these simple emission processes, two other types of emission, the excimer and exciplex emissions, are sometimes encountered with polymer systems. An excimer emission occurs from an excited associated complex which is formed between a species in the excited singlet state and a similar species from the ground state, thus:

$$A^* + A \longrightarrow (AA)^* \longrightarrow A + A + h\nu \qquad (3)$$

The exciplex emission occurs from an excited associated complex which is formed between a species in an excited state and a different ground state species, thus:

$$A^* + B \longrightarrow (AB)^* \longrightarrow A + B + h\nu \qquad (4)$$

Some polymers also give rise to high emission from excited dimer species, thus:

$$A\text{-}A \xrightarrow{h\nu} (A\text{-}A)^* \longrightarrow A + A + h\nu \qquad (5)$$

In this case both the absorption and emission spectra of the dimer are at longer wavelengths than the spectra of the corresponding monomeric species (5).

CHAPTER III

LITERATURE REVIEW

A. Accelerated Weathering of Polymers

Even though the stability of polymers to weather is best evaluated by actual outdoor exposure, this is not always practical. Much effort, therefore, has been extended to develop accelerated weathering devices, however, to obtain a meaningful correlation with outdoor exposure, as many as possible of the outdoor factors such as light intensity and spectral distribution of sunlight, temperature, and humidity and wetness need to be simulated in an accelerated testing unit. Since sunlight seems to be the major agent influencing the outdoor aging of polymers, considerable effort has been extended to analyze the spectral distribution and intensity levels of sunlight. The ultraviolet portion of sunlight (ranging from 290 to 400 nm) that reaches the earth's surface constitutes a little over 3% of the total radiation from the sun (7). The intensity levels at different parts of the spectrum have been shown to vary considerably with geographical location, season, and time of day (7). Despite these variations in the intensity of sunlight, attempts have been made to simulate it along with other weathering conditions. Figure 4 shows the spectral ranges of sunlight compared to several light sources used to weather polymers (7).

1. Accelerated weathering devices. One of the first light sources used in weathering studies and one still occasionally used today, is the carbon arc Weatherometer (8). The main disadvantage of

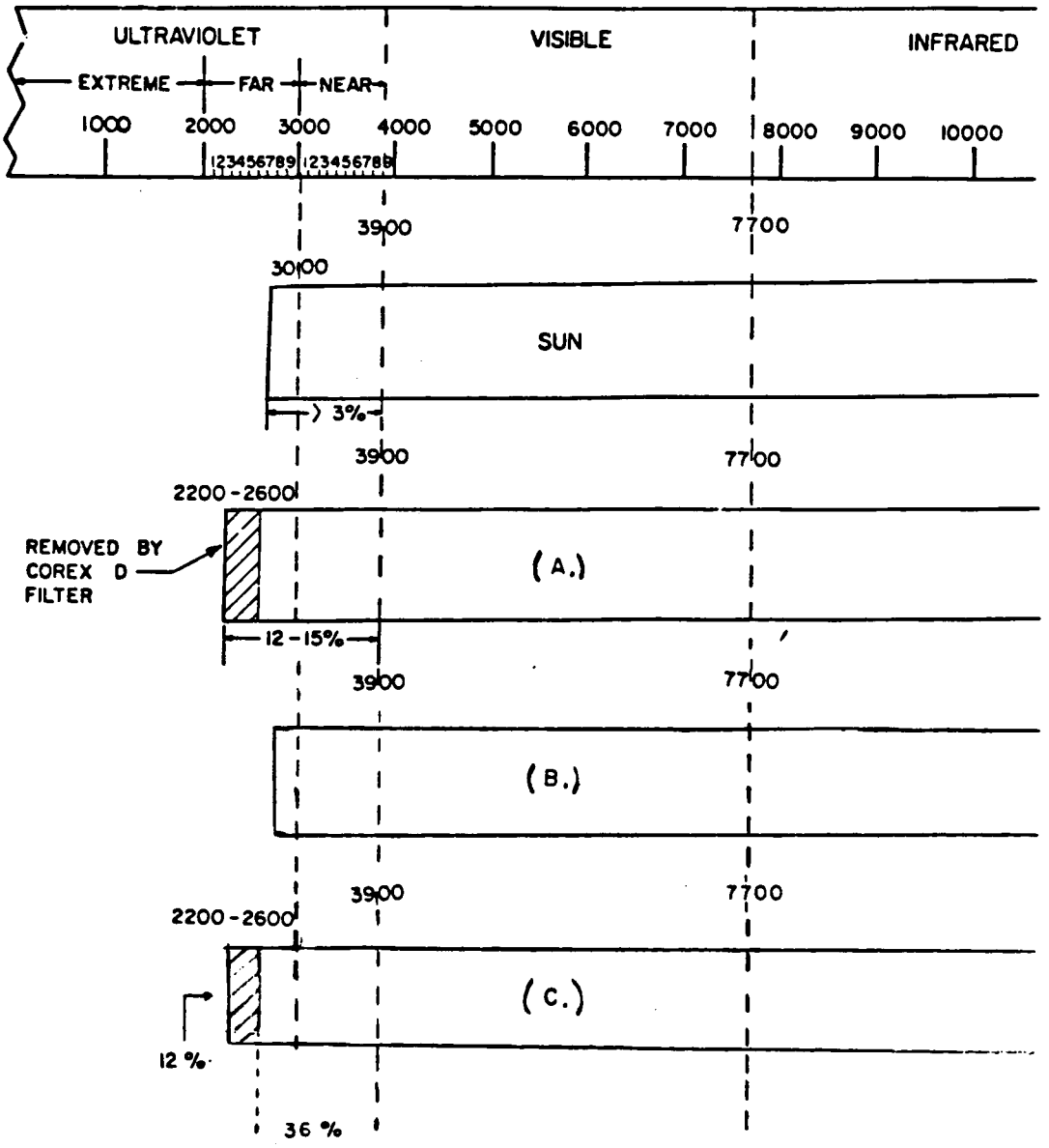

Figure 4. Spectral distribution in Angstroms of sunlight at earth's surface and a. the carbon arc, b. xenon arc, and c. high pressure quartz mercury arc.

this light source is that it does not correlate well with sunlight. Unless suitable filters are used, the spectrum includes wavelengths between 220 and 260 nm which do not occur in sunlight at the earth's surface. Nevertheless, this light source has been found to be useful in correlating the stability of paint enamels with their natural sunlight exposure (8).

The fluorescent sunlamp (8) is another source which has been used in weathering polymers. This light source contains phosphorus which converts the 254 nm emission from medium pressure mercury lamps to light containing longer wavelengths. Its emission (which has a peak at 313 nm) is considerably less intense in the longer wavelength UV region as compared to sunlight, and has much emission below 313 nm (Figure 5) (8). To overcome the lack of intensity in the longer wavelength region, fluorescent sunlamps can be used in combination with a blacklight source (Figure 5). The light stability of polymers such as polyester, polyolefins, and rigid poly(vinyl chloride) exposed to the fluorescent sunlamp/blacklight, have been found to correlate well with outdoor exposure data (8).

Another common light source which has been used extensively in weathering studies is the xenon arc (8). A xenon arc Weatherometer has facilities for controling both temperature and humidity. The emission of this light source is compared with that of sunlight in Figure 6 (8). In some weatherometers, inner quartz and outer pyrex glass filters are used; and between these filters are infrared filter screens which help eliminate some of the short-wavelength ultraviolet light not present in sunlight. Other types of filters, such as the

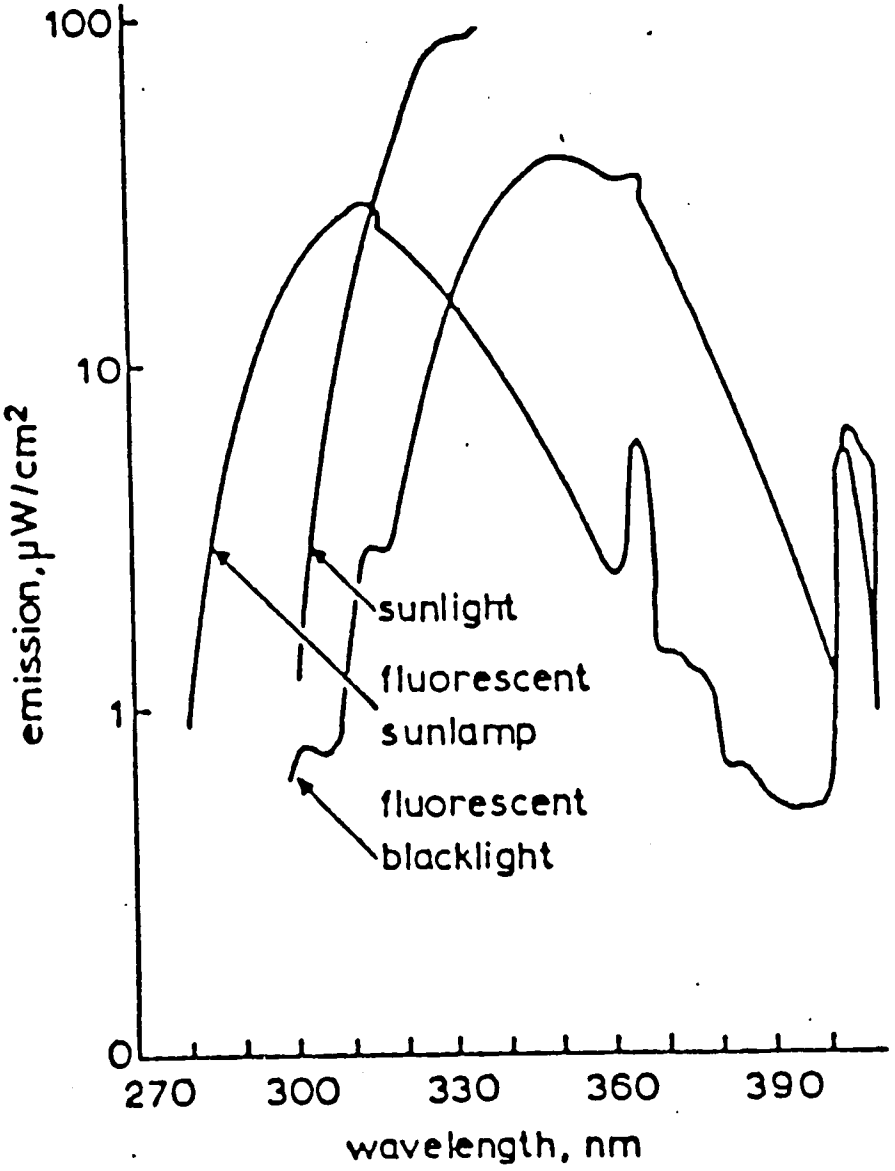

Figure 5. Ultraviolet spectral distributions of the fluorescent sunlamp and fluorescent blacklight.

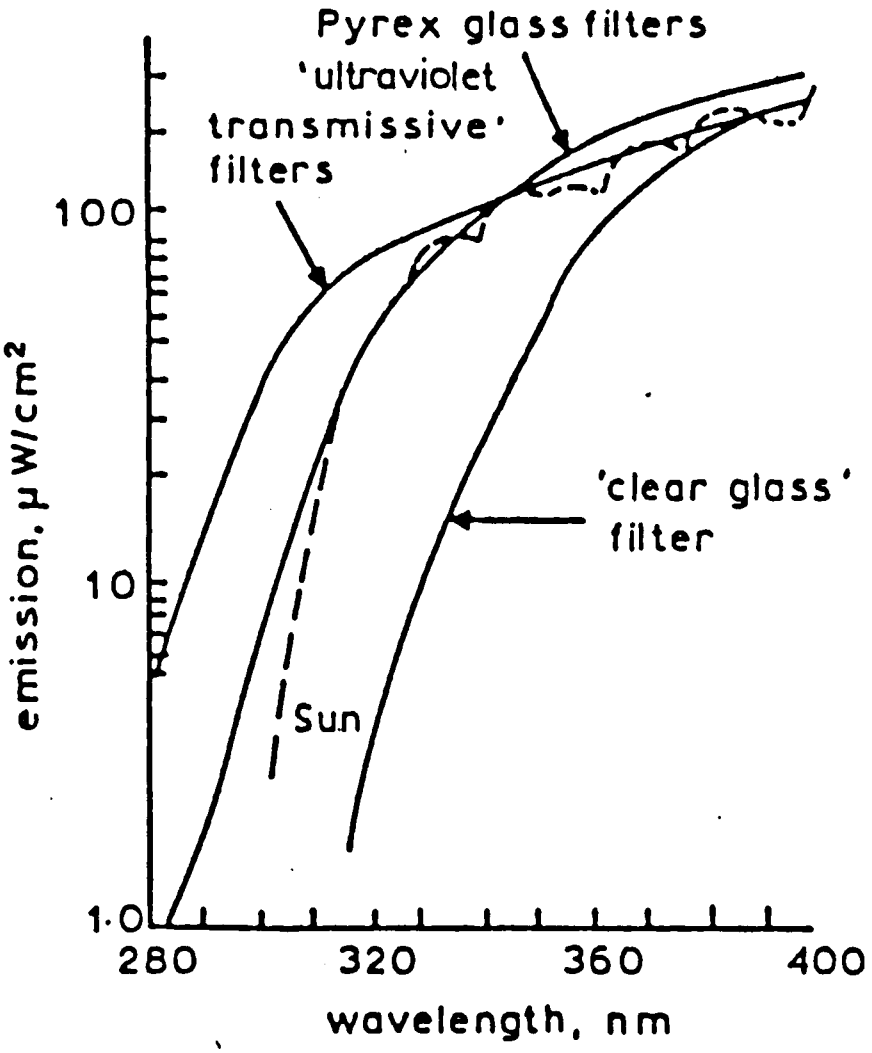

Figure 6. Spectra energy distribution of a xenon arc through various types of filters compared to sunlight at the earth's surface.

inner borosilicate and outer soda lime filters have been used successfully. With these filters, the xenon arc source has a spectrum most similar to light. This similarity, however, is not sufficient enough to give reproducible results. Wall and workers determined from a careful comparison of xenon arc spectra with sunlight that the xenon arc is lower in intensity at wavelengths greater than 335 nm (9). They attributed discrepancies in nylon breaking strength after aging in sunlight and xenon arc exposures to the fact that scissionable bonds in nylon absorb at wavelengths above 335 nm, where xenon arc intensity is lower.

The mercury arc is another light source that has been used extensively in weathering polymers (8). This light source is used in photochemical studies where monochromatic radiation is desired. There are three main types of mercury lamps; low, medium and high pressure arcs with main emission lines at 254, 365, and 436 nm. For the high pressure mercury arc, 36% of the emitted energy is between 260 and 390 nm. A good correlation has been obtained between sunlight and high pressure mercury arc exposures for the weathering of vinyl polymers and copolymers.

2. Light intensity measurement of light sources. The light intensity of most artificial light sources decrease on prolonged use. It is therefore important to measure the amount of incident light on the irradiated sample. Light intensity can be measured using several methods, but the most commonly used method for the weathering studies involves the use of chemical actinometers. There are three types of chemical actinometers; gaseous, liquid and solid actinometers.

Gaseous actinometers which use CO_2, O_2, HBr, or acetone to measure light intensities, are used for monitoring incident light in the far-ultraviolet region (10) and therefore their use is restricted. Only the liquid and solid actinometers can be used to measure light intensities from sunlight, or from the artificial light sources previously discussed. These two types of chemical actinometers will be described in more detail below.

a. Liquid actinometers. Some common liquid actinometers are solutions of benzophenone (11), 2-hexanone (11), uranyl oxalate (12) and potassium ferrioxalate (13). The third and fourth liquid actinometers are the ones most frequently used for measuring light intensity during outdoor exposure of plastics, but both have their disadvantages. Some disadvantages of uranyl oxalate as an actinometer is that its preparation and subsequent analysis of the solutions were tedious, and the solutions often froze in the winter. Potassium ferioxalate is also inadequate for long term weathering of plastics because of its instability to light. It is, however, now widely used by photochemists to measure light intensities over a range of wavelengths from 250 to 578 nm. The compound is photolyzed in aqueous solution of sulphuric acid and the Fe^{+3} ions of potassium ferrioxalate are photoreduced to Fe^{+2} ions. The following reactions occur during the photolysis of the actinometer (13).

$$[Fe^{+3}(C_2O_4)_3]^{-3} \xrightarrow{h\nu} [Fe^{+2}(C_2O_4)_2]^{-2} + C_2O_4^{-}$$

$$[Fe^{+3}(C_2O_4)_3]^{-3} + C_2O_4^{-} \xrightarrow{h\nu} [Fe^{+2}(C_2O_2)_2]^{-2} + (C_2O_4)^{-2} \qquad (6)$$

$$[Fe^{+3}(C_2O_4)_3]^{-2} \xrightarrow{h\nu} [Fe^{+2}(C_2O_4)_2]^{-2} + 2CO_2$$

Since the photoproduct $Fe(C_2O_4)_2$ does not absorb visible light, the Fe^{+2} ions can complex with 1,10-phenanthroline, producing a red-colored complex which has a high absorption coefficient, and therefore the number of Fe^{+2} ions can be determined spectrophotometrically at 510 nm (13).

b. Solid actinometers. Of the three types of chemical actinometer, solid actinometers give the most accurate measurement of light intensity since polymer films are usually used, and they can be mounted at an angle identical to that of the specimen being tested (11). Polyethylene films have sucessfully been used as actinometers (11). The temperature coefficient can be closely monitored during weathering and the analysis requires monitoring of an infrared absorption at 1710 cm^{-1}.

Other polymer systems such as poly(phenylene oxide) have been used as actinometers, and have been found to give reliable results in comparison with other techniques for measuring light intensity (11). The use of this actinometer has the same advantages discussed above, but it can be analyzed spectrophotometrically. During irradiation, the polymer darkens in color and the chromophore can be quantitatively assessed in an ultraviolet spectrophotometer at 340 nm.

Thus far, examples of films used as solid actinometers have been described. Solid actinometer compounds dispersed in polymer films have also been widely used. For example, o-nitrobenzaldehyde dispersed in poly(methylmethacrylate) undergoes photoisomerization to o-nitrosobenzoic acid (14).

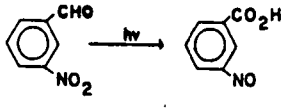

(7)

This technique has the same advantage of film actinometers, and the isomerization is readily followed by the disappearance of the nitro peak at 1520 cm^{-1} in the infrared spectra of the acrylic film.

B. Photolysis and Photooxidation of Aliphatic Polyamides

During the photolysis and photooxidation of aliphatic polyamides, the mechanical properties deteriorate, and the polymer darkens. Changes in tensile strength and elongation, determined from stress-strain curves, have been used by several scientists in determining the amount of deterioration of the polymer. Moore (15) examined the effect of sunlight and other UV sources on bright and delustered yarns of Nylon 6, 66, and 610 under varying atmospheric conditions (vacuum, O_2, N_2, humidity). Humidity had little effect on the tensile strength of Nylon 66, although bright yarns lost more strength under dry conditions than wet. At wavelengths greater than 300 nm, moisture enhanced the degradation of delustered yarns slightly. In general, it was found that the delustered yarns were more sensitive to UV radiation at wavelengths greater than 340 nm, and bright yarns were more sensitive to wavelengths below 300 nm. In all cases, oxygen resulted in greater losses in tenacity. In general, the tenacity and extensibility of the samples decreased with increase in exposure time (delustered yarns lost strength more rapidly than the bright yarns). This seems strange since in most cases where a decrease in tensile strength is observed, the elongation usually increases. However, this strange occurrence has been observed by other researchers (16, 17, 18, 19). Achhammer and workers (16), for

instance, investigated the effect of heat, sunlight and UV (from an RS sunlamp) on a series of aliphatic polyamides and found that all samples lost tensile strength and elongation. Stephenson and workers (17, 18) examined the effect of UV light (at various wavelengths) on Nylon 66. They found that the polymer shows a greater decrease in tensile strength and elongation at lower wavelengths (369 nm had considerably less effect then 314 and 244 nm). Stephenson and workers (19) also investigated the effect of UV light on Nylon 66 under nitrogen and under vacuum. When the polymer was irradiated at 253.7 nm for periods up to 180 hours (under both conditions) the tensile strength and elongation increased initially and then decreased. The decrease in tensile strength and elongation was much greater for samples exposed in nitrogen than under vacuum.

These early studies demonstrated the deterioration of mechanical properties that result from the photolysis and photooxidation of polyamides. The changes in mechanical properties and in color (yellowing) are correlated with the changes in chemical structures of the polymer that occur after irradiation. Thus, the extent of photo- and photooxidative degradation, or any other type of degradation, may be estimated through the use of chemical analysis and various spectroscopic techniques such as electron spin resonance (ESR), gas chromatography (GC), mass spectrometry, and ultraviolet-visible (UV-VIS) and infrared spectrometry (IR). Utilizing these analytical techniques, several workers have proposed mechanisms for the photo- and photooxidative degradation of polyamides and model compounds. Their studies and propose mechanisms will be discussed in the

following pages. Also, since heat is generated during the photochemical process, the thermal and thermooxidative degradations will be included.

1. Photolysis studies and proposed mechanisms. Stephenson and workers (18) examined the possible chain scission and crosslinking for polyamides and various other polymers exposed in both nitrogen, and vacuum, at 253.7 nm for periods up to 800 hours. Gels were formed in all polymers more readily in vacuum than in nitrogen, except none was formed when polyester was exposed in nitrogen. Nylon 66 forms 70% gel after 100 hours of irradiation in vacuum, and only 45% gel after 100 hours in a nitrogen atmosphere. For most of the polymers studied, in general, crosslinking occurs almost twice as much in vacuum than in nitrogen. In another photolysis study done by Stephenson and colleagues (19), nylons were irradiated at wavelengths less than 300 nm and the off gases, hydrogen and methane were monitored by GC. From their study, considerably more hydrogen was liberated from polyamides irradiated in vacuum than in nitrogen. The evolution of methane was comparable for the two atmospheres. Rafikov and Tsi-Pin (20) studied the effects of UV light on nylon films by ESR, UV, and IR spectrometry. Films were exposed to the full spectrum of a high pressure quartz mercury arc and to wavelengths greater than 300 nm at periods up to 140 hours. Chromatography showed that the full spectrum lamp exposure resulted in the evolution of H_2 and CO, and small quantities of short chain hydrocarbons. After 120 hours of UV exposure ($\lambda \geq 300$ nm), 18.9 mL of H_2/1000 polyamide chain units were liberated. Stephenson (19), however, reported only 0.2 mL of H_2 evolved from

Nylon 66 films irradiated at 253.7 nm for 120 hours in vacuum. From calculations of the amount of CO evolved per 1000 polymer chains for a polymer of M_w=16,000, Rafikov and Tsi-Pin (20) determined that on 120 hours of exposure, less than two C-N chain bonds were cleaved, with subsequent evolution of CO, but approximately 18 C-H bonds were ruptured to liberate H_2. Their study shows, therefore, that if only a portion of the radicals formed from C-H bond cleavage recombine, then crosslinking of the polyamide would predominate over chain scission. An increase in intrinsic viscosity, M_v, and the Huggins constant (indicating chain branching) were observed. After 5 hours of exposure, an insoluble gel was formed and the amount of gel increased upon further irradiation. Rafikov and Tsi-Pin (20) concluded that the formation of crosslinks is greater than chain scission, but the number of crosslinks formed was small.

Rafikov and Tsi-Pin (20) did not observe any crosslinking of polyamides exposed for 140 hours at wavelengths greater than 300 nm in vacuum. With increased exposure time, the intrinsic viscosity of the photolyzed samples decreased. Gases evolved were primarily H_2 and CO, but the amounts were much lower than those obtained on exposure at the full UV spectrum. ESR measurements indicated that a radical formed at all wavelengths was $-CH_2-\dot{C}H-NH-CO-CH_2-$. When two of these radicals on adjacent chains come close enough to form a bond, crosslinking can occur, as seen on the next page.

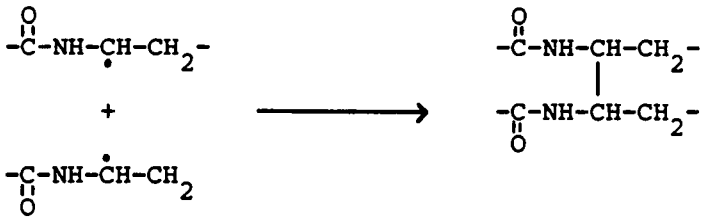

(8)

It has been suggested by Zimmerman (21) that such crosslinking is sterically impossible when radicals occur on adjacent polymer chains that are hydrogen-bonded at the amide groups. Crosslinking is therefore less likely to occur in the crystalline regions. Most workers, however, believe that there is no reason why this process should not occur in the amorphous regions of nylons, where the breaking and formation of hydrogen bonds is more frequent, and the radicals can migrate through the polymer.

In addition to crosslinking, as previously mentioned, direct scission of the polyamide chains also occurs during photolysis. ESR analysis (20, 22, 23) of the photolysis degradation products of polyamides, and studies of amide model compounds (15, 19, 24, 25, 26) show that chain scission occurs primarily at the methylene group adjacent to the nitrogen in the chain. Despite the evidence of a $-CH_2-NH-$ bond cleavage, scission at the amide linkage -CO-NH- has been proposed by several workers (15, 19, 20, 27) to be the dominant process, which accounts for evolved CO gas detected by mass spectrometry and GC. Heuvel and Lind (27) observed initial degradation at the amide linkage by low temperature ESR measurements. Stephenson, et. al. (29) and Rafikov and Tsi-Pin (20) proposed scission at the amide bond, as visualized in Figure 7, to account for the photodegradation products, even though such cleavage was not

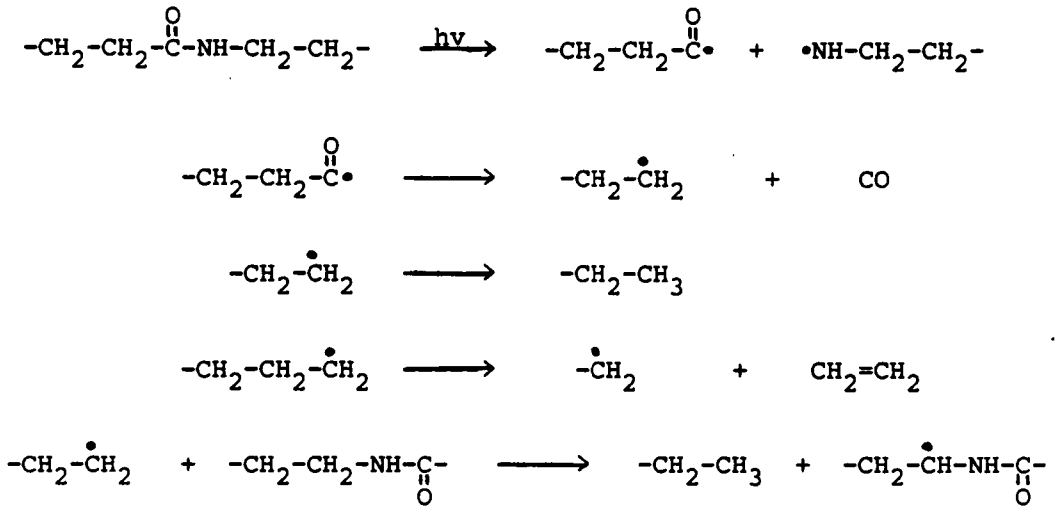

Figure 7. Amide bond scission.

directly observed by them. Stephenson (19) also proposed the formation of primary amine chains and low molecular weight primary amine compounds such as methyl-, ethyl-, and propylamines as a result of photolysis. Formation of methane and ethane were also suggested.

Even though Stephenson's research was done at wavelengths less than 300 nm, while Rafikov and Tsi-Pin's work was done at wavelengths greater than 300 nm, both reported similar results. From paper chromotography and mass spectral data of photolyzed ($\lambda < 300$ nm) N-alkylamides, Moore proposed the photolysis mechanisms of aliphatic polyamides as seen in Figure 8 (15). His scission mechanism accounts for the formation of n-pentanoic acid resulting from the hydrolysis of irradiated Nylon 66. According to Stowe, Formes and Gilbert (28), the disproporation reaction between polymers is less likely due to polymer rigidity, and therefore, the PH in Figure 8 is probably ——CH_2—— on an adjacent chain.

2. Photooxidation studies and proposed mechanisms. The photooxidation mechanisms for polyamides have been proposed from photooxidative studies of model compounds, namely N-alkyl and N,N'-dialkyl amides. Lockard and Sagar (29) studied the photooxidation of N-alkylamides, and from their study, N-acylamides, formyl-amides, and unsubstituted amides were isolated. Sharkey and Mochel (26) photooxidized solutions of ^{14}C labeled N-pentyl-1-^{14}C-hexanamide with UV light (at $\lambda \geq 300$ nm) for 285 hours at 50°C. Upon examination of the degradation products, they found that significant amounts of CO_2 and CO were derived from the methylene group next to the nitrogen. It was also established that n-valeraldehyde and its degradation products

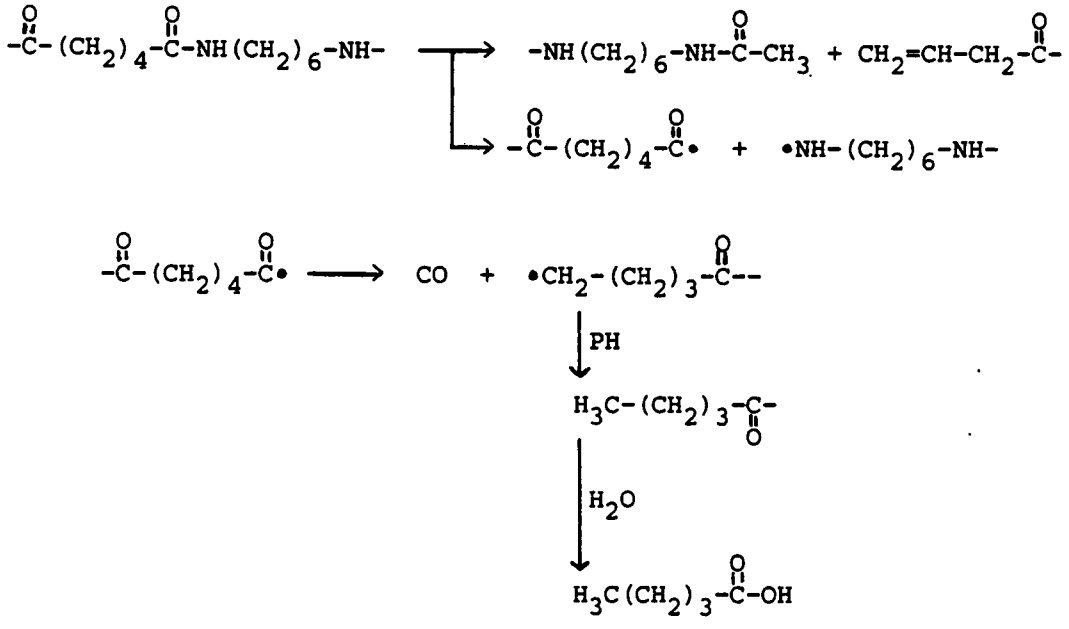

Figure 8. Photolysis mechanisms of aliphatic polyamides.

came from the amine portion of the molecule; that substitution of the hydrogens on the methylene adjacent to the nitrogen prevented oxidation attack; and that amides (hexanamide was isolated) and carboxylic acids (hexanoic acid was detected) are products of photooxidation. From these findings, the photooxidation mechanism, as seen in Figure 9, was proposed. In Sharkey and Mochel's study (26), no evidence for the initial photolytic scission was found, but products could have been formed and then oxidized to hexanoic acid and valeraldehyde. The initial photolytic scission has, however, been observed by Golemba and Guillet (30) at low temperatures by ESR. Using IR and mass spectrometric techniques, Moore (15), and Burnett and Riches (24), proposed photooxidation mechanisms (from their studies of N-alkyl amides) similar to Sharkey and Mochel. Kroes (31) showed that the mechanism suggested by Sharkey and Mochel also holds for polyamides.

The photodegradation and yellowing of Nylon 66 fabrics and model compounds were studied by Marek and Lerch (25). Samples were exposed in a Fadometer in the presence of air, moisture and heat (50^{o}C). Based upon the Ehrlich reaction (test for pyrroles), Marek and Lerch proposed the formation of pyrroles from succinaldehyde and ammonia in the photooxidation of Nylon 66 to explain the yellowing of fabrics. Similar conclusions were drawn by Margolin, Postnikov and Shlyapintokh (32) in their photooxidation study of polycaproamide. Without much evidence, they also suggested the possible formation of pyrroles during photooxidation, but their samples were irradiated at wavelengths around 254 nm.

Initiation:

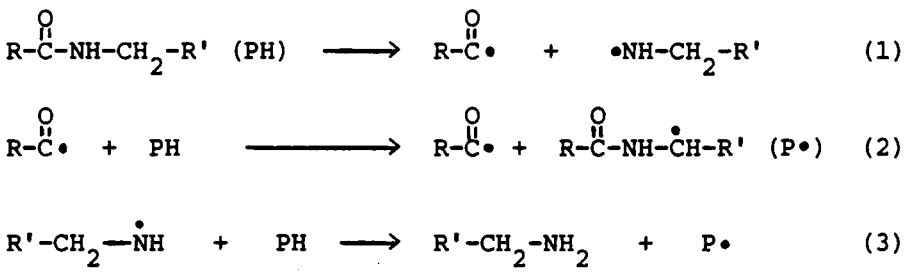

Propagation:

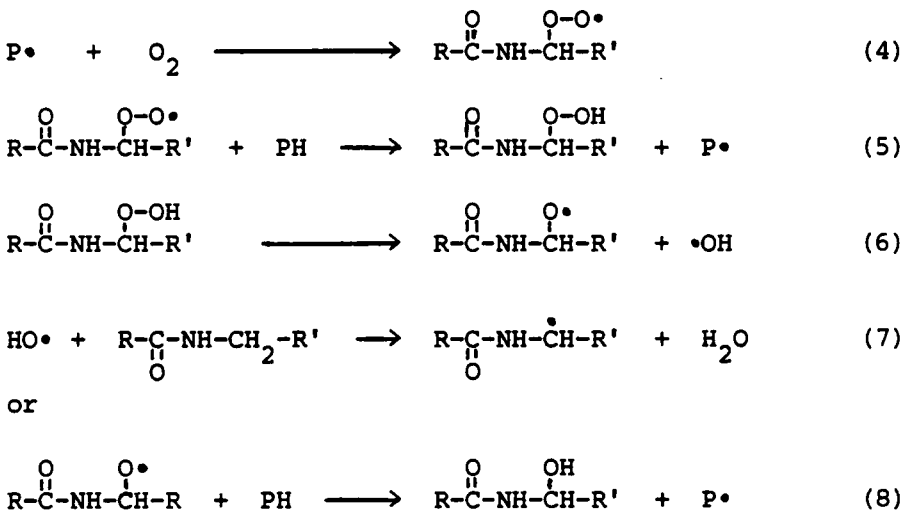

Subsequent reactions:

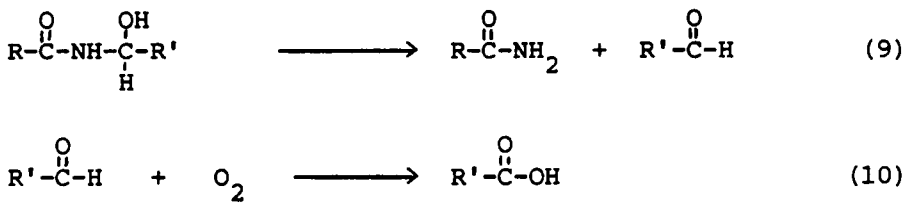

Figure 9. Photooxidation mechanism.

Ly Tang, Sallet and Lemaine (33) proposed photooxidation mechanisms of polyundecanamides at short and long wavelengths. IR and UV spectrometry, and hydroperoxide titrations were used as analytical tools in their study. The photooxidation mechanisms at 254 nm and at wavelengths greater than 300 nm can be seen in Figures 10 and 11, respectively. The formation of imides occurs at 254 nm, or at wavelengths greater than 300 nm when heat (60°C) is also present.

Most of the mechanisms mentioned thus far involve initial scission at the carbon-nitrogen bond of the amide group during photooxidation ($\lambda \geq 300$ nm), but the amide group does not absorb light above 290 nm. This fact led many workers (34, 35, 36, 37) to postulate the involvement of impurity chromophores in the photooxidation step. For photooxidized polyamides, in particular, Nylon 6 and 66, an absorption band centered at 290 nm has been the subject of much attention. Ford (38) showed that the absorption at 290 develops on irradiation and continues to increase on further storage in the dark. Phosphorescense studies by Allen, McKellar and Phillips (39) indicated that α, β-unsaturated carbonyl groups were responsible for the absorption at 290 nm and that these groups are important initiators of photooxidation.

3. Thermal degradation. The thermal degradation of polyamides and model compounds has been the subject of much investigation. When aliphatic polyamides are heated above their melting point for extended periods of time, changes occur in color (darking), and in the average molecular weight as determined by viscometry. Korshak and workers (40) showed that when Nylon 66 is heated at 270°C, in a nitrogen

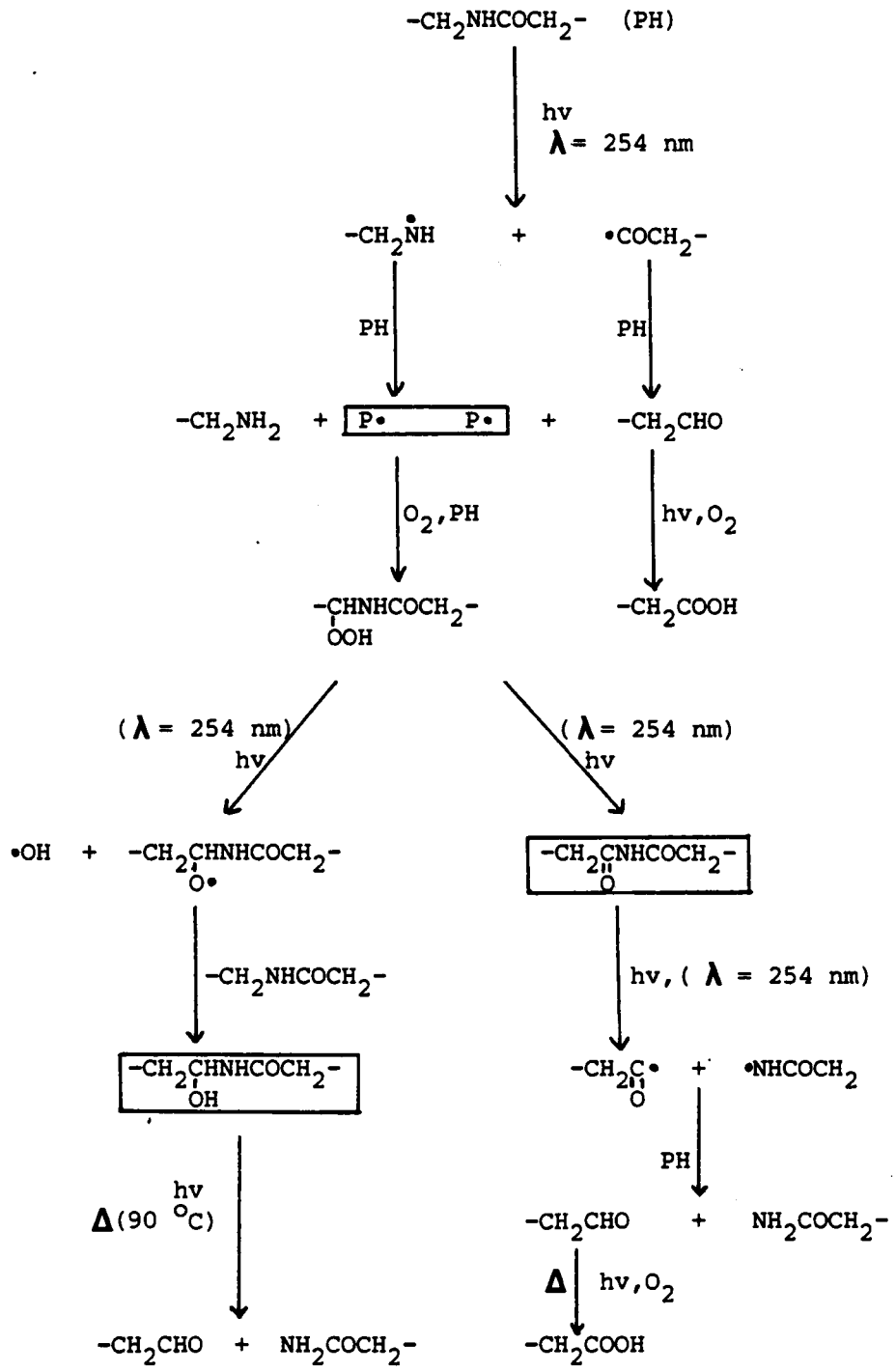

Figure 10. Photooxidation of Polyundecanamide at 254 nm.

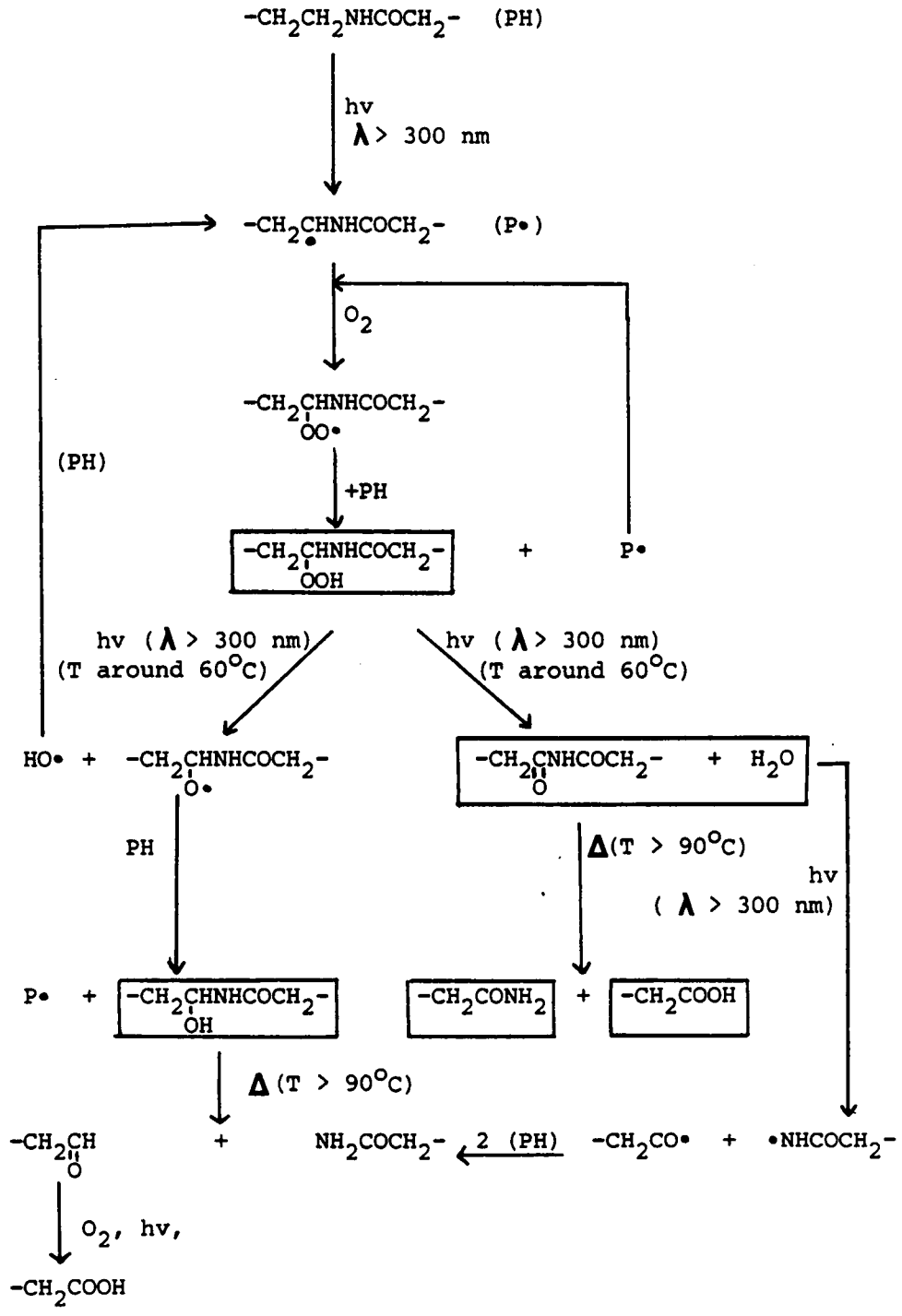

Figure 11. Photothermal Oxidation of Polyundecanamide at λ > 300 nm.

atmosphere, no changes in molecular weight is noted, but when the polymer is heated at 300°C, within 2 hours, a drastic decrease in molecular weight occurs. Futhermore, when nylon is heated at 330°C, rapid gelation and color formation occurs. The proposed mechanisms resulting in the gelation and formation of off products will be discussed in the following pages.

Some products of thermally degraded amides and polyamides (aliphatic) have been identified as carbon dioxide, water, ammonia, hexamethylenediamine, n-hexylamine, n-heptylamine and methylamine (41, 42). Thermal degradation is believed to originate from the hydrolysis of the amide bond, resulting in the formation of amines and thermally unstable carboxylic acids (41, 42).

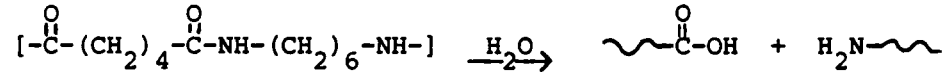

(9)

At 350°C, deamination of some of the amines and decarboxylation of the acids occur. The carboxyl groups can also participate in branch formation. With increased thermal exposure of polyamides, Kroes (43) proposed that primary amines couple (with the elimination of ammonia), and the carboxyl end of a carboxylic acid condenses with the center amine to form the resulting branched dihexylamine (B).

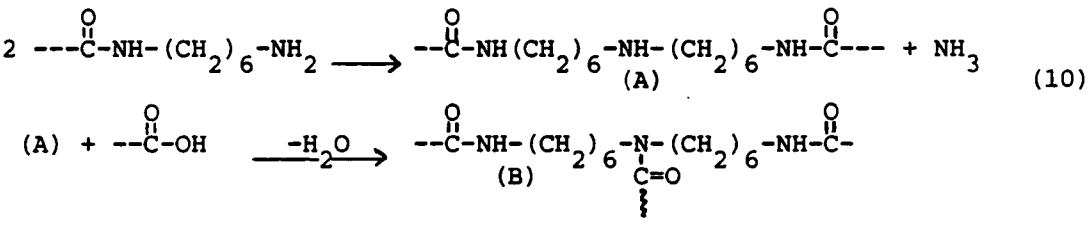

(10)

Kamerbeek and workers (44) have identified the dihexyl amine in gelled nylons. Also, water was one of the main products detected in their study, (even from materials extensively dried). The above reaction is one source of water, but according to Kamberbeek and workers, the major source of water is from thermal cracking followed by dehydration.

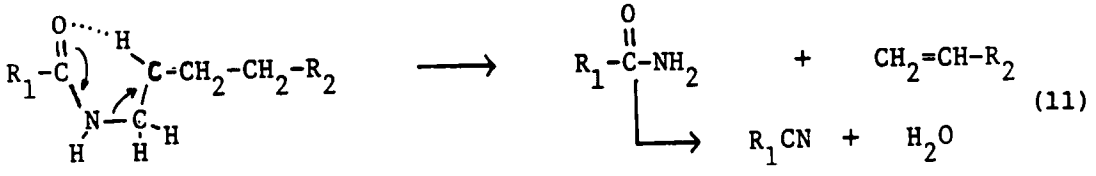

(11)

At high temperatures, the primary amide is unstable and the nitrile is formed. Nitrile groups have been detected in both the volatile fractions and the solid residue by several researchers (16, 45).

In addition to the products previously mentioned, various substituted cyclopentanone derivatives such as I and II have been analyzed by Goodman (41, 42) as degradation products of adipic acid (cyclopentanone was not observed by Goodman).

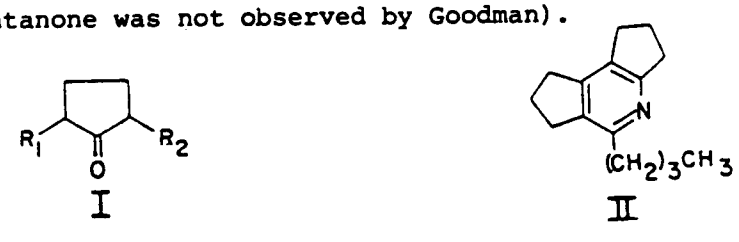

(12)

Goodman suggested that Compound I could originate from the cyclization of the acid end group in polyamides and model compounds:

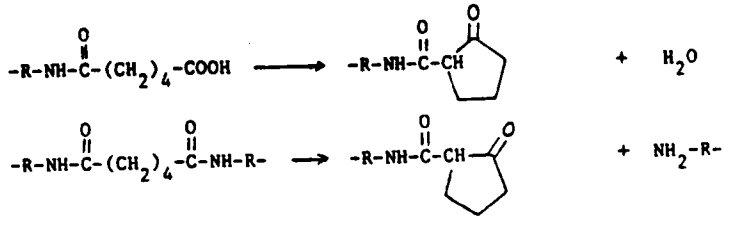

(13)

The cyclopentanone group must undergo additional reactions in order to form Compound I. Even though Goodman did not directly observe cyclopentanone, he believed that cyclopentanone was formed, and then underwent further reactions. For instance Compound II could possibly be derived from cyclopentanone.

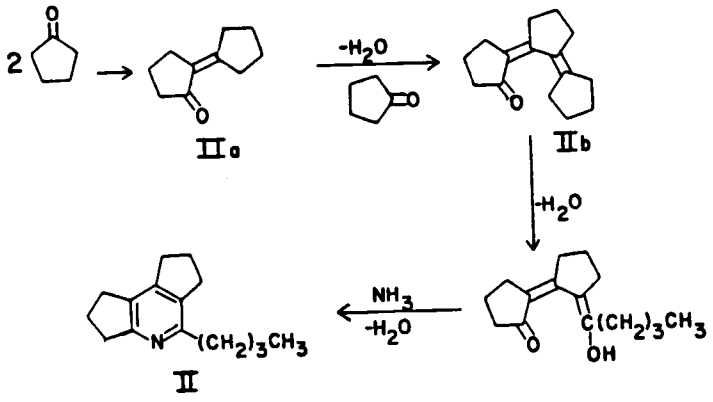

(14)

Further, Goodman (41, 42) found that thermally degraded Nylon 66 and dibutyl adipamide gave a positive Ehrlich reaction (test for pyrroles), but only a very small amount was detected. It was believed by some researchers (43, 44) that the strong UV absorption at 290 nm (which appears in thermally degraded Nylon 66 films) was probably due to pyrroles, but Goodman suggested that the absorption was probably Compound II, since it absorbs at 284 nm. Recall that photodegraded Nylon 66 films also exhibit a strong UV absorption at 290 nm which was once believed to be due to pyrroles (25) but recent studies suggest that the absorption is probably due to α, β-unsaturated carbonyl compounds (39). In the thermal studies of Nylon 66, no one has explored the possibility of the absorption at 290 nm as being due to α, β-unsaturated carbonyl compounds.

Peebles and Huffman (46) studied the thermal degradation of Nylon 610 and 66, and analysis of the volatile materials showed that it not only contained carbon dioxide, water, ammonia, hexylamine, hexamethylenediamine, 2-cyclopentylcyclopentanone(IIa), 2-cyclopentylidinecyclopentanone(IIb), but it also contained cyclopentanone (not observed by Goodman), hexamethyleneimine, a cyclic monomer (III), and 1,2,3,5,6,7-hexahydrodicyclopentapyridine (IV), which has an intense UV absorption at 287 nm.

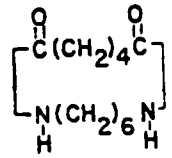

III

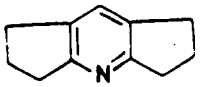

IV

(15)

Using NMR spectroscopy, Peebles and Huffman (46) showed that Compound IV, not II, was responsible for the UV absorption at 290 nm. Pyrroles were not detected. Compound III was observed in the mass spectra of the volatile products.

4. Oxidative thermal degradation. Heating polyamides in the presence of oxygen results in chain scission and crosslinking (44). At 250°C Nylon 66 becomes brittle after 2 hours. At 70°C, the polymer becomes brittle after 2 years (44). The degradation appears to result from a free radical chain reaction, and initiation is believed to occur at the carbon alpha to the nitrogen. There have been several studies (47, 48) on the oxidative thermal degradation of polyamides and model compounds. The overall scheme for the oxidative thermal degradation of N-alkylamides at 100°C can be seen in Figure 12. Hydroperoxides, imides, primary amides, aldehydes and carboxylic acids have been detected as oxidative thermal degradation products. The

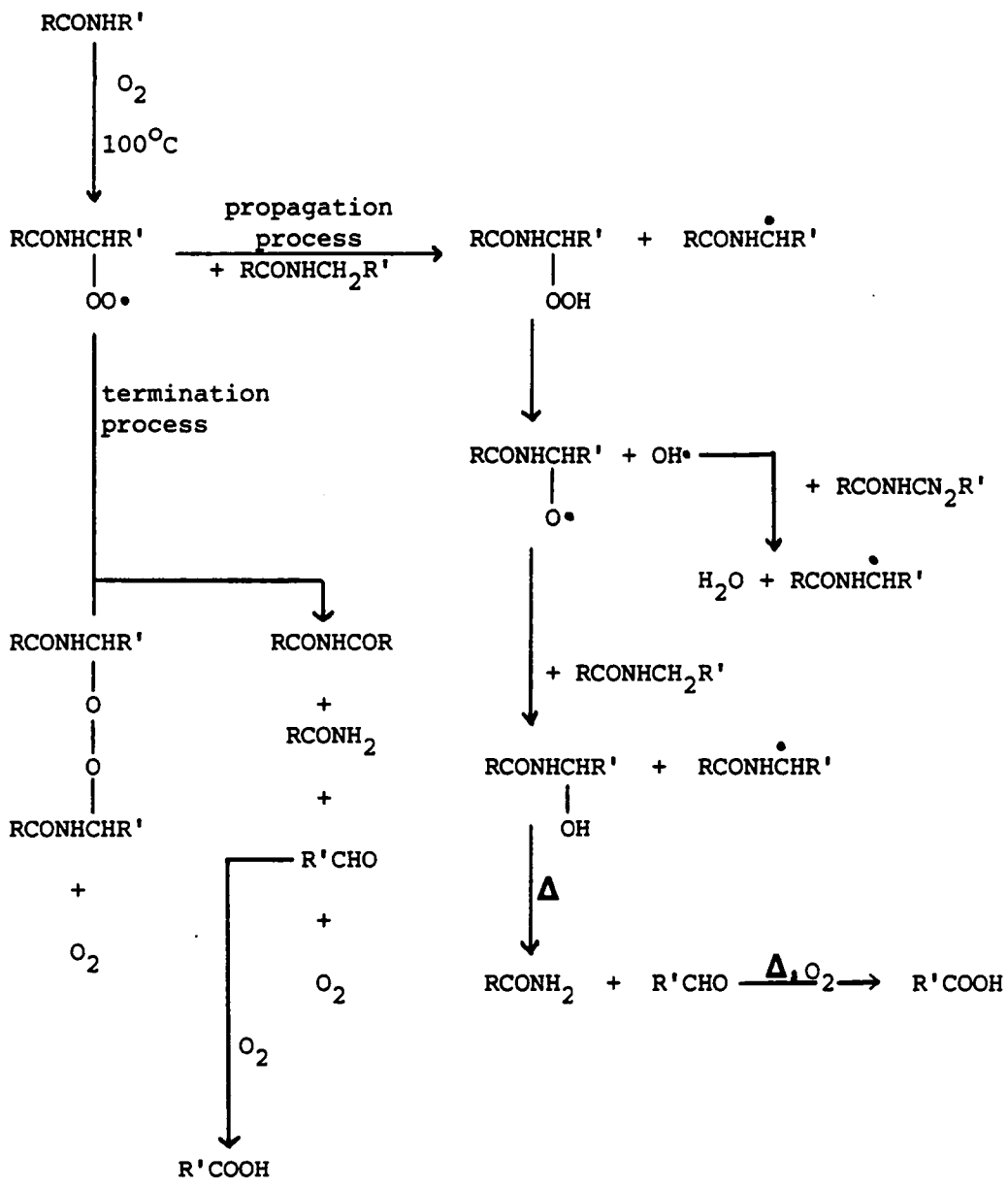

Figure 12: Oxidative Thermal Degradation of N-Alkyl Amides at 100°C.

formation of hydroperoxides greatly speeds up the degradation process (47, 48). The peroxide-catalyzed chain degradation mechanism is supported by the fact that small amounts of antioxidants drastically reduce thermal degradation in nylons.

C. Photostabilization of Polyamides

The ultraviolet stability of light-sensitive polymers can be improved by the use of photostabilizers. In some cases, a photostabilizer may also increase the thermal stability of the polymer. The photostabilization of polymers involves the retardation or elimination of the various photophysical and photochemical processes that occur during photodegradation or photooxidation. The photostabilization of polymers can be obtained in several ways (49).

1. Ultraviolet screening: The photostabilization involves the prevention of ultraviolet radiation from penetrating into the material, thus limiting the degradation process to a thin surface layer.
2. Ultraviolet absorption: The photostabilizers absorb primary ultraviolet radiation and secondary luminescence light (fluoresence or phosphorescence) of longer wavelengths than those which were previously absorbed.
3. Intersystem crossing: A polymeric ultraviolet absorber is excited to a triplet state in which a photochemical rearrangement or some other photochemical reaction can occur to prevent further degradation.

4. Internal conversion: The absorbed light energy is converted into vibrational energy by a radiationless process without any change in spin multiplicity.
5. Quenching: The photostabilizers or quenchers deactivate the excited singlet or triplet state of a polymer.

A large number of compounds, both organic and inorganic, have been recommended as photostabilizers for polyamides. It is believed that most of the commercial UV stabilizers for polyamides act as screening agents, but quenching may also play a role (50). Golemba and Guillet (30) described several methods available for the photostablization of several polymers. For polyamides, some of the photostabilizers described include UV screeners (such as carbon black) UV absorbers (such as benzophenones and benzotriazoles) and UV quenchers (such as nickel chelates). Inorganic additives such as the salts of trivalent chromium have also been used to photostabilize polyamides (51, 52). Other chromium compounds (such as di- and hexavalent chromium salts) have been used but, during the addition to nylon, the divalent chromium is oxidized and the hexavalent form is reduced to the trivalent chromium. Chromium dyes have also been shown to protect polyamides against UV radiation (53). Not only do the chromium compounds improve the light stability of polyamides, but they also increase their thermal stability.

Titanium dioxide (TiO_2) which is a delusterant often incorporated in Nylon 66 greatly increases the rate of photooxidation of the polymer. The crystal structure of TiO_2 is an important determinant of the photostability of Nylon 66; the anatase form is generally more

photoactive than the rutile form (54, 55). Certain additives, particularly Mn^{+2}, reduce the photocatalytic effect of TiO_2 (56). Cu salts protect nylons from heat and UV degradation, but they are not effective in the presence of TiO_2 and light (56). Co-stabilizers (alkyl iodides (57) and stannous salts (58)) are often used with Cu salts to protect polyamides from light. Organic compounds such as 2,4-dibromoaniline, o- and p-iodoaniline, and 2-amino-3,5-diiodo-benzoic acid (59); iodine or bromine substituted phenols (60); hydroxybenzothiazole and hydroxybenzimidazole (61); and 2-mercapto-benzothiazole (62), are synergistic with Cu salts in improving the thermal and photostability of polyamides. Mixtures of Cu and Mn also exhibit a synergistic effect (63). Other metal stabilizers include Al, Co, and Ni (64). Manganese hexametaphosphate, and Al, Cr, Mn, and Cu salts of anthranilic and phenolic acids are also reported as UV stabilizers (64).

Organic phosphorous compounds (65), and phosphine or phosphite complexes of CuI (66) have been shown to afford protection against light. A mixture of an organic phosphite with manganese(II) acetate provides both thermal and UV protection, as does combination of a phosphorous compound (H_3PO_4, H_3PO_3, NaH_2PO_4 or Na_3PO_4), a halogen compound (NaBr, KBr, KI, etc.) and a copper compound such as copper(II) acetate (67).

CHAPTER IV

EXPERIMENTAL

A. Materials and Equipment

1. Materials. All materials were used as received, unless otherwise indicated.

a. Polymers and fibers used in the study.

Nylon 66 additive free chips (Dupont, Zytel Resin, NC101).

Nylon 66 additive free fibers (Dupont, bright filaments, 30 denier).

Nylon 66 additive free spunbonded nonwoven fabrics (Monsanto, 0.3 and 1.0 oz/yd^2).

Poly(methyl methacrylate) beads (Rohm and Hass, Plexiglas V811).

b. Chemicals used in the study.

Benzyl alcohol (Fisher Sci., ACS Certified).

Carbon tetrachloride (Fisher Sci., ACS Certified).

Cobalt (II) sulfate heptahydrate ($CoSO_4$ $7H_2O$, J. T. Baker, reagent grade).

Copper (I) chloride (CuCl, J. T. Baker, reagent grade).

Copper (II) sulfate pentahydrate ($CuSO_4$ $5H_2O$, J. T. Baker, reagent grade).

Dichlorodimethylsilane (Aldrich).

p-Dimethylaminobenzaldehyde, 99% (Fisher Sci., ACS Certified, m.p. 74^{o}C).

Ethanol (Fisher Sci., ACS Certified).

Ferric chloride (J. T. Baker, reagent grade).

Formic acid, 88% (Fisher Sci., ACS Certified).

Hydrochloric acid (Fisher Sci., ACS Certified).

Hydroxylamine hydrochloride, 99% (J. T. Baker, reagent grade).

Manganese (II) chloride, anhydrous ($MnCl_2$, J. T. Baker, reagent grade).

Methanol (Fisher Sci., ACS Certified).

Nickel sulfate heptahydrate ($NiSO_4$ $7H_2O$, J. T. Baker, reagent grade).

o-Nitrobenzaldehyde (Eastman Kodak, m.p. 42-44°C).

Phenolphthalein (Fisher Sci., ACS Certified).

Phosphoric acid (Fisher Sci., ACS Certified).

Potassium hydrogen phthalate (Fisher Sci., ACS Certified).

Potassium hydroxide (J. T. Baker, reagent grade).

2-Propanol (Fisher Sci., reagent grade).

Pyrrole (Aldrich).

Toluene (Fisher Sci., ACS Certified).

c. Miscellaneous materials used in the study.

Glass plate (1 1/4 x 6 in.) - Used for a sample holder during irradiation in the specially constructed UV apparatus.

Metal fabric holder (1.75 x 5 in., Atlas Type SL).

Pasteur pipettes (Fisher Sci.) - Used as droppers.

Pyrex filter - A 1 x 5 in. pyrex plate with 1/8 in. legs at each corner of the plate. The pyrex filter eliminates wavelengths less than 300 nm.

Teflon tape, 1/2 inch wide (Fisher Sci.).

2. Equipment.

Atlas weatherometer - A commonly used apparatus for exposing fibers and fabrics to UV light. A xenon arc lamp is used as the light source.

Cary 213 ultraviolet-visible spectrophotometer.

Fourier transform infrared spectrophotometer (Digilab, Model FTS-20C).

Hewlett-Packard mass spectrometer (Model 5980-A).

Mettler balance (Model P160).

Perkin-Elmer infrared grating spectrophotometer (Model 1330).

Ultraviolet chamber - A specially constructed apparatus for exposing samples to UV light. A Hanovia high pressure mercury vapor lamp is used as the light source. The lamp is mounted onto a piece of wood in order to vary its distance from the sample. Inside the wooden chamber, there is a water-cooled condenser whose interior contains a quartz tube in which the sample is placed. The sample container system is designed to run in the presence of air for photooxidation studies, or under vacuum in the absence of air for photolysis studies.

B. Exposure Procedures

1. Preparation of the Nylon 66 films used in the photo- and photooxidation studies. Nylon 66 additive free chips (20g) were stirred with 60 mL of 88% formic acid for 4 hours at 25°C and then, with the aid of a Gardner knife, was cast as a viscous solution onto a glass surface which had been previously reacted with dichlorodimethylsilane in order to facilitate the removal of the film. The film was allowed to air dry in the absence of light for 6 months prior to UV exposure. A similar procedure was used to prepare Nylon 66 films containing photostabilizing additives (CuCl or $MnCl_2$), except the wt:wt ratio of stabilizer to chips was 230 to 1. The average thickness of the prepared films was 2-4 mils.

2. Calibration of the light source (14).

a. Preparation of poly(methyl methacrylate) film containing the solid state actinometer, o-nitrobenzaldehyde. Poly(methyl methacrylate) beads (17.8g) were stirred in toluene (80 mL) at room temperature until a viscous solution was formed. Solid o-nitrobenzaldehyde was then added to the solution; stirring was continued for an additional hour. The solution was cast onto a glass surface (previously treated with 10% dichlorodimethylsilane dissolved in carbon tetrachloride) using a Gardner knife. After evaporation of the toluene for 8 hours at 25°C, an acrylic film containing 0.51 M o-nitrobenzaldehyde, and having an average thickness of 0.27 μm was obtained.

b. Calibration procedure. The schematic of the UV chamber used for the calibration of the light source is depicted in Figure 13. The Hanovia high pressure mercury vapor lamp was calibrated by first pouring a special aqueous solution of salts (5% $CoSO_4 \cdot 7H_2O$, 4% $CuSO_4 \cdot 5H_2O$, and 36% $NiSO_4 \cdot 7H_2O$) into the exterior of the quartz tube, so that the optimum bandpass filter was centered at 3200 Å (68). The salt solution was irradiated for one hour at a distance of 6.8 cm from the quartz tube center. The poly(methyl methacrylate) film containing the solid state actinometer, o-nitrobenzaldehyde, was then placed on a glass plate which was centered inside of the quartz tube, and irradiated until the substance in the film photoisomerized to o-nitrobenzoic acid. In order to avoid an induction time problem during initial irradiation of the film, aluminum foil was placed around the outer portion of the quartz container, and the lamp was left on for 10 minutes prior to UV exposure of the films. Photoisomerization of the solid state actinometer normally took 10 minutes of exposure time, and was monitored by the disappearance of the NO_2 peak at 1520 cm^{-1} in the infrared spectra of the acrylic film. At 3200 Å, this calibration method gave a value of 9.92×10^4 erg/cm^2 sec for the light intensity of the Hanovia high pressure mercury vapor lamp. Compared to the original intensity of 5.32×10^5 erg/cm^2 sec, at the same wavelength, the experimental value is 18.7% of the original light intensity and is in good agreement with the value of 20% which results after 10 hours of irradiation as described in the literature by the lamp's supplier (69).

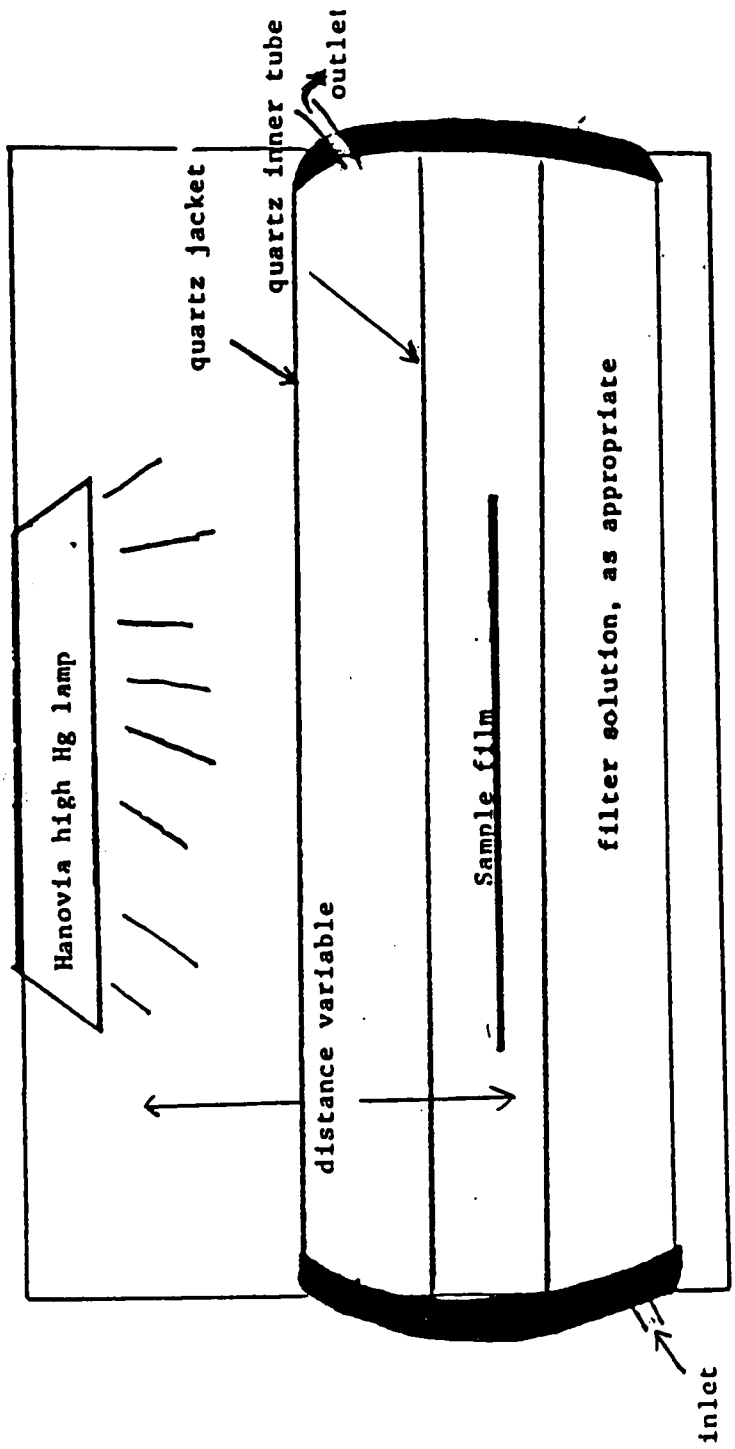

Figure 13. Schematic of the UV chamber used for photolysis and photooxidation.

3. Irradiation Procedures.

a. Procedure for photolyzing nylon samples in the specially constructed UV apparatus. The UV apparatus used in the photolysis study is depicted in Figure 14. Nylon 66 films, with and without photostabilizing additives, were prepared for exposure by placing them on a glass plate that slid into the quartz tube of the UV apparatus at a distance of 6.8 cm from the light source. The system was closed, and all glass joints were sealed with Teflon tape. A vacuum was pulled for 24 hours over the entire system, after which time stopcocks 1 and 4 were closed, and the pump turned off. Under vacuum, individual films were irradiated for 24, 48 and 96 hours with the calibrated Hanovia lamp. During irradiation, the quartz chamber was cooled by passing water through the condenser surrounding it, and the volatile products formed were trapped in a dry ice/isopropanol bath. After photolysis of the films was complete, stopcock 3 was closed, and the trap was then disconnected from the system for mass spectral analysis of the volatile products.

b. Procedure for photooxidizing nylon samples in the specially constructed UV apparatus. Nylon 66 films (with and without photostabilizing additives) and spunbonded nonwoven fabrics were placed on a glass plate that slid into the quartz tube of the UV apparatus at a distance of 6.8 cm from the lamp. Nylon filaments were prepared in a similar manner, but the continuous fibers were wrapped around the glass plate instead of being placed on it. A pyrex filter was placed above the samples in order to protect them from wavelengths less than 300 nm. Prior to irradiation, teflon tape was wrapped around the

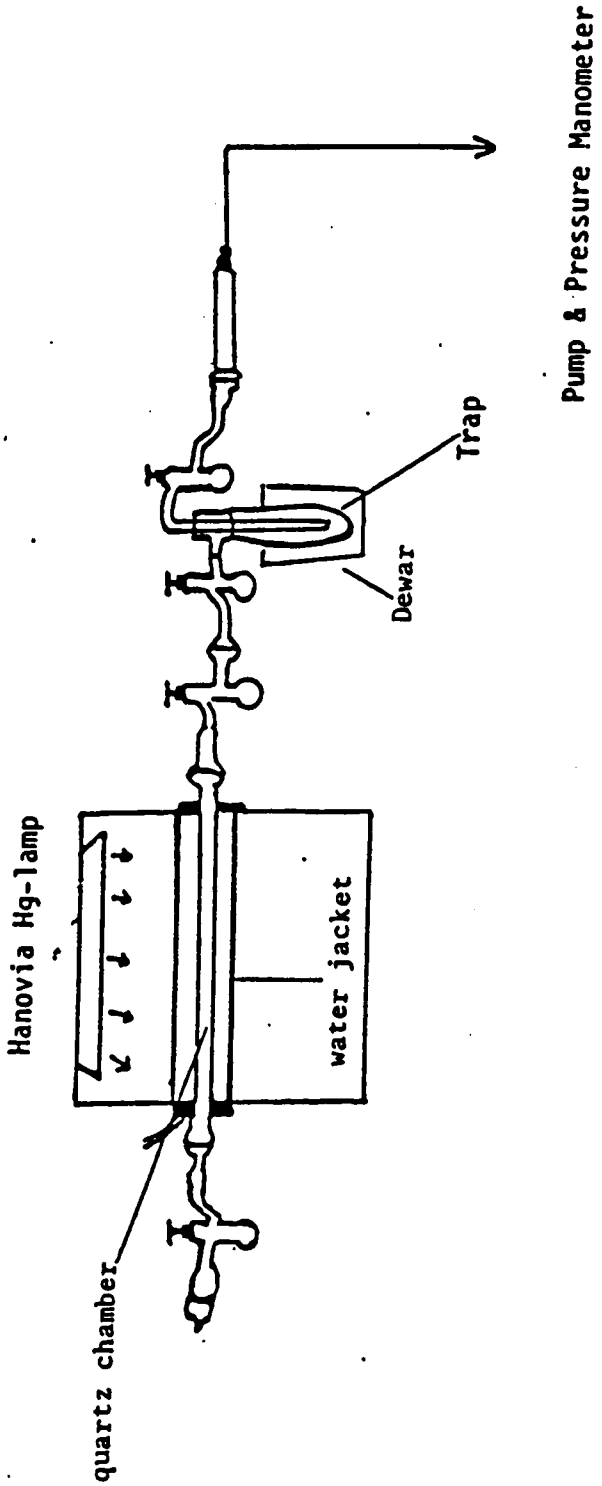

Figure 14. Ultraviolet exposure chamber.

glass joints, and a vacuum was pulled over the system for 24 hours to seal the joints and to remove any volatile products from previous exposures. Before the samples were actually exposed, air was allowed to flow through the system for one hour. After the system was closed, the nylon films, fibers and nonwoven webs were individually irradiated for 24, 48 and 96 hours in the UV chambers. During the photooxidation period, volatile products were trapped in a dry ice/isopropanol bath for mass spectral analysis.

c. Procedure for photooxidizing nylon samples in a Weatherometer (70). Nylon 66 fibers and nonwoven fabrics were first mounted onto metal holders that hooked directly onto a rotating rack in the Weatherometer. The samples were exposed to a xenon arc lamp for 48, 96, 144 and 195 hours (equivalent to 48-195 hours of noon sunlight) at 45^{o}C and 54% relative humidity. Borosilicate inner and soda lime outer filters (those recommended for simulation of exposure of materials for testing their lightfastness) were used during irradiation.

C. Spectrometric Analysis of Exposed and Unexposed Nylon 66 Samples.

1. Mass spectrometric analysis.

a. Analysis of the volatile products trapped in the specially designed UV apparatus. After photolysis or photooxidation of the nylon fibers (with and without photostabilizing additives), fabrics, and films, the gaseous products which had been collected in the trap of the specially constructed UV apparatus were analysed by direct introduction into an electron ionization type Hewlett-Packard mass

spectrometer. The ion source heater was set between 192-195°C, the gain was set at 3, and the ionization potential was kept constant at 70 eV. The direct probe heater was not used in the analysis of the volatile products.

b. Analysis of the exposed and unexposed nylon samples by solid-state mass spectrometry. Photolyzed, photooxidized, and unexposed nylon films (with and without photostabilizing additives), fibers, and nonwoven fabrics were analyzed (as previously described) in a mass spectrometer under the same conditions. The direct probe heater, however, was used for these solid samples. The nylon sample under investigation was first placed in a capillary tube and put in a nest holder that was subsequently placed in the insertion probe. After the system was pumped down, the insertion probe was pushed into the mass spectrometer, the direct probe heater was turned on, and data were collected. The direct probe begins to warm up at 27°C, and then increases to 79°C, 228°C, 330°C, and 380°C at retention times of 1, 2, 3, and 4 minutes, respectively. After four minutes, the direct probe heater was turned off.

2. Analysis by ultraviolet/visible spectroscopy. Photolyzed, photooxidized, and unexposed Nylon 66 films (with and without photostabilizing additives) were scanned in a Cary 213 ultraviolet/visible spectrophotometer by a differential technique. In order to obtain an autobaseline, a piece of the unexposed film was taped onto both the reference and sample metal frame holders, and then scanned between 200-500 nm, with the autobaseline setting turned on. The reference position was then kept constant while the corresponding

exposed films were run at the same wavelength range. The instrument settings were a) a balance of 6.0, b) an original gain of 3.0, c) a chart display setting of 10.0, d) a scan rate of 0.5 nm/sec, and e) a period of 1.0 sec.

3. Infrared spectroscopy of films exposed in the specially constructed UV apparatus. Photolyzed, photooxidized , and unexposed nylon films (without additives) were scanned in a Perkin-Elmer infrared grating spectrophotometer. Films under investigation were taped onto the sample holder while the corresponding unexposed films were taped onto the reference holder. The nylon samples were then scanned between 600 and 4000 cm^{-1}.

4. Fourier transform infrared spectroscopy (FTIR) of films exposed in the specially constructed UV apparatus. The FTIR of photolyzed and unexposed films (without additives) was attempted on a Digilab Fourier transform infrared spectrophotometer. The films under investigation were scanned between 600 and 4000 cm^{-1} in a similar manner as those scanned in the grating infrared spectrophotometer.

D. Chemical Analysis of Exposed and Unexposed Nylon 66 Samples.

1. Crosslinking studies of Nylon 66 films exposed in the specially constructed UV apparatus. The photolyzed, photooxidized, and unexposed films (with and without photostabilizing additives) were weighed (weight range 2.3 - 4.8 mg) and allowed to stand in 88% formic acid (10 mL) for three days at 25^{o}C. The insoluble part of the film (a gel), if remaining, was then placed on an evaporating dish, tilted to a 45^{o} angle, and the excess formic acid was removed with absorbent

paper prior to weighing. The gels were dried under vacuum for two days at 90°C and then reweighed to determine the soluble fraction of the original sample. The degree of swelling was computed in order to determine the relative amounts of crosslinking in the films.

2. Carboxyl end group analysis of photooxidized Nylon 66 samples (71). Analysis for carboxyl end groups was performed on Nylon 66 films (with and without photostabilizing additives), fibers, and nonwoven fabrics that had been photooxidized in the weatherometer and in the specially designed UV chambers. The samples were first dissolved in freshly distilled benzyl alcohol with heating at 155°C. Since distillation and heating of the alcohol resulted in slightly acidic products, a correction obtained by heating the alcohol for the same amount of time as the alcohol/nylon solution was required for all titrations. A 0.0585 N solution of potassium hydroxide dissolved in a mixture of 10% methanol and 90% benzyl alcohol was used as the titrant. Potassium hydrogen phthalate was used to standardize the base, and phenolphthalein (0.05%) dissolved in benzyl alcohol was used as the indicator.

3. Determination of imide groups formed in the photooxidized Nylon 66 samples (72).

a. Preparation of the reagent solution. The presence of imide groups could be determined by their conversion to colored iron (III) hydroxamate in the presence of ferric chloride and hydroxylamine hydrochloride. The hydroxylamine hydrochloride/ferric chloride reagent solution was prepared by first acidifying a 0.5% ferric chloride/ethanol solution with a few drops of concentrated

hydrochloric acid, and then saturating the solution with hydroxylamine hydrochloride. The mixture was stirred and warmed at 40°C for thirty minutes before its use.

b. Treatment of nylon samples with the reagent solution. Nylon 66 samples that had been photooxidized in the weatherometer and the specially designed UV apparatus were treated with the freshly prepared ferric chloride/hydroxylamine reagent solution. Unexposed and photooxidized films (0.003 g), fibers (0.003 g), and nonwoven fabrics (0.1 g) were dissolved with two drops of 88% formic acid in a micro test tube, and two drops of the reagent solution were added. The mixture was evaporated to dryness over a micro flame, after which a few drops of water was added. In the presence of imides, a violet or pink color was formed according to the amount of imide present.

4. Detection of pyrroles in the photooxidized Nylon 66 samples (28).

a. Preparation of the reagent (Ehrlich reagent) used to detect pyrroles. The Ehrlich reagent was prepared by dissolving p-dimethyl-aminobenzaldehyde (1.0 g) in a mixture of 88% formic acid (75 mL) and concentrated phosphoric acid (25 mL). This reagent is light sensitive and must be stored in a dark bottle.

b. Treatment of Nylon 66 with the Ehrlich reagent. The Ehrlich test for pyrroles was performed on Nylon 66 films (with and without photostabilizing additives), fibers, and nonwoven fabrics that had been photooxidized in either the Weatherometer or the specially designed UV apparatus. In the absence of light, 0.003-0.004 g of the exposed and unexposed films, wetted with one drop of phosphoric acid,

were treated with four drops of Ehrlich reagent. As controls, 7.0 x 10^{-3}M, 7.0 x 10^{-6}M, 7.0 x 10^{-9}M, and 7.0 x 10^{-12}M pyrrole/formic acid were also treated with the reagent. The treated samples were allowed to sit in the dark for twenty minutes, and were then examined for color changes. A positive test is indicated by the formation of a deep red color.

E. Tensile Properties of Exposed and Unexposed Nylon 66 Samples.

The photooxidized (exposed in the Weatherometer and UV chamber), and unexposed fibers and nonwoven fabrics were evaluated for their tensile strength, % elongation, and energy-to-rupture, using an Instron (table model). The tensile properties of single fibers, obtained from a filament bundle, were measured using a Cell A on the Instron at a full scale load of 10.0 g. The crosshead and chart speeds were set at 0.2 and 5.0 in/min, respectively. The mechanical properties of the nonwoven fabrics were obtained in a similar manner, except a Cell B on the Instron at a full scale load of 5,000 g was used, and both the crosshead and chart speeds were 5.0 in/min.

CHAPTER V

RESULTS AND DISCUSSION

Even though much research concerning the photo- and photo-oxidative degradation of polyamides has been conducted, many uncertainties still remain. This study, therefore, was directed toward elucidating the mechanism by which UV light degrades polyamides. In order to obtain additional information on the photolytic and photooxidative process, Nylon 66 films (with and without photostabilizing additives) that had been exposed for 24 or 48 hours to a high pressure mercury lamp, either under vacuum (at wavelengths greater than 300 nm) or in the presence of air (at wavelengths less than 300 nm), were analyzed by UV-VIS, and gaseous and solid state mass spectrometry. Fibers and spunbonded nonwoven fabrics which had been photooxidized with a xenon arc source (at 54% relative humidity and 45^{o}C) were also analyzed by solid state mass spectrometry. Conventional infrared spectroscopy was also attempted on the photolyzed and photooxidized films, but the films were too thick to obtain any direct distinct absorbances. Because of this, surface reflectance (ATR) Fourier Transform (FTIR) spectroscopy was performed on the photolyzed films to detect chemical changes that might have occurred on the surface of the film. There were no changes in the position of the peaks which occurred in the FTIR spectra of the exposed versus unexposed films. There were, however, changes in the intensity of the peaks. In general, the intensity of the peaks occurring in the FTIR of the photolyzed films decreased during UV

exposure. Since chemical changes could not be detected by FTIR, the photooxidized films were not analyzed by this method.

Chemical analysis (for carboxyl end groups, imides and pyrroles) were also performed on the photooxidized samples. A crosslinking study was carried out on the photolyzed, photooxidized, and unexposed films. The data generated from these chemical and spectroscopic techniques were combined with data from the literature, and the photolytic and photooxidative degradation mechanism(s) were proposed. To demonstrate the loss in strength that occurs upon irradiation, the breaking strength, % elongation at break, and energy-of-rupture were determined on the photooxidized and unexposed fibers and spunbonded fabrics. The results of these chemical tests, spectroscopic analyses, mechanical tests will be discussed in the following sections.

A. Chemical Analysis of the Photolyzed and Photooxidized Nylon 66 Samples

1. Crosslinking studies of photolyzed and photooxidized Nylon 66 films. The solubility and swelling of Nylon 66 films (with and without photostabilizing additives) that had been photolyzed and photooxidized by a high pressure mercury arc were examined. Unexposed and photooxidized Nylon 66 films were found to dissolve in formic acid almost immediately. After photolysis (UV exposure under vacuum), however, the films became insoluble due to extensive crosslinking. Table 1 shows gel data of Nylon 66 films (with and without CuCl or $MnCl_2$) that had been photolyzed for 24 or 48 hours.

Table 1. Gel data of photolyzed Nylon 66 films.

Additive	Photolysis Time (hr)	Orig. wt. (mg)	Wt. of Solvent & Gel (mg)	Wt. of Dried Gel (mg)	Ratio of Swell. Solv. to Gel (wt.)	%Gel
CuCl	24	2.9	74.7	1.4	52	48
$MnCl_2$	24	4.8	109.8	3.7	28	77
$MnCl_2$	48	3.7	81.7	2.8	28	76
None	24	3.3	49.7	2.7	17	82
None	48	2.5	47.7	2.2	21	88

The ratio of swelling solvent to gel (degree of swelling) was used to qualitatively measure the crosslink density. Systems which have the lowest degree of swelling have the greatest crosslink density. The weight of the solvent and gel is subject to experimental error in its measurement. Nevertheless, the crosslink density appears to be greatest for photolyzed films without additives, somewhat less for films containing $MnCl_2$, and the least for films with CuCl. For Nylon 66 films without additives, the amount of gel increased with time of irradiation. The degree of crosslinking for Nylon 66 (without additives) is in agreement with earlier studies by Stevenson and workers (18), who observed about 70% gel after 100 hours of exposure (at a distance of 24 cm from the light source) under vacuum. The

crosslinking observed in photolyzed Nylon 66 films is believed by most researchers to be due to the coupling of two $-CH_2-\dot{C}H-NH-CO-CH_2-$ radicals.

2. Detection of pyrroles in the photooxidized nylon samples. Earlier studies by Marek and Lerch (25) indicated the formation of pyrroles, presumably from succinaldehyde and ammonia, in the photooxidation of Nylon 66 fabrics. The Ehrlich test for pyrroles was performed on Nylon 66 films (with and without photostabilizing additives), fibers and nonwoven fabrics. The presence of pyrroles is indicated by a dark red color for high concentrations and a lighter red for diluted samples. As controls, 7.0×10^{-3}, 7.0×10^{-6}, 7.0×10^{-9}, and 7.0×10^{-12} Molar concentrations of pyrrole/formic acid were reacted with the Ehrlich reagent and a positive test was obtained for each sample up to 7.0×10^{-9}M. This test, therefore, will detect pyrroles having a concentration of about 1.0×10^{-10}M (a pale yellowish-red color was observed). The test results (for pyrrole) in all of the photooxidized and unexposed nylon samples were negative. This indicates, therefore, the improbability of pyrrole or its derivatives as photooxidation products.

3. Test for imides in the photooxidized Nylon 66 films and fibers (19). The test for imides was performed on Nylon 66 films and fibers photooxidized in the UV chamber (high pressure mercury arc), and on Nylon 66 films (with and without $MnCl_2$ or CuCl), fibers and nonwoven fabrics which had been photooxidized in the Weatherometer. Imide groups react directly with hydroxylamine to give hydroxamic acid.

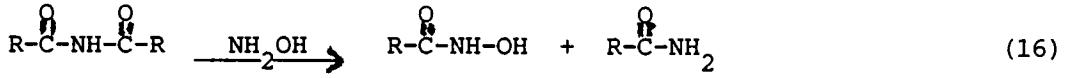

(16)

If $FeCl_3$ is present as the above reaction occurs, the colored iron III hydroxamate is formed. A violet or pink color is formed according to the amount of imide present. Table 2 shows that some of the fibers, films and nonwoven fabrics gave at least moderatly positive tests for the presence of imide groups. In general, a higher concentration of imides was detected in the nylon samples exposed in the Weatherometer (54% relative humidity, 45°C). Nylon films containing $MnCl_2$ which were exposed in the Weatherometer gave similar results as Nylon 66 without additives, except a lower concentration was observed. Photooxidized films containing CuCl, on the other hand, gave negative imide tests. The additive CuCl, therefore, appears to suppress the formation of imides.

4. Carboxyl end group analysis of photooxidized Nylon 66 films, fibers and nonwoven fabrics (71). Titration of the carboxyl groups present in Nylon 66 proved to be extremely useful in obtaining additional information on the photooxidative degradation mechanism of aliphatic polyamides. The carboxyl end group analysis of Nylon 66 films, fibers and nonwoven fabrics, that had been exposed by either a high pressure mercury lamp or xenon arc (Weatherometer), can be seen in Table 3. In general, the carboxyl concentration of the photooxidized nylon samples increased from 24 to 48 or 96 hours of exposure, but then decreased after further irradiation. This seems to suggest that during the photooxidation process, carboxyl end groups are formed and upon further irradiation, decarboxylation or

Table 2. Results of the imide tests performed on photooxidized Nylon 66.

Nylon Sample	Exposure time (hr)	Exposure source (a)	Results of Imide Test
Fibers	0	Mercury lamp	-
	48		+
	96		-
Film	0	Mercury lamp	-
	48		+
	96		-
Film	0	Weatherometer	-
	48		-
	96		+
	144		++
Film/$MnCl_2$	0	Weatherometer	-
	48		-
	96		+
	144		+
Film/CuCl	0	Weatherometer	-
	48		-
	96		-
	144		-
Fibers	0	Weatherometer	-
	48		+
	96		-
	147		++
	195		+
Nonwoven fabrics	0	Weatherometer	-
	48		-
	96		+

(a) At 54% RH and 45°C in the Weatherometer.

- = Negative; white color.

+ = Positive, but very low concentration; pinkish white color.

++ = Positive; pinkish white color.

Table 3. Carboxyl end group analysis of photooxidized Nylon 66 films, fibers, and nonwoven fabrics.

Nylon Sample	Exposure time (hr)	Exposure source (a)	Meq. COOH/ g Ny 66	x-y (b)
Film	0	None	4.31	0.00
	24	Mercury lamp	4.50	0.19
	24	Weatherometer	8.17	3.51
	48	Mercury lamp	5.48	1.17
	48	Weatherometer	12.83	8.17
	96	Mercury lamp	9.01	4.70
	96	Weatherometer	8.17	3.51
	144	Weatherometer	5.83	1.17
Fibers	0	None	4.78	0.00
	48	Mercury lamp	5.98	1.20
	48	Weatherometer	10.37	5.59
	96	Mercury lamp	9.97	5.19
	96	Weatherometer	5.58	0.80
	147	Weatherometer	4.78	0.00
	195	Weatherometer	4.39	-0.39
Nonwoven Fabric (c)	0	None	4.37	0.00
	48	Weatherometer	6.13	1.40
	96	Weatherometer	7.00	2.28

(a) At 54% RH and 45°C in the Weatherometer.

(b) x-y = [meq COOH/g irradiated nylon]-[meq COOH/g nonirradiated nylon].

(c) wt. of 1 oz./yd^2.

decarbonylation occurs. Samples exposed in the Weatherometer obtained a maximum number of end groups much quicker than those exposed to the mercury vapor lamp. This is probably due to the moisture (54% relative humidity) in the air which may have aided in the formation of the carboxylic acid by free radical processes, as well as by conventional hydrolysis.

$$-CH_2-CH_2-\overset{O}{\overset{\|}{C}}-NH-CH_2- \xrightarrow{H_2O} -CH_2-CH_2-\overset{O}{\overset{\|}{C}}-OH + H_2N-CH_2-CH_2- \quad (17)$$

Tables 4 and 5 show the results of the carboxyl end group analysis of Nylon 66 films containing CuCl or $MnCl_2$ that were photooxidized by either a high pressure mercury lamp, or a xenon arc (in the Weatherometer). Films containing $MnCl_2$ seem to undergo a similar photooxidation mechanism as Nylon 66 without additives, except the increase in carboxyl concentration after irradiation is small. A different mechanism seems to be occurring for nylon films containing CuCl since there was no increase in carboxyl concentration upon photooxidation. In fact, upon irradiation of the Nylon 66/CuCl film, the carboxyl groups decreased with increase in irradiation time.

B. Spectroscopic Analysis of the Photolyzed and Photooxidized Nylon 66 Samples.

1. Analysis of the photolyzed and photooxidized samples by UV-VIS spectrometry.

a. Analysis of the photolyzed films by UV-VIS spectrometry. Ultraviolet spectroscopy seems to be a useful analytical tool for

Table 4. Carboxyl end group analysis of Nylon 66 films containing CuCl or $MnCl_2$ which were photooxidized by a High Pressure Mercury Arc.

Additives in Films	Exposure time (hr)	Meq. COOH/ g Ny 66	x-y (a)
$MnCl_2$	0	4.31	0.00
	24	4.11	-0.20
	48	4.70	0.39
	96	4.70	0.39
CuCl	0	4.50	0.00
	24	3.92	-0.59
	48	3.92	-0.59
	96	3.92	-0.59

(a) x-y = [meq COOH/g irradiated nylon]-[meq COOH/g nonirradiated nylon].

Table 5. Carboxyl end group analysis of Nylon 66 films containing CuCl or $MnCl_2$ which were photooxidized in the Weatherometer (a).

Additives in Films	Exposure time (hr)	Meq. COOH/ g Ny 66	x-y (b)
$MnCl_2$	0	4.66	0.00
	24	5.83	1.17
	48	7.00	2.34
	96	5.83	1.17
	144	5.83	1.17
CuCl	0	4.66	0.00
	24	3.50	-1.16
	48	2.33	-2.33
	96	2.33	-2.33
	144	3.50	-1.16

(a) At 54% RH and 45°C.

(b) x-y = [meq COOH/g irradiated nylon]-[meq COOH/g nonirradiated nylon].

obtaining additional information on the photodegradation of Nylon 66. Even though it is difficult to extract a great deal of information from a UV spectrum, generalizations can still be formulated. From the UV spectra of Nylon 66 films (with and without photostabilizing additives) that had been photolyzed for 24 and 48 hours, a maximum absorption at 290 nm and a secondary absorption around 250 nm was observed (Table 6). The unexposed films did not exhibit any absorption between 200 and 500 nm. In general, bands of high intensity which appear above 210 nm represent α, β- or α, β, γ, δ-unsaturated carbonyl compounds, or a diene or polyene. For all of these absorbing species, the longer the length of the conjugated system, the longer the observed wavelength will be. For photolyzed Nylon 66 it is unlikely that a diene or polyene structure is responsible for the absorptions at 254 and 290, since at least 3 to 4 extended double bonds are required to obtain these wavelengths. It is possible, however, that the observed wavelengths at 254 and 290 represent α, β- or α, β, γ, δ-unsaturated carbonyl compounds. The conjugation of a double bond with a carbonyl group leads to intense absorption corresponding to a $\pi \rightarrow \pi^*$ transition of the carbonyl group. In simple α, β-unsaturated carbonyl compounds, the absorption is usually observed between 220 and 255 nm. The $\pi \rightarrow \pi^*$ transition is affected in a predictable manner by structural changes of the chromophore (absorbing species). Woodward and Nielsen (73) examined the ultraviolet spectra of a large number of α, β-unsaturated carbonyl compounds and devised a set of empirical rules which allow for the prediction of the wavelength at which the $\pi \rightarrow \pi^*$ transition will

Table 6. UV spectra of photolyzed Nylon 66 films.

Additive	Irrad. Time (hr)	Maximum Absorption		Secondary Absorption	
		Wavelength (nm)	Absorption	Wavelength (nm)	Absorption
None	0	-	-	-	-
None	24	290	[1.33]	248	[1.19]
None	48	288/292	1.9	250/254	1.20
$MnCl_2$	0	-	-	-	-
$MnCl_2$	24	280/293	[0.66]	242/248	[0.75]
$MnCl_2$	48	286/294	1.54	251	1.43
CuCl	0	-	-	-	-
CuCl	24	294	[0.79]	252/270	[0.6 - 0.7]

occur in unknown α, β-unsaturated carbonyl compounds. Their rules can be seen in Tables 7 through 9. Table 10 compares the wavelengths (either observed or calculated) of several α, β- and α, β, γ, δ- -unsaturated carbonyl compounds. Undoubtedly, it would be extremely difficult to pinpoint the exact unsaturated carbonyl compounds responsible for the absorptions at 254 and 290 in photolyzed Nylon 66.

In addition to these structural changes that occur during the photolysis of Nylon 66, generally speaking, it seems that photostabilizing additives such as CuCl and $MnCl_2$ reduce the formation of the unsaturated carbonyl compounds. Also, it appears at a first glance that the intensities of the absorption bands at 254 and 290 increase during photolysis, but from mass spectral examination of the photolyzed films, it was found that oxygen was present in all films irradiated for 24 hours under vacuum (even though only a very small amount was detected in the volatile fractions). Therefore what appears to be an increase in intensity due to irradiation, may actually be due to differences in the amount of oxygen during exposure.

b. Analysis of the photooxidized films by UV-VIS spectrometry. The UV data for the 24, 48 and 96 hour photooxidized films (with and without $MnCl_2$) can be seen in Table 11. The unexposed films did not exhibit any absorption between 200 and 500 nm. For films without the photostabilizing additive $MnCl_2$, an absorption centered around 255 nm was observed, and its intensity increased with longer exposure times. The incorporation of additives (such as $MnCl_2$) in the Nylon 66 films decreases the formation of the absorbing species responsible for this

Table 7. The rules for enones

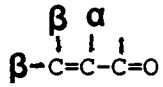

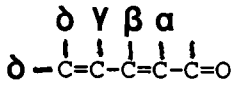

Base values:			
6-Membered ring or acyclic parent enone			215 nm
5-Membered ring parent enone			202
Acyclic dienone			245
Increments for:			
Double bond extending conjugation			30
Alkyl group or ring residue		α	10
		β	12
	γ and higher		18
Polar groupings:			
	-OH	α	35
		β	30
		δ	50
	$-OCOCH_3$	α, β, δ	6
	$-OCH_3$	α	35
		β	30
		γ	17
	-Cl	α	15
		β	12
	-Br	α	25
		β	30
	$-NR_2$	β	95
Exocyclic double bond			5
Homocyclic diene component			39
Solvent correction			variable
			———
λ_{max} EtOH (calc) = Total			

Table 8. The rules for α, β-unsaturated aldehydes.

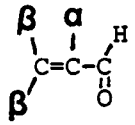

PARENT	208 nm
With α or β alkyl groups	220
With α, β or β, β alkyl groups	230
With α, β, β alkyl groups	242

Table 9. The rules for α, β -unsaturated acids and esters.

Base values for:

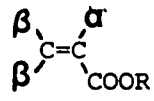

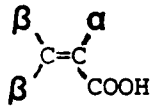

With α or β alkyl group	208 nm.
With α, β or β, β alkyl groups	217
With α, β, β alkyl groups	225
For an exocyclic α, β double bond	add 5 nm
For an endocyclic α, β double bond in a 5- or 7-membered ring	add 5 nm

Table 10. The calculated or observed maximum wavelengths of several α, β-unsaturated carbonyl compounds.

α, β-unsaturated carbonyl compounds	Maximum Wavelengths
Enones	
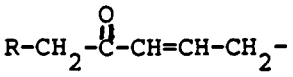	Calculated λ_{max} = 227
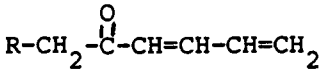	Calculated λ_{max} = 245
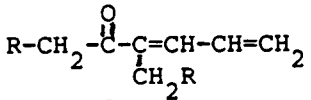	Calculated λ_{max} = 255
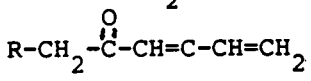	Calculated λ_{max} = 257
α, β-unsaturated Aldehydes	
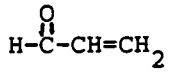	Calculated λ_{max} = 206
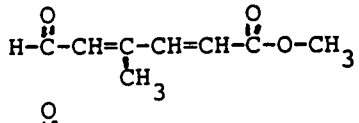	Calculated λ_{max} = 272
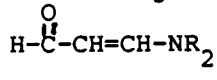	Calculated λ_{max} = 300
α, β-unsaturated Acids	
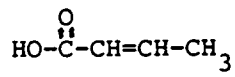	Observed λ_{max} = 205
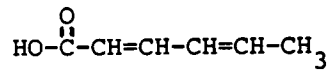	Observed λ_{max} = 254
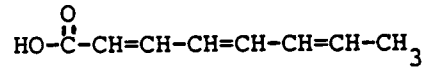	Observed λ_{max} = 294

Table 11. UV spectra of photooxidized Nylon 66 films.

Additive	Irrad. Time (hr)	Maximum Absorption	
		Wavelength (nm)	Absorption
None	0	-	-
None	24	253/256	0.16
None	48	255/257	0.54
None	96	255/257	1.00
$MnCl_2$	0	-	-
$MnCl_2$	24	242/248	0.12
$MnCl_2$	48	246	0.40
$MnCl_2$	96	242	0.32

absorption. As in the photolyzed films, the absorption at 255 nm could also represent an α,β-unsaturated carbonyl compound. It is interesting to note that the photooxidized films do not exhibit any absorption at 290 nm. This is contradictory to earlier work done by Ford (38) and Allen (36) where they observed a band at 290 nm in their photooxidized films. This is, however, in agreement with the earlier photolysis studies done by this author, where oxygen was detected in the 24 hour exposed films. Recall that the presence of a small amount of oxygen during photolysis of films seemed to lower the intensity of the band at 290. When the films were irradiated in the diliberate presence of high concentrations of oxygen, there was no peak at 290 nm.

2. Analysis of the photolyzed and photooxidized samples by mass spectroscopy. In a mass spectrometer, molecules are subjected to bombardment by a stream of high energy electrons, converting some of the molecules to ions (74). The ions are accelerated in an electric field and separated according to their mass-to-charge (m/e) ratio in a magnetic or electric field. The ions with a particular m/e ratio are detected by a device which counts the number of ions that strike it. The detector output is amplified and then fed to a recorder which traces a mass spectra (a graph of the amount of particles detected (% Abundance)) as a function of the m/e ratio. Samples studied by mass spectrometry may be gases, liquids or solids. Before the ions can be formed, some method must be used to convert the sample to the vapor state in order to obtain a stream of molecules flowing into the ionization chamber. For gases, the substance is already vaporized and

therefore the gaseous sample is directly introduced into the ionization chamber (gas phase mass spectrometry). For less volatile materials, the sample is heated to provide a greater vapor pressure and the volatilized material is then ionized. With non-volatile solids, a direct probe method of introducing the sample is used (solid state mass spectrometry). The solid is placed in the probe which is then inserted through a vacuum lock into the ionization chamber. The probe is heated, and vapor from the solid sample is evolved in close proximity to the stream of high energy electrons. Solid state mass spectrometry can be used to study molecules or macromolecules with vapor pressures lower than 10^{-9} mm Hg at room temperature (74).

Photolyzed Nylon 66 films (with and without photostabilizers) and fibers were analyzed by both gas phase and solid state mass spectrometry. In the solid state m/e determinations, a graph of retention times versus the fragmentation temperature for each of the photolyzed and photooxidized samples indicated that the slopes were similar at retention times less than 1.6 minutes. The mass spectra of the exposed and unexposed Nylon 66 samples were therefore compared at retention times less than 1.6 minutes. Also, in order to insure that formic acid (the solvent used to prepare Nylon 66 films) was not trapped in the films, a series of mass spectra of Nylon 66 films, with and without formic acid, were examined at early retention times. Mass spectral results are discussed in the following pages.

a. Mass spectral analysis of controls with and without formic acid. Table 12 demonstrates that Nylon 66 films which were cast from formic acid and then dried properly did not produce solvent related m/e fragmentations that would interfere in the mass spectral interpretation of the irradiated films. From the mass spectra (at early retention times) of Nylon 66 which had been cast from formic acid and not allowed to dry, the m/e peaks 18, 28, 29, 44, 45 and 46 were observed (Appendix Figure B.1). These fragmentations are the same as those observed by Happ and Stewart (75) in their mass spectral study of formic acid. The m/e fragmentations observed from the mass spectra of improperly dried films can therefore be attributed to: H_2O (18), CO (28), HCO (29), CO_2 (44), COOH (45) and HCOOH (46). When Nylon 66 films were dried under vacuum at 90°C for two days, formic acid was not detected in the films; i.e., the m/e fragmentations 29, 45 and 46 were not observed (Figure B.2). The m/e peaks 18, 28 and 44 were present, but these fragmentations could be attributed to the thermal degradation of the nylon. Since heating of the samples before exposure could interfere with the mass spectral interpretation of the photodegraded samples, the films used in this study were air dried in the absence of light, for 6 months prior to irradiation. The mass spectra of the air dried films had the same m/e fragmentations as the heat dried samples, except the peaks appeared at a much longer retention time and therefore would not interfere with the mass spectral interpretation of the photodegraded films (Figures B.3 and B.4). Analysis of the photolyzed and photooxidized Nylon 66 samples by mass spectrometry will be discussed in the following sections.

Table 12. The m/e abundances of formic acid and Nylon 66 films cast from formic acid.

m/e	Relative Abundance HCOOH (a)	Nylon 66 HCOOH	Nylon 66 Dried (b)	Nylon 66 (c)
18	26	+	+	+
28	83	+	+	+
29	100	+	-	+
44	91	+	+	+
45	46	+	-	-
46	57	+	-	-

(a) Happ, G. P.; Stewart, D. W. J. Am. Chem. Soc. **1952**, 74, 4440.

(b) Nylon 66 dried under vacuum at 90°C for two days.

(c) Nylon 66 air dried in the absence of light for 6 months.

b. Analysis of photolyzed Nylon 66 films by mass spectrometry of gaseous and solid state products. The m/e fragmentations and % abundance obtained from the solid state mass spectra of the photolyzed and unexposed Nylon 66 films (with and without $MnCl_2$ or CuCl) may be observed at early retention times in Appendix Tables A.1, A.2, A.3, and A.8 through A.13, while those obtained from the mass spectra of the volatile photolysis products can be seen in Tables A.5 through A.7. Also, the gaseous and solid state mass spectra of the unexposed and photolyzed films (with and without additives) can be seen in Figures B.3 through B.6, and B.8 through B.20. The mass spectra of the volatile fractions evolved during photolysis contained m/e 18 and 17 which is due to H_2O and HO• that forms from traces of water remaining in the amorphous regions of the nylon. The most abundant fragment, m/e 28, is most likely due to CO and $CH_2{=}CH_2$. Ethylene (m/e 28) could be formed by disproportionation reactions from almost any alkyl radical.

$$R\text{-}CH_2\text{-}\dot{C}H_2 \longrightarrow R\bullet + CH_2{=}CH_2 \qquad (18)$$

Another major peak, m/e 44, could be due to CO_2 which may be formed if H_2O or O_2 were accidently present during photolysis, (Figure 15). There are several alternative explanations for the appearance of m/e 44 but these will be discussed later. Other fragmentations (m/e 29, 30, 31, 43, 44, 45, 48, and 59) will be discussed along with the mass spectral results of the photolyzed films.

Examination of the mass spectra for the 24 hour photolyzed films (with and without additives) indicated that oxygen (m/e 32) was

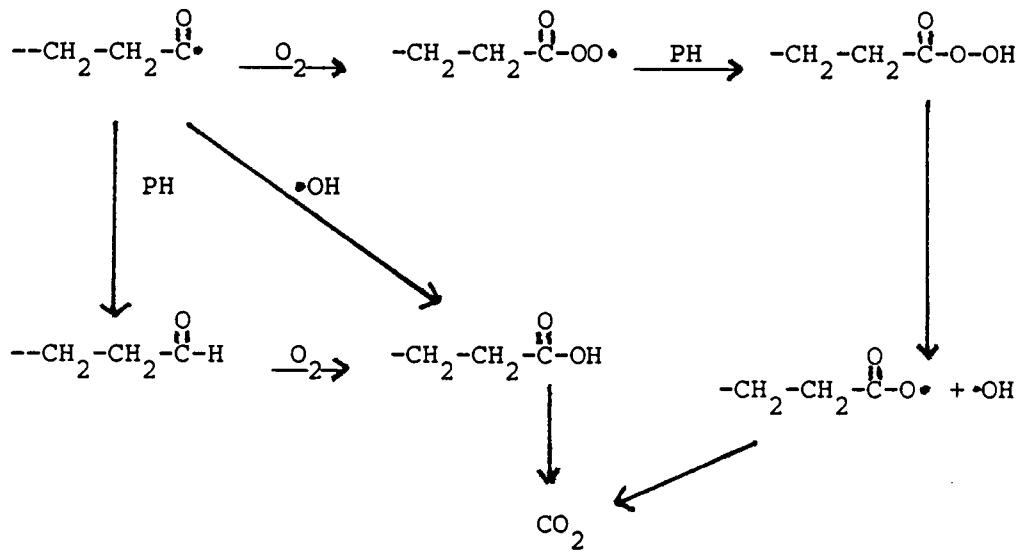

Figure 15. Possible pathways to the formation of CO_2 evolved during either photolysis or photooxidation.

trapped in the films, even though none was detected in the volatile fragments. Because of this, the mass spectral data obtained from the films which had been photolyzed for 48 hours was used to determine the photolysis mechanism which is depicted in Figures 16 and 17.

Homolytic scission at the amide linkage (Figure 16, pathway a) seems to be the dominant process to account for the evolved CO and ethylene gases (m/e 28) detected by mass spectrometry (Figure 16, pathway b). In addition to these cleavage reactions, the acyl radical can also abstract a hydrogen atom from an adjacent polymer chain resulting in the long chain aldehyde, solid A'. The mass spectral assignment of solid A' and other possible photodegradation products may be seen in Figure 18. Long chain aliphatic aldehydes should give fragments of m/e 44 (which is attributed to acetaldehyde and its tautomer) and, in this case, m/e 41 as a result of the McLafferty rearrangement (76).

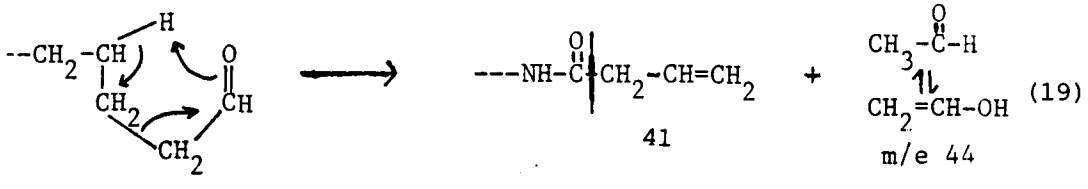

(19)

Both fragmentations occur in the mass spectra of the photolyzed films and therefore long chain aliphatic aldehydes like solid A' are possibly produced during the photolysis process. It is believed that this particular aldehyde (solid A') also leads to the formation of the α,β-unsaturated aldehyde (solid B'). The m/e fragmentations 43, 57, 69, 83, 97, 111, and 125 are consistent with solid B' and are observed at a retention time of 2.0 minutes in the mass spectra of the 48 hour

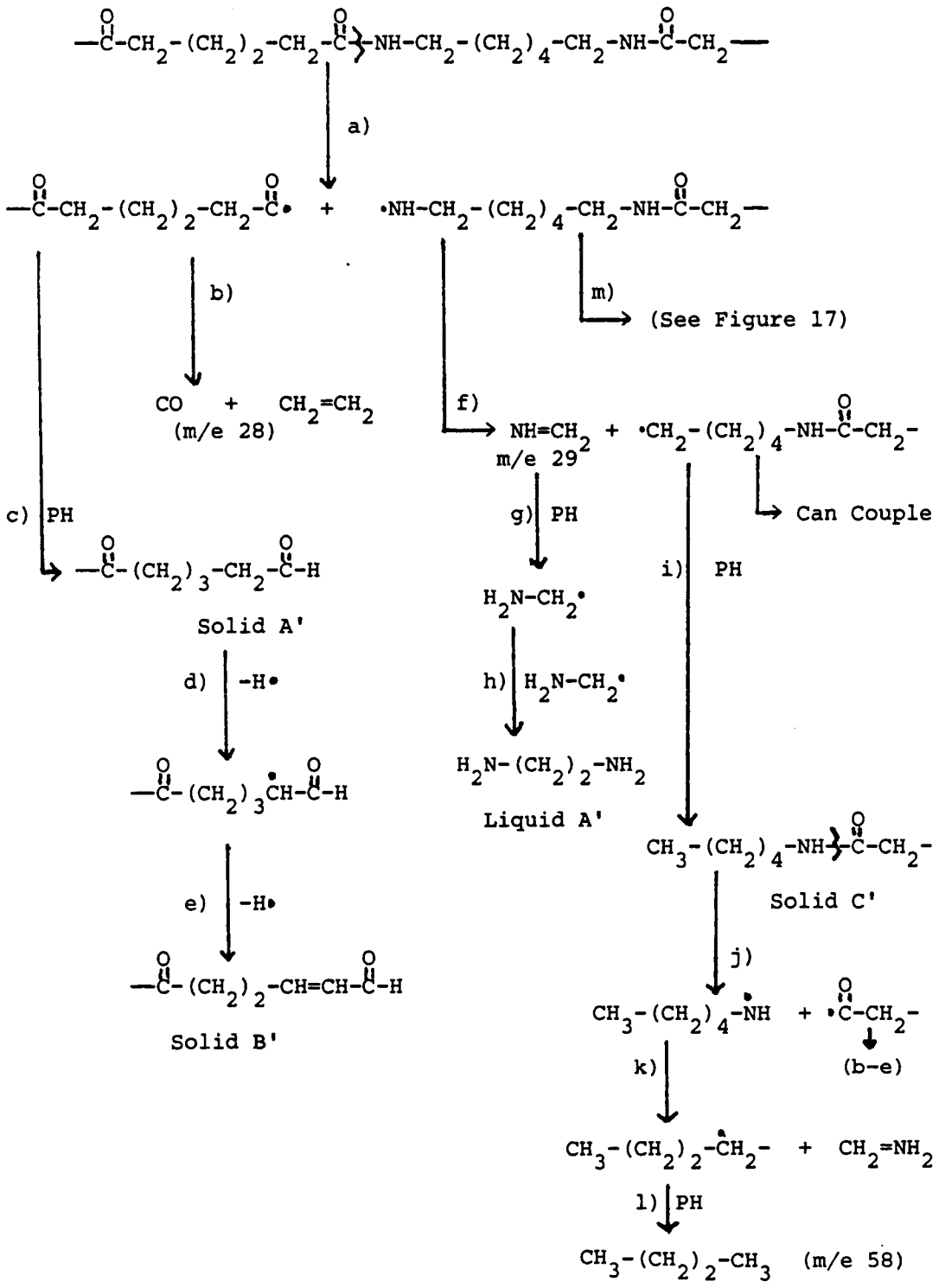

Figure 16. Photolysis mechanism; homolytic chain scission resulting in volatile and liquid products, and solid residues; A', B', and C'.

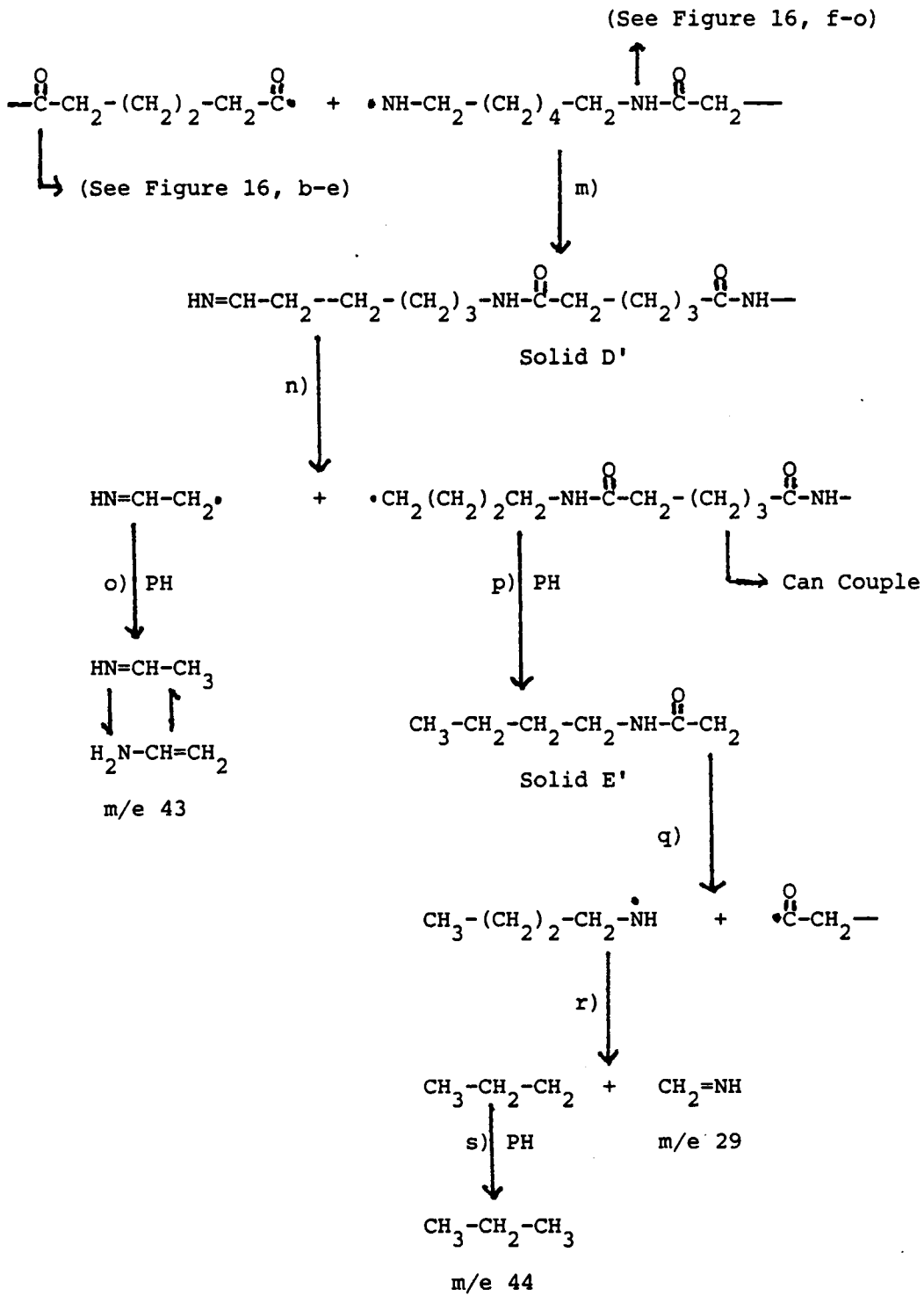

Figure 17. Photolysis mechanism; homolytic chain scission resulting in volatile and liquid products, and solid residues; D' and E'.

Solid A' :

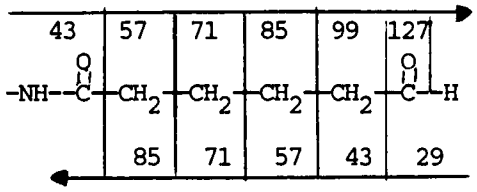

Other Fragmentations of Solid A'

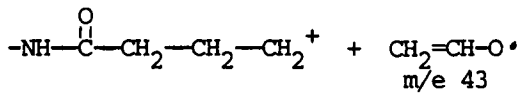

McLafferty Rearrangement of Solid A'

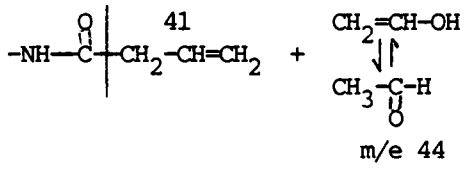

Solid B' :

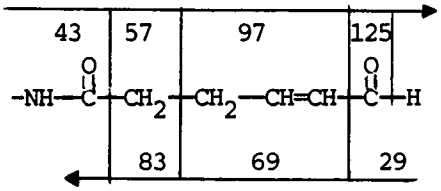

Solid C' :

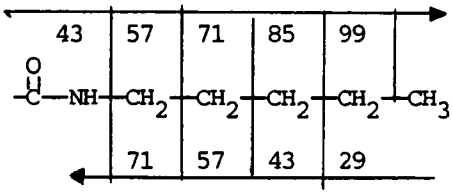

Figure 18. Mass spectral assignments of the volatile and liquid products, and solid residue possibly formed during the photolysis of Nylon 66.

Solid D' :

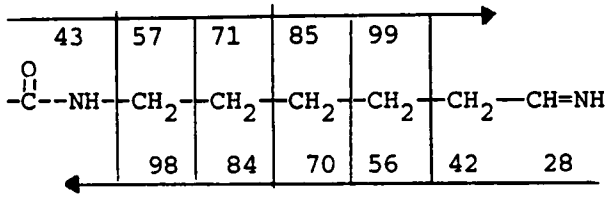

(no m/e 42, in solid MS)

Solid E' :

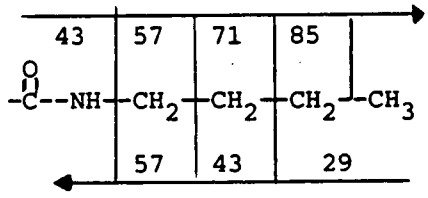

Liquid A' :

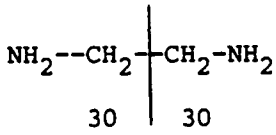

Propane gas

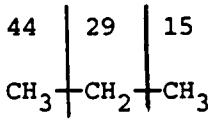

(also contains m/e 26, 28, 29, 39, 41, 42, and 43)

Butane gas

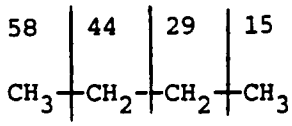

(also contains m/e 26, 28, 39, 41, 42, 43, and 57)

Figure 18. (Continued)

photolyzed films (Figure B.16). At the same retention time, the mass spectra of unexposed Nylon 66 (Figure B.4) displays similar m/e fragmentations as the exposed film. Some main differences, however, are that the unexposed film has higher molecular weight fragments (for example m/e 129 and 149), and the m/e fragment 125 is not present.

Thus far, the fate of the acyl radical which results from homolytic scission at the amide linkage of the polyamide chain has been discussed, but there has been no mention of the amine radical. Stephenson (19) had suggested that the amine radical $\bullet NH\text{-}CH_2$-- abstracts a hydrogen atom from an adjacent polymer chain resulting in the formation of primary amine chains and low molecular weight compounds such as methylamine (m/e 31), ethylamine (m/e 45) and propylamine (m/e 59). None of these low molecular weight primary amines were observed in the mass spectra of the photolyzed films (Figures B.14 - B.20), but they possibly were detected in the volatile fractions of Nylon 66 with or without additives (Tables A.5 - A.7). The main fragmentations of these three amines are m/e 30 and 31 for CH_3NH_2, m/e 29, 30, and 45 for $CH_3\text{-}CH_2\text{-}NH_2$, and m/e 29, 30, 43, 44, and 59 for the $CH_3\text{-}(CH_2)_2\text{-}NH_2$ compound (77). The presence of a m/e 30 fragmentation is usually good evidence that a primary amine is formed, but it is not conclusive (78). For long chained primary amines, the most intense peak should be the m/e 86 fragment as seen in the following fragmentation process (78).

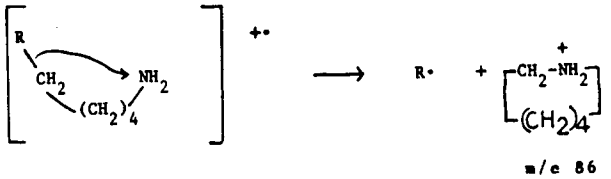

(20)

This fragmentation did not appear in any of the mass spectra of the photolyzed films (Figures B.14 - B.20), and therefore, it is concluded that long chain primary amines were not present. If these compounds were formed, they must have rapidly undergone chain scission or other consumption.

Another pathway (Figure 16, pathway f) which seems to occur at the $\cdot NH\text{-}CH_2\text{-}$ end of the polyamide chain is the homolytic cleavage which results in the evolution of methylene imine ($NH{=}CH_2$, m/e 29). The m/e 29 fragmentation ($NH{=}CH_2$) occurs in both the gaseous and solid state mass spectra of Nylon 66. From Tables A.5 through A.7, it appears that the m/e 29 fragment is slightly more abundant in the volatile fractions of the photolyzed films containing $MnCl_2$ or CuCl. Methylene imine, which is generated in the photolyzed films (without additive), can abstract a hydrogen atom from an adjacent polyamide chain and rapidly dimerize to form ethylenediamine (liquid A'). The major peaks for ethylenediamine are m/e 30, but m/e 29, 44 and 60 also occur in much smaller abundances (79). These fragmentations appear in the mass spectra of the 48 hour photolyzed Nylon 66 film at a retention time of 1.3 minutes, (Figure B.15) and a lot later in the mass spectra of the unexposed film (retention time of 2.3 minutes; Figure B.4). Ethylenediamine does not seem to form in the photolyzed films containing CuCl (Table A.13) or $MnCl_2$ (Table A.11), since the m/e 30 fragmentation does not occur in their mass spectra (79). Recall that the m/e 30 fragmentation could also indicate the presence

of primary amines (77), but this possibility has been ruled out since there are no m/e 31, 45, 58, or 86 fragmentations in the mass spectra of the photolyzed films. The only other possibility for the m/e 30 fragmentation is formaldehyde, but since the m/e 30 peak appears in the volatile fractions in extremely small amounts, then this is unlikely. Ethylenediamine is probably the main contributor to the m/e 30 peak. According to Grasselli and Ritchey (79), the abundance of the m/e 30 fragmentation in ethylenediamine is 100% while the parent peak (m/e 60) is only about 5%. The m/e 60 peak which appears in the mass spectra of photolyzed Nylon 66 must therefore be attributed to some other fragmentation. Carboxylic acids undergo rearrangement to form a strong m/e 60 fragment, but the acids must also exhibit a m/e 45 peak (COOH) which does not appear at early retention times in the mass spectra of the photolyzed samples (80). At present, the m/e 60 fragmentation that occurs in the photolyzed Nylon 66 has not been identified.

Once methylene imine is formed (Figure 16, pathway f), the alkyl radical $\cdot CH_2-(CH_2)_4-$, can undergo loss of $CH_2=CH_2$ or crosslinking, or it can abstract a hydrogen atom from an adjacent chain to form transient intermediate solid C', which undergoes a series of reactions to produce more methylene imine (or ethylenediamine), and n-butane gas (m/e 58, Table A.5).

Figure 17 depicts another route through which the amine radical $\dot{N}H-CH_2-$ can react. Further scission of the nylon chain at the $\dot{N}H-CH_2-$ fragment can lead to loss of $NH=CH-CH_2\cdot$ which subsequently abstracts a hydrogen atom from the adjacent polyamide chain and

results in the formation of ethylene imine (m/e 43). This fragmentation is observed in both the gas (Table A.5) and solid state mass spectra of the photolyzed film (Table A.9), and in the solid state mass spectra of the unexposed film, at a slightly longer retention time (Table A.1). Once ethylene imine (m/e 43) is evolved, the alkyl radical can either crosslink, as mentioned before, or undergo a series of reactions to form n-propane (m/e 44, Table A.5) and more methylene imine (m/e 29). Photolyzed Nylon 66 films containing CuCl seem to favor the degradation pathways of Figure 17, where ethylene imine (m/e 43) and n-propane (m/e 44) are formed in rather large quantities (Table A.7).

c. Analysis of photooxidized Nylon 66 samples mass spectrometry of gaseous and solid state products. The mass spectra of the volatile fractions produced during the photooxidation (in the UV chamber) of Nylon 66 films (with and without additives) and fibers, can be observed in Figures B.31 through B.41. The m/e fragments 28, 43, and 44 are similar to those observed in the volatile products resulting from photolysis; where the relative abundances of m/e 28, 29, 43, and 44 indicate the loss of CO and/or $CH_2{=}CH_2$ (m/e 28), $NH{=}CH_2$ and/or CHO (m/e 29), $CH_3CH{=}NH$ (m/e 43), and CO_2 (m/e 44).

Two other fragments, m/e 17 (OH) and m/e (HOOH), which appear in some of the spectra, are consistent with a mechanism in which hydroperoxides are intermediates in photooxidation. The photooxidation mechanism(s) which account for the formation of the volatile products can be observed in Figure 19 (for m/e 28, 29, 43, 44) and Figure 15 (for m/e 44). The gaseous products observed involve initial scission

at the carbon-nitrogen bond of the amide group during photooxidation ($\lambda \geq$ 300 nm), but the amide group does not absorb light above 290 nm. This fact led researchers to postulate the involvement of impurity chromophores (such as α,β-unsaturated carbonyl compounds) in the photooxidation process to explain the formation of the volatile products and solid residues. The solid state mass spectral data of Nylon 66 films (with and without additives) photooxidized in the UV chamber can be observed in Tables A.14 through A.19, while those of the fibers photooxidized in either the Weatherometer or UV chamber appear in Tables A.20 through A.23. The solid state mass spectral data of the photolyzed films and fibers may be compared to the mass spectral data of the unexposed samples (Tables A.1 - A.4) Also, all the mass spectra (both gaseous and solid state) of photooxidized Nylon 66 samples (with and without additives) may be seen in Figures B.21 through B.45, while the mass spectra of the unexposed samples appear in Figures B.3 - B.7. Samples photolyzed in the Weatherometer (where moisture is present and the temperature is 45^{o}C), degraded more rapidly than those photooxidized in the UV chamber, and there was a more random pattern of degradation products. In comparing the photooxidized samples with the unexposed polyamides, it was noted that the exposed nylons underwent the same mode of degradation as the unexposed samples with regard to thermal decomposition, but degradation occurred much sooner. The photooxidation mechanisms (Figures 19, 20, and 21), which explain the formation of nonvolatile

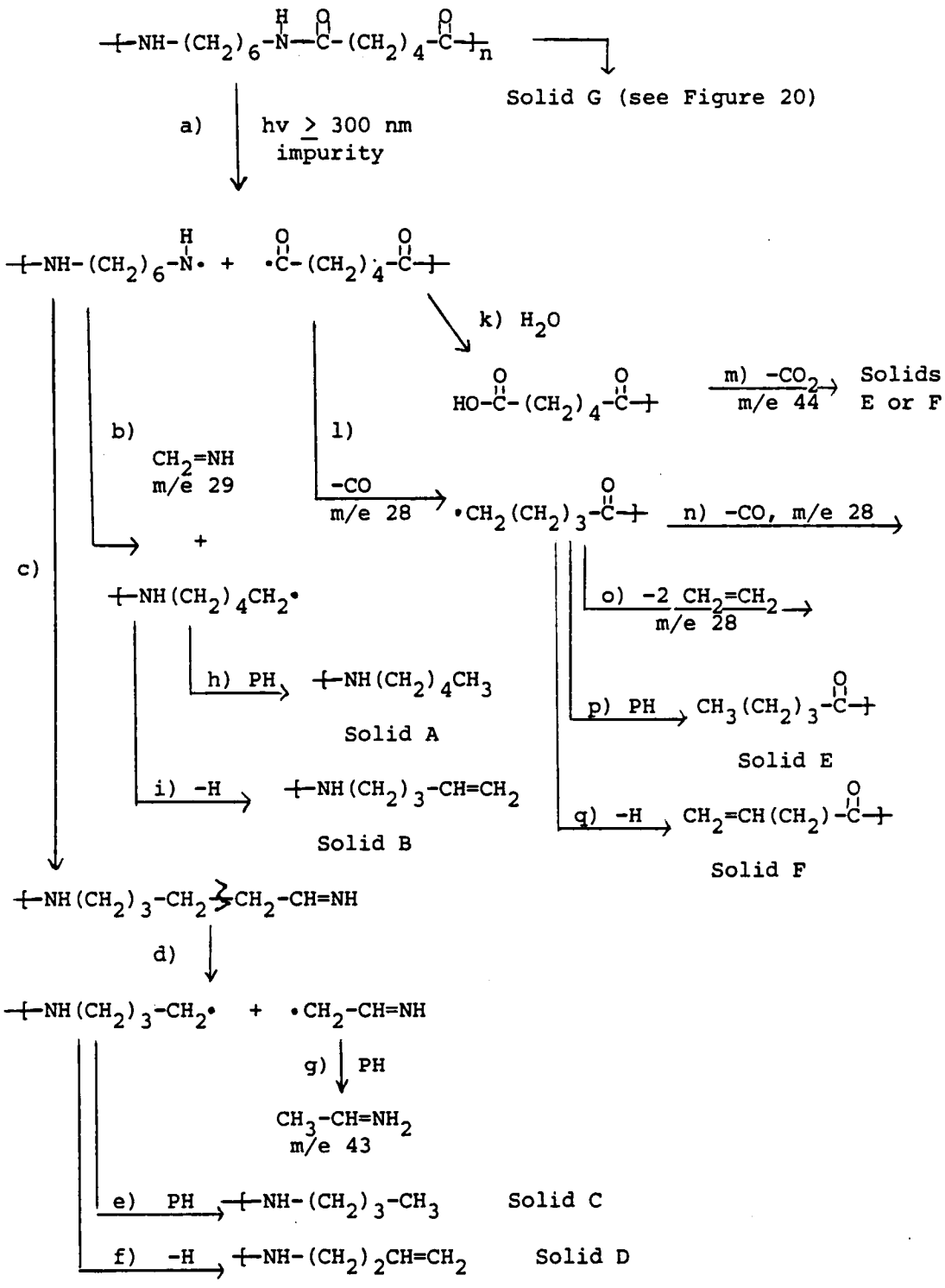

Figure 19. Photooxidation mechanism; homolytic chain scission resulting in volatile products (m/e 28, 29, 43, and 44).

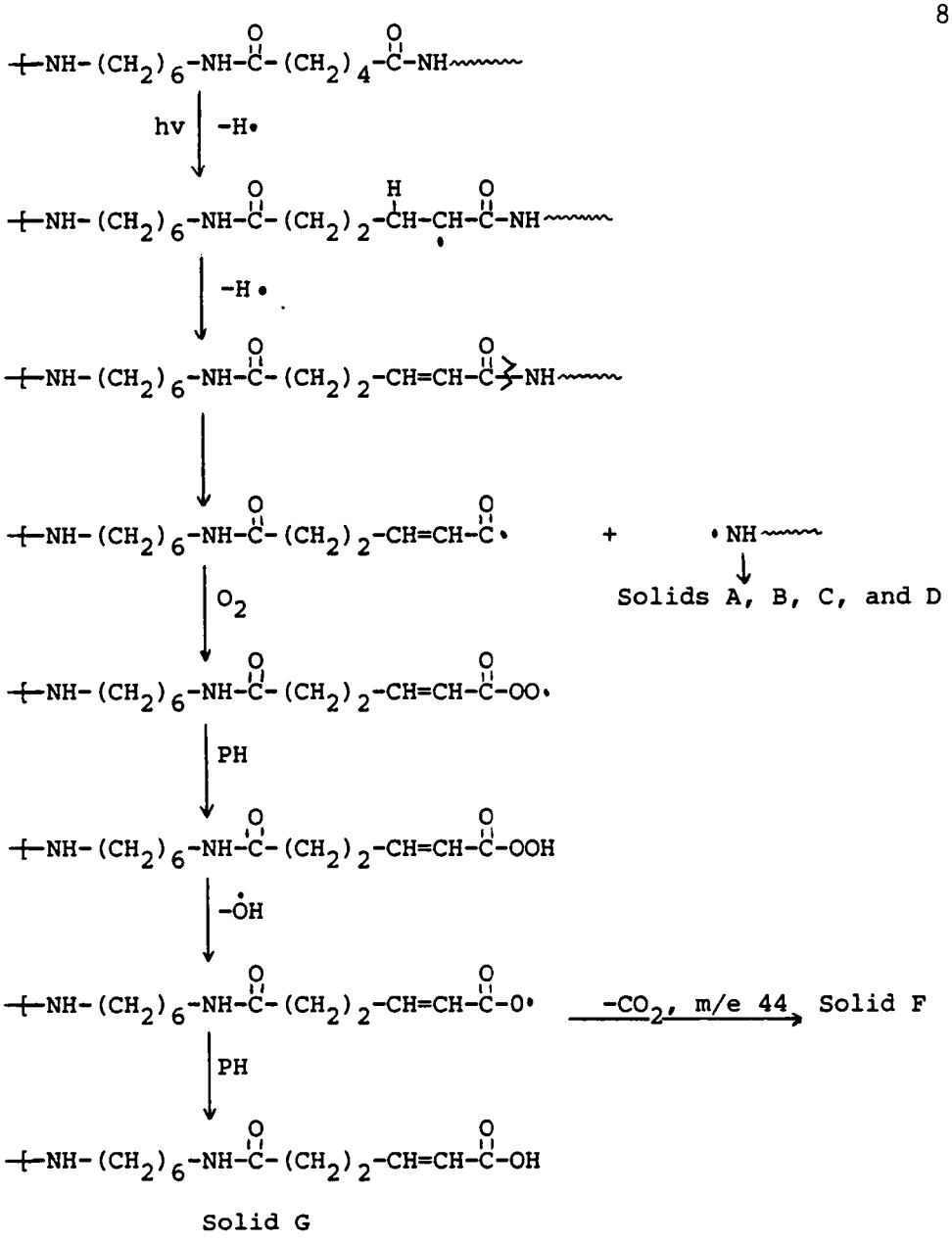

Figure 20. Photooxidation mechanism; hydrogen abstraction, homolytic cleavage between -NH-CO- , and oxidation.

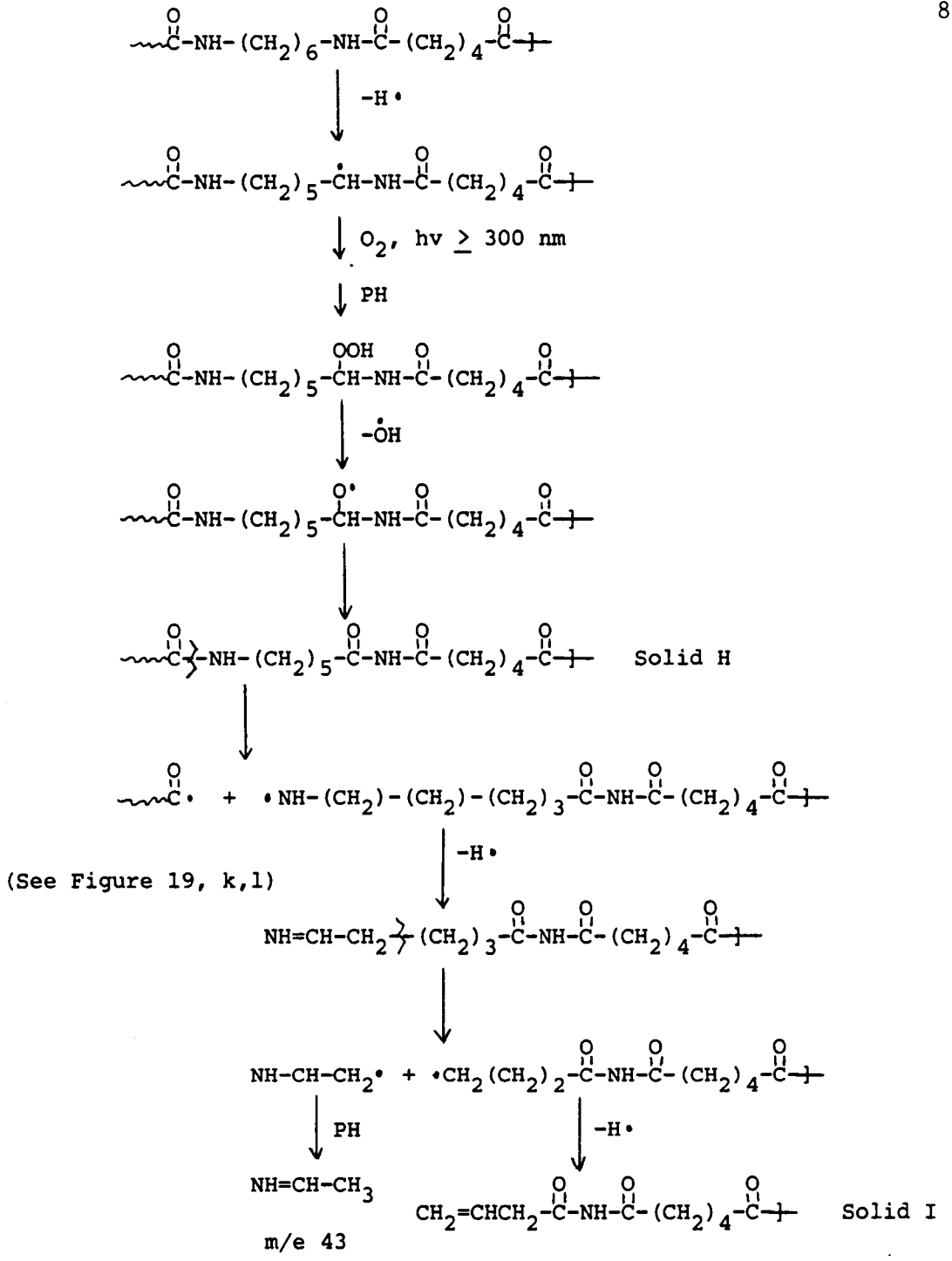

Figure 21. Photooxidation mechanism; hydrogen abstraction followed by oxidation, and then homolytic cleavage between -NH-⟩CO-.

photooxidation products, were therefore devised from mass spectral data at early retention times, and correlated with the results of the chemical tests and UV data.

The photooxidation process involves random chain scission, hydrogen abstraction and the oxidation of the nylon chain. Homolytic cleavage at the amide linkage, followed by the loss of methylene imine (m/e 29), results in the alkyl radical $-NH-(CH_2)_4-CH_2^{\bullet}$, which could either abstract a hydrogen atom to form solid A, or disproportionate to produce Solid B (Figure 19: b, h, and i). The mass spectral assignments of solids A and B and other possible residual photooxidation products, can be seen in Figure 22. There doesn't seem to be much mass spectral evidence for solid A since m/e 86 is not observed at early retention times. The unsaturated species (solid B), however, probably exists.

Since random scission may occur, loss of ethylene imine (m/e 43) from the amine end of the polymer chain may also be formed, and the resulting alkyl radical, $-NH-(CH_2)_3-CH_2^{\bullet}$, could possibly result in the saturated and unsaturated compounds, solids C and D. Again, there does not seem to be much evidence for the saturated species (solid C) since the m/e 72 fragmentation appears at higher retention times. Unlike the fragmentation at the amine radical end, after the loss of CO from the carbonyl part of the chain, the saturated compound, solid E, seems to be produced in addition to the unsaturated species solid F.

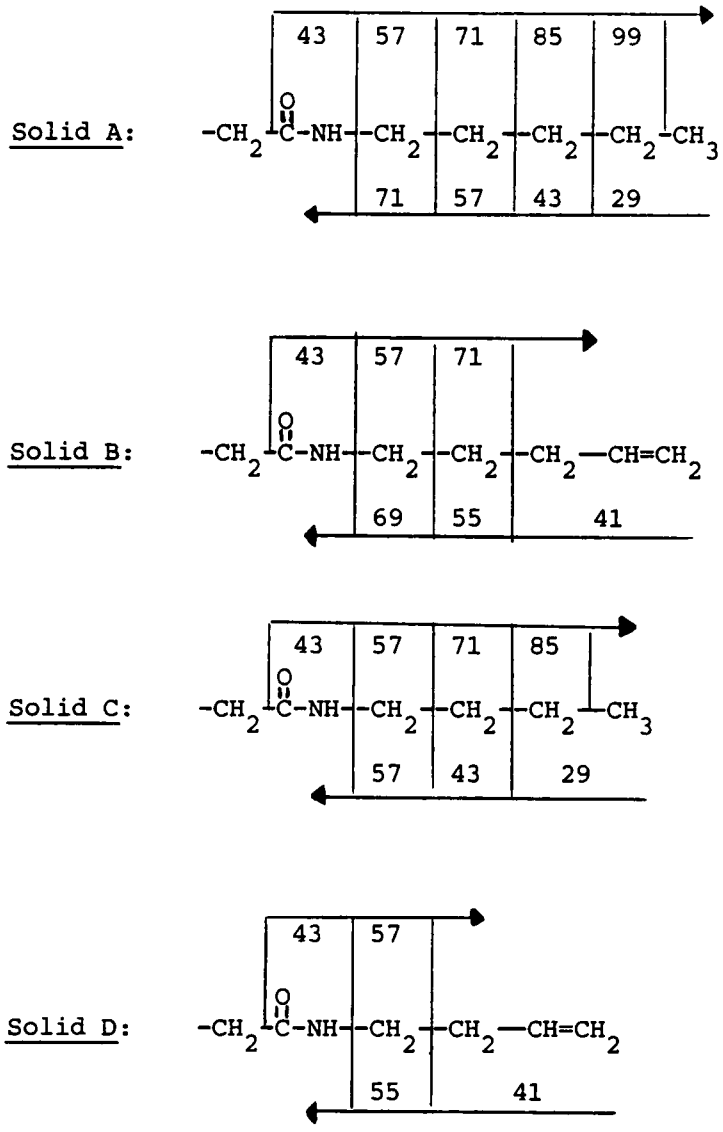

Figure 22. Mass spectral assignments of solids A - I.

Solid E:

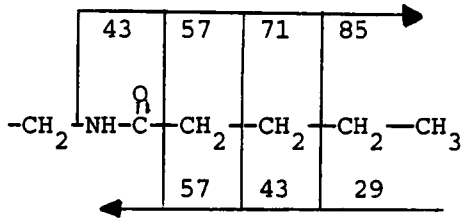

Solid F:

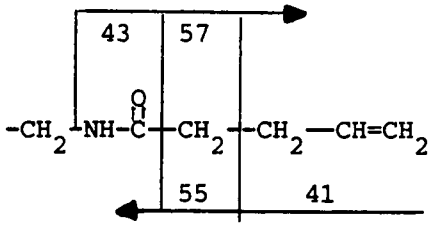

Solid G:

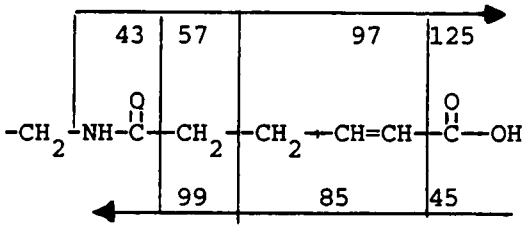

Solid H:

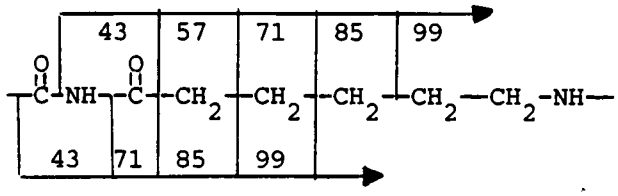

Solid I:

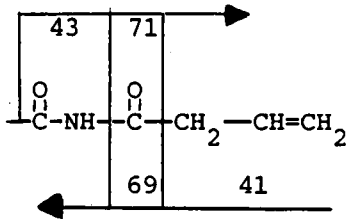

Figure 22. (Continued)

As previously discussed in the photolysis section, long chain saturated and unsaturated aldehydes (solids A' and B') may also be formed from the acyl radical. The mass spectral assignments for solids A' and B' can be seen in Figure 18. Again, as observed in the photolyzed samples, m/e 27 or 127 (fragments which should occur in long chained aldehydes) did not appear in the mass spectra of the photooxidized samples. The α,β-unsaturated aldehyde (solid B'), on the other hand, was detected in the photooxidized nylons, and again it is probably formed from the transient compound, solid A'. Earlier studies suggested the production of saturated aldehydes as intermediates to the formation of the carboxylic acids (26).

(21)

Common mass spectral fragmentations for unsaturated carboxylic acids can be seen as follows (76):

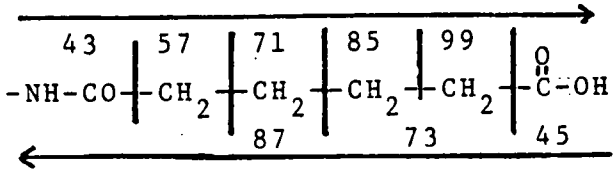

(22)

McLafferty Rearrangement:

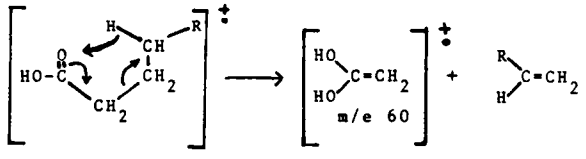

(23)

When m/e 45 and 60 appear together in a mass spectra, there is a good chance that a long chain saturated carboxylic acid is present. At early retention times (before 1.4 min), m/e 45 and 60 appeared in the mass spectra of a few photooxidized samples, but in most cases these

fragments occurred between 1.8 and 2.0 minutes. These same peaks appeared much later in the unexposed samples. For fibers, at 1.8 minutes, the % abundance of the m/e 45 and 60 fragments was found to correlate well with the concentration of COOH obtained from the end group analysis (Table 13). This type of correlation, however, was not observed in the films. The pathways which result in unsaturated carboxylic acids can be seen in Figure 15 from the previous section. Decarboxylation has been observed from mass spectral (m/e 44) and carboxyl end group analysis.

A series of reactions that also seem to occur at the carboxyl end of the chain can be seen in Figure 20, where initial formation of unsaturated sites, followed by scission at the α, β-unsaturated amide linkage and then oxidation, hydrogen abstraction, and loss of OH leads to the α, β-unsaturated carboxylic acid, solid G. The mass spectral and possibly UV (λ_{max} = 252 nm) data of photooxidized Nylon 66 correlate with the formation of this compound. Figure 21 depicts the photooxidation mechanism resulting in the formation of imides (solids H and I). Rafikov and Tsi-Pin (20) showed that the $-CH_2-CH-NH-CO-CH_2-$ radical was formed during both photolysis ($\lambda \leq 300$ nm) and photooxidation ($\lambda \geq 300$ nm). During photolysis, this type of radical couples with another radical on an adjacent chain and produces either crosslinks or branches. In the photooxidation process, however, oxygen rapidly couples with the $-CH_2-\dot{C}H-NH-CO-CH_2-$ radical to produce hydroperoxides and/or imides (such as solid H). Subsequent cleavage of ethylene imine (m/e 43) from solid H and loss

Table 13. The correlation between the carboxyl end group analysis and % abundance of m/e 45 and 60 for photooxidized Nylon 66 fibers.

Nylon Sample	Exposure Source (a)	Exposure time (hr)	% Abundance of m/e 45	% Abundance of m/e 60	COOH Conc. (b)
Fiber	Mercury lamp	0	-	-	4.78
		48	12	12	5.98
		96	20	25	9.97
Fiber	Weatherometer	48	12*	23	10.37
		96	6*	12	5.58
		147	5	17	4.78
		195	4*	12	4.39

(a) At 54% RH and 45°C in the Weatherometer.

(b) Meq COOH/g Nylon 66.

* m/e 45 peaks which first appeared at 2 min in mass spectra.

of H• can lead to the formation of the imide solid I. The mass spectral data (Tables A.14 - A.23) correlate with the chemical analysis of imide groups (see Table 2).

The mass spectra of photooxidized and unexposed Nylon 66 films containing $MnCl_2$ is similar to that of Nylon 66 without additives. $MnCl_2$, however, appears to retard modes of degradation that occur without additives. CuCl, on the other hand, seems to alter decomposition modes of Nylon 66. From the mass spectra, it can be seen that CuCl suppresses the formation of imides and all of the solid residues depicted in Figure 22 that have m/e fragmentations above 71. End group analysis of Nylon 66 samples show that with an increase in photooxidation, the concentration of carboxylic groups decreases, possibly due to decarboxylation or decarbonylation. The mass spectra of the volatile fractions of Nylon 66/CuCl, however, do not seem to be much different from that of Nylon 66 alone or with $MnCl_2$.

C. Tensile Properties of Photooxidized Fibers and Nonwoven Fabrics.

The tensile properties of photooxidized bright Nylon 66 films, which had been exposed in the specially constructed UV apparatus and the commonly used Weatherometer, were measured in order to demonstrate the loss in strength that occurs upon irradiation. The breaking strength (mg/m), % elongation, and energy-to-rupture was observed (Table 14). Since only a portion of the filaments as a fiber bundle were exposed to the light source, the loss in tensile properties of the fibers was gradual, even after long exposure (the decrease in tensile properties was greater in the samples exposed in the UV

Table 14. Tensile properties of Nylon 66 fibers and fabrics before and after UV exposure

Nylon Sample	Exposure time (hr)	Exposure source (a)	Breaking Strength (mN) (b)	%Elongation-at-break	Energy-to rupture (μJ)
Fibers	0	Mercury lamp	38.6	16	2,386
	48		32.4	14	1,672
	96		28.8	13	1,439
Fibers	24	Weatherometer	32.4	16	1,997
	48		33.0	16	1,984
	96		33.3	16	1,978
	147		31.5	16	1,668
	195		30.6	15	1,668
Nonwoven Fabric (c)	0	Weatherometer	33,354	112	513,142
	48		16,795	122	303,890
	96		14,470	95	215,470

(a) At 54% RH and 45°C in the Weatherometer.

(b) Fiber tensile properties were measured at a crosshead speed of 0.2 in/min and a chart speed of 5 in/min using a Cell A on an Instron, at a full scale load of 10 grams.

(c) Crosshead and chart speeds were 5 in/min using a Cell B and a full scale load of 5000 grams.

chamber than the ones exposed in the Weatherometer). The nonwoven fabrics, on the other hand, experienced a 50% loss in tensile strength and a comparable loss in % elongation and energy-to-rupture after exposure.

CHAPTER VI

CONCLUSION

The main objective of this research project was to elucidate the mechanism(s) by which Nylon 66 degrades in sunlight by combining data obtained from mass spectrometry and other analytical tools with data from the literature. Nylon 66 films (with and without $MnCl_2$ and CuCl), fibers, and nonwoven fabrics were photolyzed (at $\lambda \leq 300$ nm) and photooxidized (at $\lambda \geq 300$ nm) in a specially constructed UV apparatus, equipped with a high pressure mercury vapor lamp and a reattachable trap for collecting gaseous products formed during the UV exposures. Bright Nylon 66 fibers and nonwoven fabrics were also photooxidized in an Atlas Weatherometer (xenon light source) where moisture was present and the temperature was 45°C. In order to obtain additional information on the photolytic and photooxidative processes, Nylon 66 films (with and without $MnCl_2$ and CuCl) and fibers which had been photolyzed and photooxidized in the UV chamber, and Nylon 66 fibers which had been photooxidized in the Weatherometer, were analyzed by mass spectrometry. Nylon 66 films (with and without photostabilizing additives) which had been photolyzed and photo-oxidized by a mercury arc were also analyzed by UV-VIS spectrometry, and a crosslinking study was performed on these samples. Transmission IR and ATR-FTIR were unsuccessfully attempted on some of these films. Chemical investigation (for carboxyl end groups, imides and pyrroles) of the photooxidized films and fibers proved useful in obtaining additional information on the photooxidation process, and the data

produced were correlated with the % abundance and m/e peaks of the nylon samples. Also, in order to demonstrate the loss in strength that occurs from irradiation, the tensile properties such as the energy-of-rupture, % elongation, and breaking force were measured for the photooxidized nylon fabrics and fibers. Mechanisms consistent with the data obtained from the chemical and spectroscopic analysis have been proposed to explain the pathways by which Nylon 66 photodegrades.

As observed in earlier photolysis and photooxidation studies, random chain scission at the amide linkage appears to be the initial reaction for the formation of the volatile products and solid residues obtained during both processes. During these processes, the loss of volatile substances such as CO, ethylene, CO_2, and methylene- and ethylene imine leaves fragmentations in the solid phase that possibly contain α,β-unsaturated carbonyl compounds, and other compounds containing sites of unsaturation. In addition to the volatile products mentioned above, other gases and volatile liquids such as n-propane, n-butane, methyl-, ethyl-, and propylamines also seemed to appear in the volatile fractions of the photolyzed samples. The above volatile products evolved during both processes, except for methylene- and ethylene imine, have previously been observed by several workers.

In some of the photooxidized samples, especially those which were exposed in the Weatherometer, imides were detected by chemical analysis. Also, end group analysis correlated well with mass spectral assignments and loss of tensile strength of photooxidized fibers. Although earlier studies had suggested the formation of pyrroles as

photooxidation products, in this study during photooxidation, there was no evidence of pyrroles. In agreement with previous investigations, crosslinking was not observed in the photooxidized samples, but was observed in the photolyzed samples (without additives) where the degree of crosslinking increased upon exposure.

From both the photolysis and photooxidation studies of Nylon 66 containing $MnCl_2$ and CuCl, it was found that $MnCl_2$ retards photo-degradation without much mechanistic change (except that it suppressed the formation of ethylenediamine), while CuCl drastically alters the mode of decomposition. For instance during photolysis, CuCl suppressed the formation of ethylenediamine, as well as the degree of crosslinking. Likewise, during photooxidation, it suppresses the formation of imides and seems to prevent the initial formation of carboxyl end groups. Until this study, none of the earlier photolysis or photooxidation studies had examined the chemistry occurring during the photodegradation of Nylon 66 or any other aliphatic polyamide containing photostabilizing additives.

LIST OF REFERENCES

LIST OF REFERENCES

1. Stevens, M. P.; "Polymer Chemistry an Introduction"; Addison-Wesley Publishing Co. Inc.; Reading, Mass., 1975; p 277.

2. Grayson, M. A.; Wolf, C. J.; "Applied Polymer Spectroscopy "; E. Brame, Jr., Ed.; Accademic Press, New York, 1978; pp 221-239.

3. Luderwald, I; Merz, F. Angew. Mackromol. Chemie **1978**, 74, 165.

4. McKellar, J. F.; Allen, N. S.; "Photochemistry of Man-Made Polymers"; Applied Science Publishers LTD; London, 1979, p 1-29.

5. Turro, N. J.; "Modern Molecular Photochemistry"; Benjamin Cummings Publishing Co. Inc.; Menlo Park, Calf., 1978, p 22.

6. Ref. 5, pp 4-5.

7. Stowe, B. S.; Fornes, R. E.; Gilbert, R. D. Polymer Plast. Technol. Eng. **1974**, 2, 159-197.

8. Ref 4, pp 261-267.

9. Wall, M. J.; Frank, G. C. Polymer Plast. Technol. Eng. **1971**, 41, 38.

10. Ref. 4, p 269.

11. Ref. 4, pp 269-272.

12. Ranby, B.; Rabek, J. F.; "Photodegradation, Photooxidation and Photostabilization of Polymers", John Whiley & Sons, Inc., New York, 1975, p 474.

13. Ref. 14, p 472.

14. Cowell, G. W.; Pitts, J. N., Jr. J. Am. Chem. Soc. **1968**, 90, 1106.

15. Moore, R. F. Polymer **1963**, 4, 493.

16. Achhammer, B. G.; Reinhart, F. W.; Kline, G. M. J. Res. Nat. Bur. Stand. **1951**, 46, 391.

17. Stephenson, C. V.; Moses, B. C.; Willcox, W. S. J. Polym. Sci. **1961**, 55, 451.

18. Stephenson, C. V.; Moses, B. C.; Burks, R. E., Jr.; Wilcox, W. S. J. Polym. Sci. **1961**, 55, 465.

19. Stephenson, C. V.; Lacey, J. C., Jr.; Wilcox, W. S. J. Polym. Sci. **1961**, 55, 477.

20. Rafikov, S. R.; Tsi-Pin, S. Vysokomol. Soedin **1961**, 3, 56.

21. Zimmerman, J. Vysokomol. Soedin **1960**, 46, 151.

22. Szocs, F.; Becht, J.; Fisher, H. Eur. Polym. J. **1971**, 7, 173.

23. Verma, G. S. P.; Peterlin, A. Kolloid-Z **1970**, 236, 111.

24. Burnett, G. M.; Riches, K. M. J. Chem. Soc., B **1966**, 12, 1229.

25. Marek, B.; Lerch, E. J. Soc. Dyers, Color. **1965**, 81, 481.

26. Sharkeyy, W. H.; Mochel, W. E. J. Amer. Chem. Soc. **1959**, 81, 3000.

27. Heuvel, H. M.; Lind, K. C. J. R. J. Polym. Sci., A-2 **1970**, 8, 401.

28. Fornes, R. E.; Gilbert, R. D.; Stowe, B. S. Text. Res. J. **1973**, 43, 704

29. Lock, M. W.; Sagar, F. B. Proc. Chem. Soc. **1960**, 358.

30. Golemaba, F. J.; Guillet, J. E. J. Paint Technol. **1969**, 41, 315.

31. Kroes, G. H. Rec. Trav. Chem. Pays-Bas. **1962**, 81, 624.

32. Margolin, A. L.; Postnikov, L. M.; Shlyapintokh, V. Ya. Vysokomol. Soyed. **1977**, A19, 1954.

33. Tang, L.; Sallet, D.; Lemaine, J. Macromolecules **1982**, 15, 1432.

34. Anton, A. J. Appl. Polym. Sci. **1965**, 9, 1631.

35. Betts, A. T.; Uri, N. Chem. Ind. (London) **1967**, 512.

36. Allen, N. S. Polym. Degrad. Stab. **1982**, 4, 239.

37. Allen, N. S.; McKellar, J. F.; Wilson, D. J. Photochem. **1976**, 6, 377.

38. Ford, R. A. J. Coll. Sci. **1957**, 12, 271.

39. Allen, N. S.; McKellar, J. F.; Phillips, G. O. J. Polym. Sci., Polym. Chem. Ed. **1974**, 12, 1233.

40. Korshak, V. V.; Slonimshii, G. L.; Krongauz, E, S. Isvest. Akad. Nauk. USSR, Otdel. Khim. Nouk **1958**, 221.

41. Goodman, I. J. Polym. Sci. **1954**, 13, 175.

42. Goodman, I. J. Polym. Sci. **1955**, 17, 587.

43. Kroes, G. H. Rec. Trav. Chim. **1963**, 82, 979.

44. Kamberbeek, B.; Kroes, G. H.; Grolle, W. "Thermal Degradation of some Polyamides," (Soc. Chem. Ind. Monographs) Society of Chem. Ind., London, 1961, vol. 13, 357.

45. Edgar, O. B.; Johnson, D. H. J. Chem. Soc. **1958**, 3925.

46. Peebles, J. H., Jr.; Huffman, M. W. J. Polym. Sci. (A-1) **1971**, 9, 1807.

47. Lock, M. V.; Sager, B. F. J. Chem. Soc. B. **1966**, 690.

48. Sagar, B. F. J. Chem. Soc. B. **1967**, 1047.

49. Ref. 12, p 362.

50. Lappin, G. R.; "Encyclopedia of Polymer Science and Technology," Interscience, New York, 1969, vol. 14, 129.

51. Desson, R. G.; Hatfield, H. R.; Wood, L.; Appl. 1951; British Patent 649,481; 1951.

52. Stettele, W.; Appl. 1960; Swiss Patent 347,979; 1961.

53. Newsome, O. J. Soc. Dyers Colour. **1950**, 66, 277.

54. Richards, D. B.; Bovenizer, G. W. J. Paint Technol. **1972**, 44, 90.

55. Allen, N. S.; Mc Kellar, J. F.; Philips, G. O.; Chapman, G. B. J. Polym. Sci., Polym. Lett. **1974**, 723.

56. Papers, P. P., Jr.; Morter, C.; Morter, R. L., Jr.; Appl. 1960; US Patent 3,113,120; 1963.

57. Stamatoff, G. S.; Appl. 1954; US Patent 2,705,227; 1955.

58. Twilley, I. C.; Poznick, F. P.; Appl. 1963; US Patent 3,280,053; 1966.

59. Twilley, I. C.; Poznick, F. P.; Appl. 1963; US Patent 3,294,735; 1966.

60. Camp, A. E.; Steinman, H. W.; Appl. 1964; US Patent 3,341,492; 1967.

61. Hardy W. B.; Forster, W. S.; Hosler, J. F.; Appl. 1959; US Patent 3,049,509; 1962.

62. Mikolajewski, E.; Swallow, J.; Webb, W. J. Appl. Polym. Sci. **1964**, 8, 2067.

63. Voitelev, Y. A.; Katorzhnov, I. Kim. Volokna. **1960**, 3, 3.

64. British Patent 726,792; 1955.

65. Neiman, M. B.; "Aging and Stabilization of Polymers," Consultants Bureau, New York, 1965, p 227.

66. British Patent 1,108,451; 1968.

67. E. I. du Pont de Nemours & Co.; Appl. 1955; British Patent 722,724; 1955.

68. Laporta, P.; Zaraga, F. Appl. Optics **1981**, 20, 2946.

69. Supplied by Ace Glass Inc.

70. "Atlas Fade-Ometer and Weather-Ometer, for accelerated lightfastness and weathering tests," (1978), Bulletin No. 1300C.

71. Waltz, J. E.; Taylor, G. B. Anal. Chem. **1947**, 19, 448.

72. Fishman-Goldberg, V.; Spoerri, P. E. Anal. Chem. **1959**, 31, 1735.

73. Pavia, D. L.; Lampman, G. M.; Kriz, G. S.; "Introduction to Spectroscopy," Saunders College Publishing, Phil., 1979, pp 198-206.

74. Ref. 73, pp 225 - 229.

75. Happ, G. P.; Stewart, D. W. J. Am. Chem. Soc. **1952**, 74, 4440.

76. Silverstein R. M.; Bassler, G. C.; Morril, T. C. "Spectrometric Identification of Organic Compounds," John Wiley and Sons, New York, 1981, p 26.

77. Ref. 73, p 272.

78. Ref. 74, p 30.

79. Grasselli, J. G.; Ritchey, W. M.; "Atlas of Spectral Data & Physical Constants for Organic Compounds," CRC Press, 2nd Ed., Cleveland, Ohio, 1975, p 246.

80. Ref. 73, pp 269 - 271.

APPENDIXES

APPENDIX A

MASS SPECTRA

DATA TABLES

Tables A.1 - A.4

Solid Mass Spectral Data of Unexposed Nylon 66 Films (with and without $MnCl_2$ and CuCl), and Bright Fibers.

Table A.1. Solid state mass spectral data of unirradiated Nylon 66.

Mass	Retention times (min.) 0.4	0.7	1.0	1.1	1.2	1.3	1.4	1.5	1.6	1.7
18	100	100	100	100	75	53				
28	44	58	90	100	100	100	100	100	100	70
43									63	59
44							39	65	79	56
55										44
57								59	79	100
69									47	52
71									63	59
83									42	52
85									47	44
97									53	44
149									63	89

% Abundance

Table A.2. Solid state mass spectral data of unirradiated Nylon 66/CuCl.

Mass	Retention times (min.) 0.4	0.7	1.0	1.1	1.2	1.3	1.4	1.5	1.6
18	17	24							
28	100	100	100	100	100	100	100	100	100
43									
44								17	17
55									
57									
71									

% Abundance

Table A.3. Solid state mass spectral data of unirradiated Nylon 66/$MnCl_2$.

Mass	Retention times (min.) 0.4	0.7	0.9	1.0	1.1	1.2	1.4	1.5	1.6
18	100	67							
28	71	100		100	100	100	61	45	28
43								20	25
44							47		25
55									18
57							43	35	41
69									22
71								30	28
83									22
85									18
97									22
149							100	100	100
177									16

% Abundance

Table A.4. Solid state mass spectral data of unexposed Nylon 66 fibers.

Mass	Retention times (min.) 0.3	0.7	0.9	1.0	1.2	1.3	1.4	1.7	1.9	2.2
17		15	17	16	14	17	17	12	14	7
18	49	89	81	74	67	84	75	67	73	36
28	100	100	100	100	100	100	100	100	100	100
32	24	29	26	27	23	31	27	26	29	28
43									7	12
44									8	10
55										6
57									8	13
69									6	9
71										8
83										8
85										9
97										7

% Abundance

Tables A.5 - A.7

Mass Spectral Data of the Volatile Products evolved during the 24 and 48 hour Photolysis of Nylon 66 Films (with and without $MnCl_2$ and CuCl).

Table A.5. Mass spectral data of the volatile products evolved during the 24 and 48 hour photolysis of Nylon 66.

	Fragmentations evolved after exposure for:	
	24 hours	48 hours
m/e	%Abundance	%Abundance
14	0.4	0.4
15	-	0.2
16	1.6	0.7
17	10.9	3.8
18	43.4	18.6
26	0.3	0.5
28	100	100
29	3.8	3.3
30	0.5	0.5
31	-	0.2
32	3.9	1.1
39	0.5	0.7
40	2.3	2.9
41	1.4	1.5
42	0.6	1.2
43	4.2	10.1
44	54.5	53.1
45	1.0	0.9
46	-	0.1
47	-	0.1
49	-	1.3
51	-	0.6
55	-	0.2
56	-	0.2

Table A.5 (Continued)

	Fragmentations evolved after exposure for:	
	24 hours	48 hours
m/e	%Abundance	%Abundance
57	0.3	0.5
58	0.3	3.3
59	-	0.3
69	0.4	0.6
73	4.1	0.4
84	-	1.2
86	-	0.7
96	0.4	-
97	-	0.1
130	-	0.1
133	0.8	-
191	0.6	-
193	0.6	-
199	-	0.2
201	-	0.3
204	0.8	-
206	-	0.4
207	2.9	-
248	0.4	-
264	0.6	-
266	0.9	8.4
280	8.4	0.3
281	2.1	-
282	1.1	-

Table A.6. Mass spectral data of the volatile products evolved during the 24 and 48 hour photolysis of Nylon 66/$MnCl_2$.

	Fragmentations evolved after exposure for:	
	24 hours	48 hours
m/e	%Abundance	%Abundance
12	0.1	-
14	0.4	0.3
15	0.2	0.3
16	0.5	0.9
17	0.5	8.8
18	3.2	50.7
19	-	0.2
26	0.6	0.4
27	3.1	-
28	100	100
29	3.8	4.7
30	0.8	0.5
31	-	0.4
32	0.5	0.7
38	0.2	-
39	0.7	0.6
40	1.9	3.1
41	1.7	2.0
42	1.3	1.0
43	7.3	4.6
44	49.1	44.9
45	0.8	1.4

Table A.6. (Continued)

	Fragmentations evolved after exposure for:	
	24 hours	48 hours
m/e	%Abundance	%Abundance
46	0.2	0.2
55	0.2	-
56	0.2	0.2
57	0.2	0.6
58	1.5	0.4
59	0.1	0.3
60	0.3	-
69	0.7	-
71	0.1	-
73	0.5	0.7
100	0.1	-
130	-	0.3
198	0.2	-
199	0.4	0.2
200	0.5	-
201	0.2	0.3
206	-	0.3
219	0.1	-
280	-	0.4

Table A.7. Mass spectral data of the volatile products evolved during the 24 and 48 hour photolysis of Nylon 66/CuCl.

	Fragmentations evolved after exposure for:	
	24 hours	48 hours
m/e	%Abundance	%Abundance
14	0.3	0.3
15	0.4	0.1
16	0.9	0.8
17	5.6	6.3
18	23.8	31.1
26	1.1	0.4
27	4.2	-
28	100	100
29	6.2	4.0
30	0.9	0.7
31	0.5	0.1
32	0.8	1.0
37	0.2	-
38	0.4	-
39	2.0	0.5
40	2.6	3.0
41	4.6	1.5
42	3.5	0.7
43	27.5	4.0
44	79.2	53.3
45	1.9	1.1
46	0.3	0.2
55	0.9	0.1
56	1.3	0.1
57	3.4	0.5

Table A.7. (Continued)

	Fragmentations evolved after exposure for:	
	24 hours	48 hours
m/e	%Abundance	%Abundance
58	8.1	0.3
59	1.2	-
60	0.4	-
69	1.5	0.2
70	0.6	-
71	1.1	-
72	0.4	-
73	1.6	0.4
84	0.3	-
85	0.9	-
96	0.4	-
100	0.3	-
130	-	0.1
131	0.4	-
191	0.4	-
198	0.3	0.3
199	0.4	0.4
200	-	0.1
201	0.6	0.4
204	0.4	-
206	2.8	0.4
207	0.5	-
218	0.2	-
266	0.2	-

Tables A.8 - A.13

Mass Spectral Data of Nylon 66 Films (with and without $MnCl_2$ and CuCl) Photolyzed for 24 and 48 hours.

Table A.8. Solid state mass spectral data of Nylon 66 photolyzed for 24 hours.

Mass	Retention times (min.) 0.4	0.7	0.9	1.0	1.1	1.2	1.3	1.4	1.6	1.7
18		21	20	17	16	17	17			19
28	100	100	100	100	100	100	100	100	100	100
32	30	21	27	21	24	19	25	24	23	20
43										15
44										
55										
57										

% Abundance

Table A.9. Solid state mass spectral data of Nylon 66 photolyzed for 48 hours.

Mass	Retention times (min.) 0.3	0.5	0.8	1.0	1.2	1.3	1.4	1.5	1.6	1.7
18	100	100	100						31	25
28	92	59	60	100	100	100	100	100	100	72
29						43	41	59	42	38
30						38			39	34
41										25
43							41	50	58	67
44					40	53	46	82	77	75
55									46	50
57							36	55	77	100
60						38	36	41		
69									42	56
71									42	69
81										28
83									39	60
85										59
95										34
97									31	56
111										31

% Abundance

Table A.10. Solid state mass spectral data of Nylon 66/$MnCl_2$ photolyzed for 24 hours.

Mass	Retention times (min.) 0.4	0.7	0.9	1.0	1.1	1.3	1.4	1.6	1.7	1.8
18		18								
28	100	100	100	100	100	100	100	100	100	100
32	24	27	30	24	32	34	27	32	27	26
43									22	16
44										22
57									20	33
69										18
71										24

% Abundance

Table A.11. Solid state mass spectral data of Nylon 66/$MnCl_2$ photolyzed for 48 hours.

Mass	Retention times (min.) 0.4	0.7	0.9	1.0	1.1	1.2	1.4	1.5
18	100	100	100	53	53	53	47	45
28	57	60	93	100	100	100	73	61
43		73	79	73	93	71	60	51
44				60	73	59	100	100
55			57				33	36
57		60	79	87	93	82	60	73
60								27
69			71	60	60	53	33	42
71			57	73	67	53	33	42
83							27	30
85							27	27
97								30

% Abundance

Table A.12. Solid state mass spectral data of Nylon 66/CuCl photolyzed for 24 hours.

Mass	Retention times (min.) 0.4	0.7	0.9	1.0	1.1	1.2	1.3	1.4	1.5	1.6
18	36	24	18	16				15		
28	100	100	100	100	100	100	100	100	100	100
32	20	20	16	20	24	28	20	25	26	24
43							17	19	20	24
44				16	24	22	30	37	43	52
55										
57										
60										
69										
71										
86										
98										

% Abundance

Table A.13. Solid state mass spectral data of Nylon 66/CuCl photolyzed for 48 hours.

Mass	Retention times (min.) 0.4	0.7	0.9	1.0	1.1	1.2	1.3	1.4	1.5	1.6
18	17	20								
28	100	100	100	100	100	100	100	100	100	100
32	23	25	29	23	23	30	27	27	25	23
43										
44										
55										
57										
71										

% Abundance

Tables A.14 - A.21

Solid State Mass Spectral Data of Hylon 66 Films (with and without $MnCl_2$ and CuCl), and Bright Fibers Photooxidized in the UV Chamber under a Pyrex Filter.

Table A.14. Solid state mass spectral data of Nylon 66 films photooxidized for 48 hours in the UV chamber under a pyrex filter.

Mass	Retention times (min.) 0.4	0.7	0.9	1.0	1.1	1.2	1.4
17		12	15	15	23	11	15
18	100	100	100	100	100	100	75
28	43	22	32	36	39	39	35
29					12	11	13
41			9	10	23	18	24
42							15
43		14	28	32	52	68	69
44		19	27	40	68	92	100
45						13	20
55		9	12	16	20	26	37
56							12
57		13	23	25	33	43	45
58							11
59					17	26	35
60				11	20	31	43
69	14	13	20	24	29	31	28
70							10
71		9	11	17	24	29	32
73		9	23	23	24	36	36
83			9		14	17	15
85			10		16	17	21
99						10	9

% Abundance

Table A.15. Solid state mass spectral data of Nylon 66 films photooxidized for 98 hours in the UV chamber under a pyrex filter.

Mass	Retention times (min.) 0.4	0.7	0.9	1.0	1.1	1.2	1.4
18		100	100	21	8	6	7
28		60	83	27	10	7	8
29							4
41					8	8	9
43			67	27	14	13	15
44					8	9	13
45							4
55					7	9	12
56							4
57					12	13	13
59							5
67					9	10	9
69							3
73				23	25	28	29
83							3
85				100	100	100	100
86					7	8	8
99							3

% Abundance

Table A.16. Solid state mass spectral data of Nylon 66/$MnCl_2$ films photooxidized for 48 hours in the UV chamber under a pyrex filter.

Mass	Retention times (min.) 0.3	0.4	0.7	0.9	1.0	1.1	1.2	1.4
17			20					
18			100	100	83	63	56	56
28			42	56	48	48	50	42
41			24	27	17	25		21
43	100		78	95	63	73	61	49
44	83		84	100	100	100	100	100
55			29	43	33	40	30	36
56								17
57			29	54	33	35	35	42
59	83		46	49	32	30	30	19
60						23		
69				22	17	23	17	25
71				24	19			21
72			29	27	23	28	22	19
73			24	32	27	28	28	18
83								17
85				22			20	19
86			29	27	23	28	22	19
97								17

% Abundance

Table A.17. Solid state mass spectral data of Nylon 66/$MnCl_2$ films photooxidized for 96 hours in the UV chamber under a pyrex filter.

Mass	Retention times (min.) 0.3	0.4	0.5	0.7	1.0	1.2	1.4
17		20	18	18	14		
18	100	100	100	100	100	100	100
28	95	33	52	54	48	58	95
41				16	19	24	33
43				34	45	56	69
44		12	14	36	47	62	95
55				15	24	28	39
57				21	32	40	49
60					16	28	39
69				16	26	28	33
71				16	15	20	21
73				14	22	24	51
83					16	20	23
85							23

% Abundance

Table A.18. Solid state mass spectral data of Nylon 66/CuCl films photooxidized for 48 hours in the UV chamber under a pyrex filter.

Mass	Retention times (min.) 0.4	0.7	0.9	1.1	1.2	1.4	1.5	1.8
18	14	31	28	18	18	19	22	16
28	100	100	100	100	100	100	100	100
32	22	27	26	26	30	24	25	24
43		9	11	12	8	15	17	19
44	8	9	12	12	13	30	33	46
55						10	8	13
57			10	10	9	14	14	21
69		8				10	11	15
71						11	12	12
85								

% Abundance

Table A.19. Solid state mass spectral data of Nylon 66/CuCl films photooxidized for 96 hours in the UV chamber under a pyrex filter.

Mass	Retention times (min.) 0.4	0.7	0.9	1.0	1.1	1.2	1.4	1.5	1.6
18		24	24	27	21	19	14	20	15
28	100	100	100	100	100	100	100	100	100
32	28	31	20	27	25	28	28	30	22
41									9
43			8	12	15	13	12	17	32
44			10	13	18	21	25	36	64
55						9		12	21
57				12	15	14	11	17	35
59									10
69					10		9	14	21
71					8	9		11	18
73									10
83									15
85									15
97									15

% Abundance

Table A.20. Solid state mass spectral data of Nylon 66 fibers photooxidized for 48 hours in the UV chamber under a pyrex filter.

Mass	Retention times (min.) 0.3	0.7	0.9	1.0	1.2	1.3	1.4	1.5
17	6	21	21	21	16	21	21	18
18	31	100	100	100	100	100	100	35
28	100	85	84	84	63	67	81	100
29							4	4
32	21	24	22	21	18	20	22	26
41				3	3	5	7	9
43		5	7	8	8	11	14	19
44			3	4	3	5	7	10
45								3
55			4	5	5	7	10	12
56			3	4	5	7	13	17
57		5	8	10	11	17	24	32
60						3	4	7
69			3	4	4	6	8	12
70							3	4
71			5	6	5	18	11	12
73					3	4	6	10
81					2		3	4
83				3	3	5	5	9
84								4
85				3	4	5	8	9
98								4

% Abundance

Table A.21. Solid state mass spectral data of Nylon 66 fibers photooxidized for 96 hours in the UV chamber under a pyrex filter.

Mass	Retention times (min.) 0.3	0.7	0.9	1.0	1.2	1.3	1.4
17	22	20	19	19	20	15	10
18	100	100	100	100	100	72	45
28	77	40	50	54	85	100	100
29			3	4	6	7	9
32	19	11	14	14	22	26	22
41		4	7	8	16	22	22
42					5		
43	4	7	11	18	33	38	40
44			4	5	9	15	13
45			3	5	9	13	15
55		6	11	14	23	34	33
56		5	8	13	17	23	17
57	9	13	21	29	46	56	54
60			4	6	14	17	19
67			2	3	6	7	9
69	5	7	13	15	26	40	39
70		3	5	7	11	14	16
71	4	6	13	17	28	34	40
73		2	6	7	14	21	26
81		3	5	7	12	13	15
82			4	5	7	9	10
83		5	10	14	24	31	32
84		3	6	6	12	16	16
85		4	9	11	21	27	27
99			4	4	8	10	12
112				3	5	7	8
125				3	6	7	8

% Abundance

Tables A.22 - A.23

Solid State Mass Spectral Data of Bright Nylon 66 Fibers Photooxidized for 48 and 147 hours in the Weatherometer.

Table A.22. Solid state mass spectral data of Nylon 66 fibers photooxidized for 48 hours in the Weatherometer.

Mass	Retention times (min.) 0.3	0.5	0.7	0.9	1.0	1.2	1.3	1.4
17	16	19	22	20	19	22	8	
18	100	100	100	100	100	97	53	67
28	98	81	69	63	70	87	100	100
29	2				3	5	6	
32	25	24	16	18	18	22	9	25
41	6		3	6	10	13	11	31
43	11	5	7	12	18	38	45	86
44			2	3	5	8	6	17
55	9	4	6	9	16	19	25	50
56					4	5	10	
57	13	9	9	17	22	40	56	75
60	6				3	5		
67					3	8		
69	9	4	6	8	13	11	16	64
70	3			4	5	6		19
71	9	4	6	11	16	22	32	64
73	8				7			
81				3	6	12	11	19
82				3	5	13		
83	7	3	5	9	12	25	13	50
84	3		2	3	5	8	7	
85	6	3	4	8	11	25	19	45
91				2	3	7		
95			2	3	5	10	6	22
96					2			
97	5	3	4	7	14	8	14	47
98	2			3	3			
99	2			3	4			17
125					3	6	5	

% Abundance

Table A.23. Solid state mass spectral data of Nylon 66 fibers photooxidized for 147 hours in the Weatherometer.

Mass	Retention times (min.) 0.3	0.5	0.7	0.9	1.0	1.2	1.3	1.4
17	12	18	18	20	20	19	17	12
18	100	100	100	100	100	100	85	59
28	59	63	57	58	68	96	100	100
29				2	2	3		
32		16	15	18	21	23	27	28
41			2	3	4	5	7	8
42		1						
43		8	21	26	30	31	25	26
44		1	3	3	4	6	8	6
55		1	1	4	4	11	10	18
56						2	2	4
57		2	4	6	10	16	14	24
58		1	7	5	6	7	4	6
59			2					
60						4	5	6
67								3
69			2	4	5	10	9	16
70				2		3	3	6
71		1	2	5	5	11	12	19
73						3	4	7
81						3	3	6
82				2	3		3	4
83		1	2	3	6	8	8	18
84						4	5	9
85			2	4	5	8	10	15
95						3	4	5
96								3
97			1	3	5	8	8	14
98						3	4	9
99							3	6
112							2	5
125							2	4

% Abundance

APPENDIX B

MASS SPECTRA

FIGURES

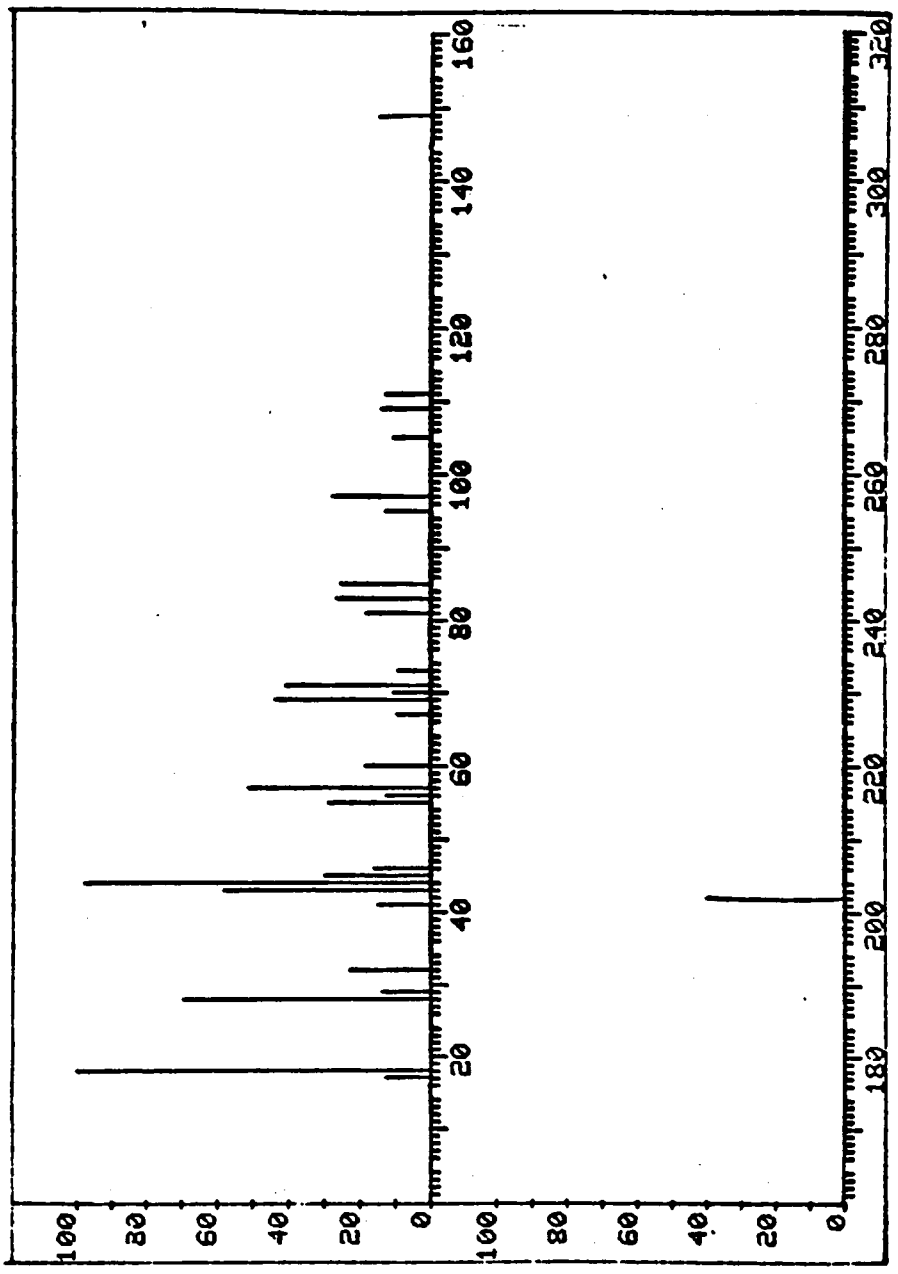

Figure B.1. Mass spectra of Nylon 66 cast from formic acid but not dried (1.2 min).

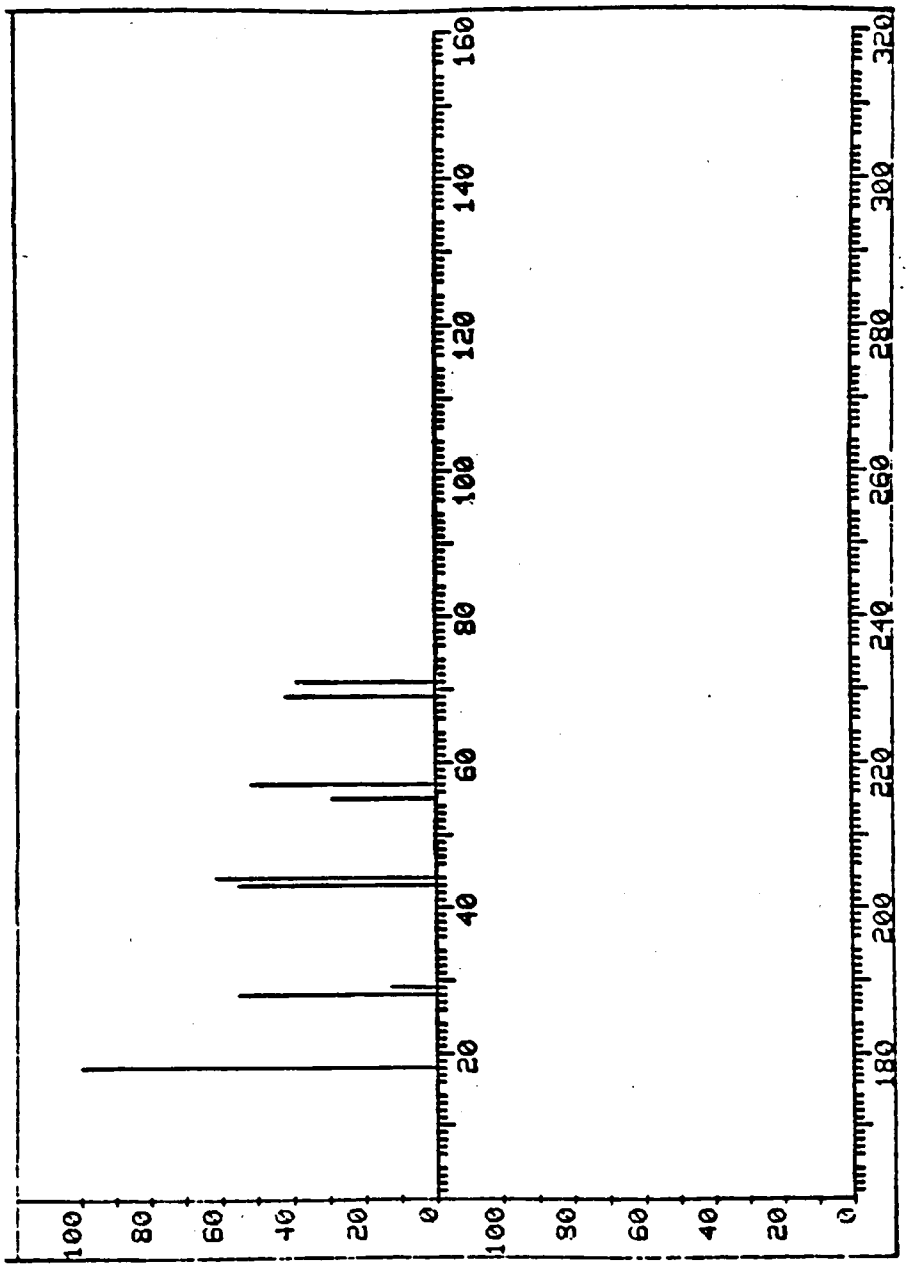

Figure B.2. Mass spectra of Nylon 66 cast from formic acid and dried at 90°C under vacuum (1.7 min).

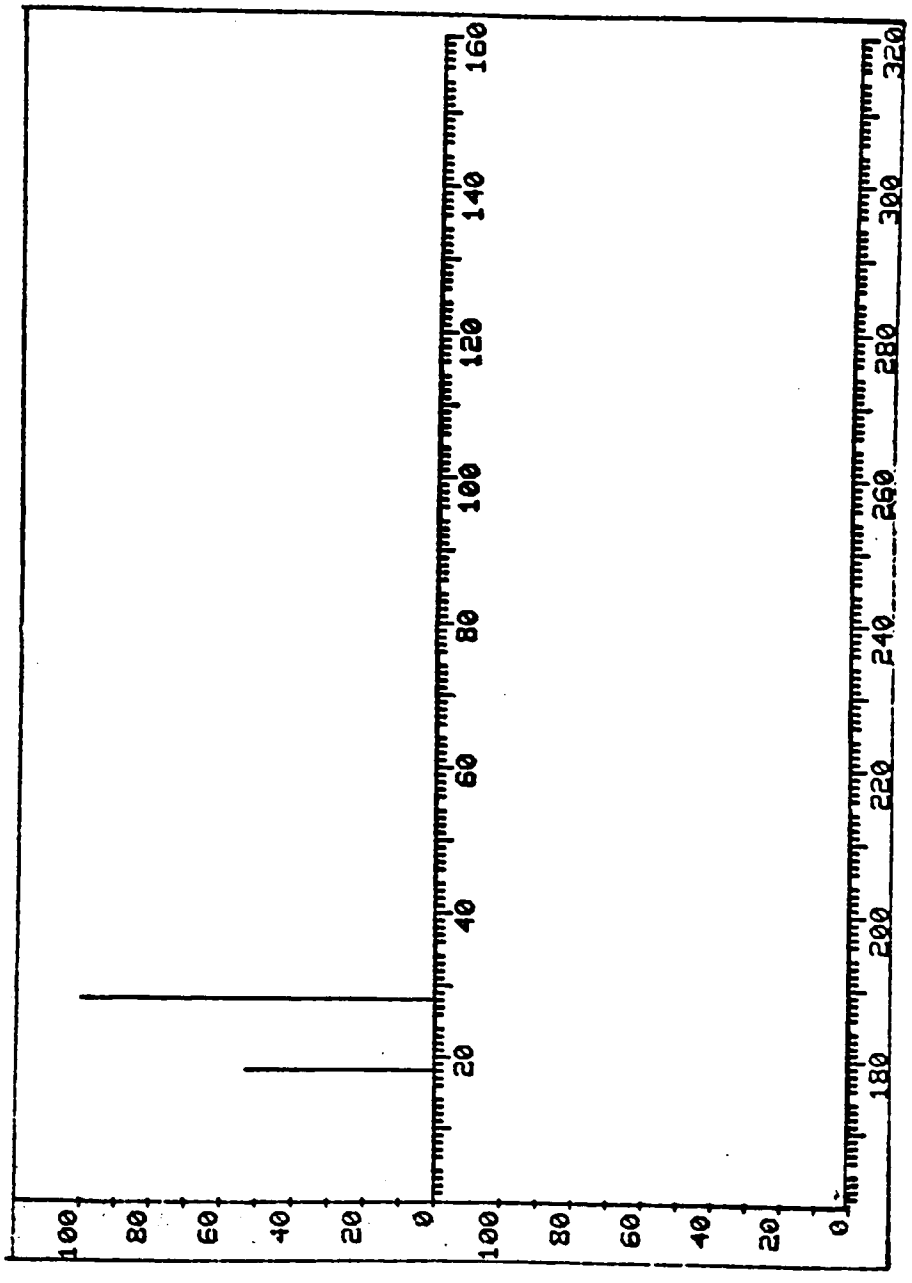

Figure B.3. Mass spectra of unexposed Nylon 66 film (1.3 min).

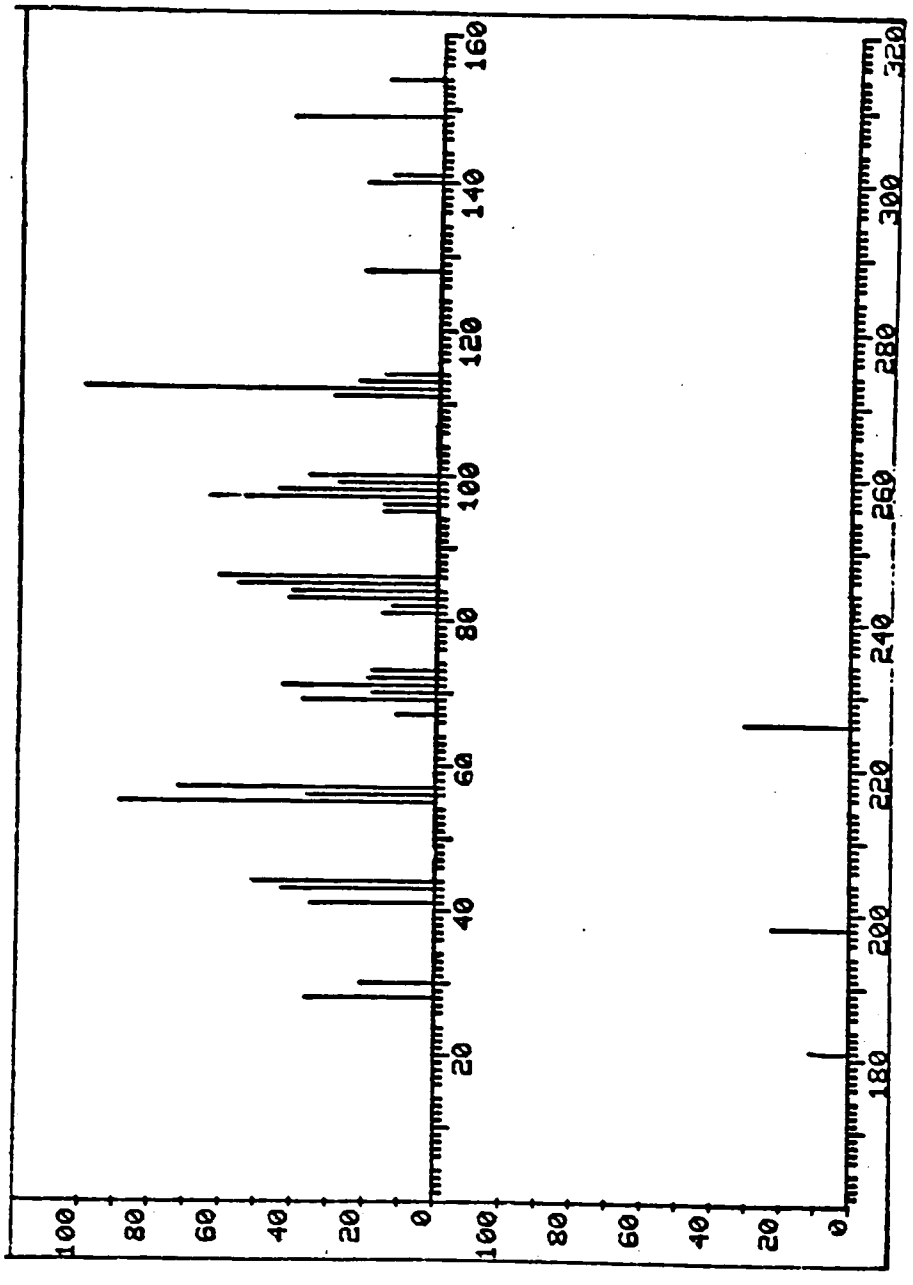

Figure B.4. Mass spectra of unexposed Nylon 66 film (2.3 min).

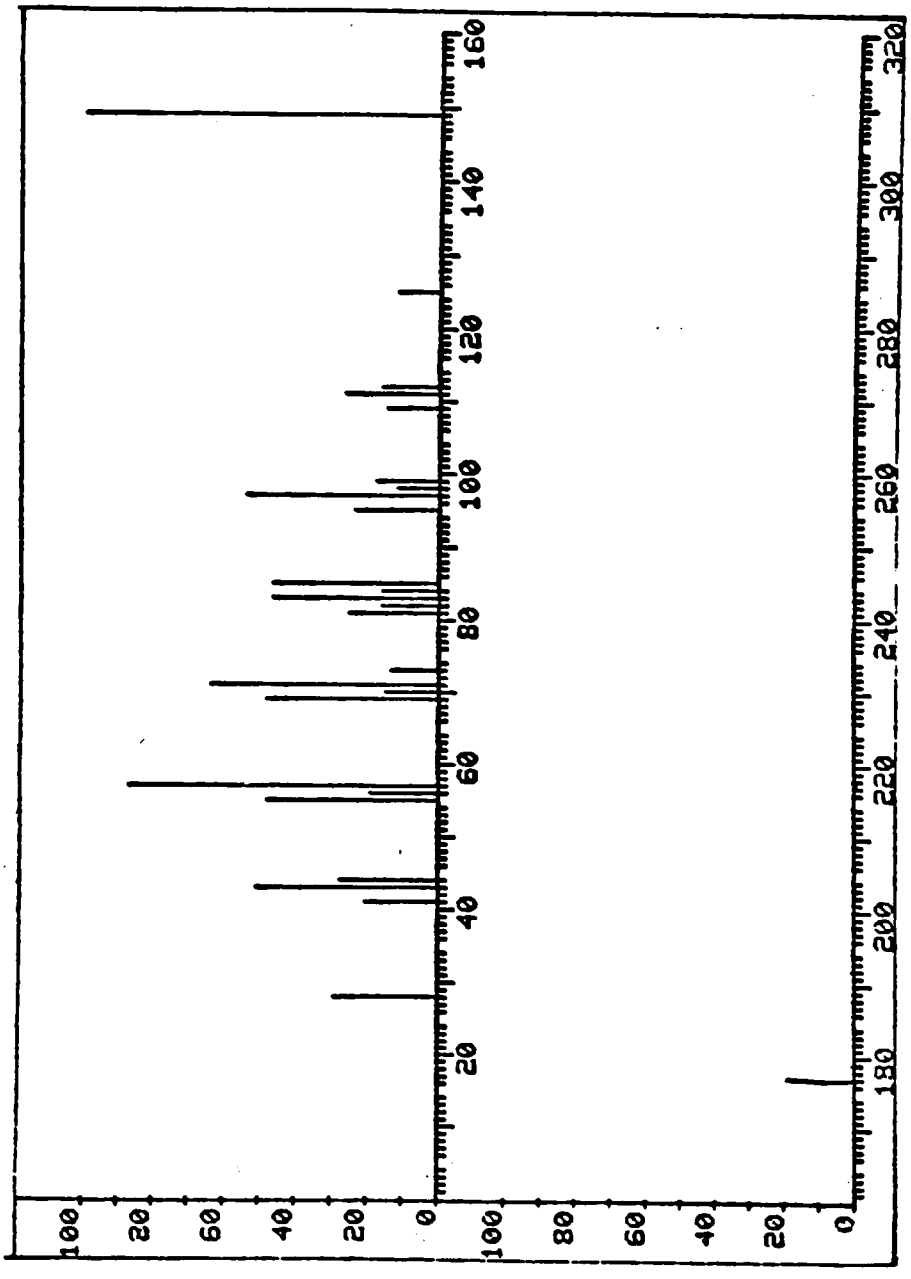

Figure B.5. Mass spectra of unexposed Nylon 66/$MnCl_2$ film (1.9 min).

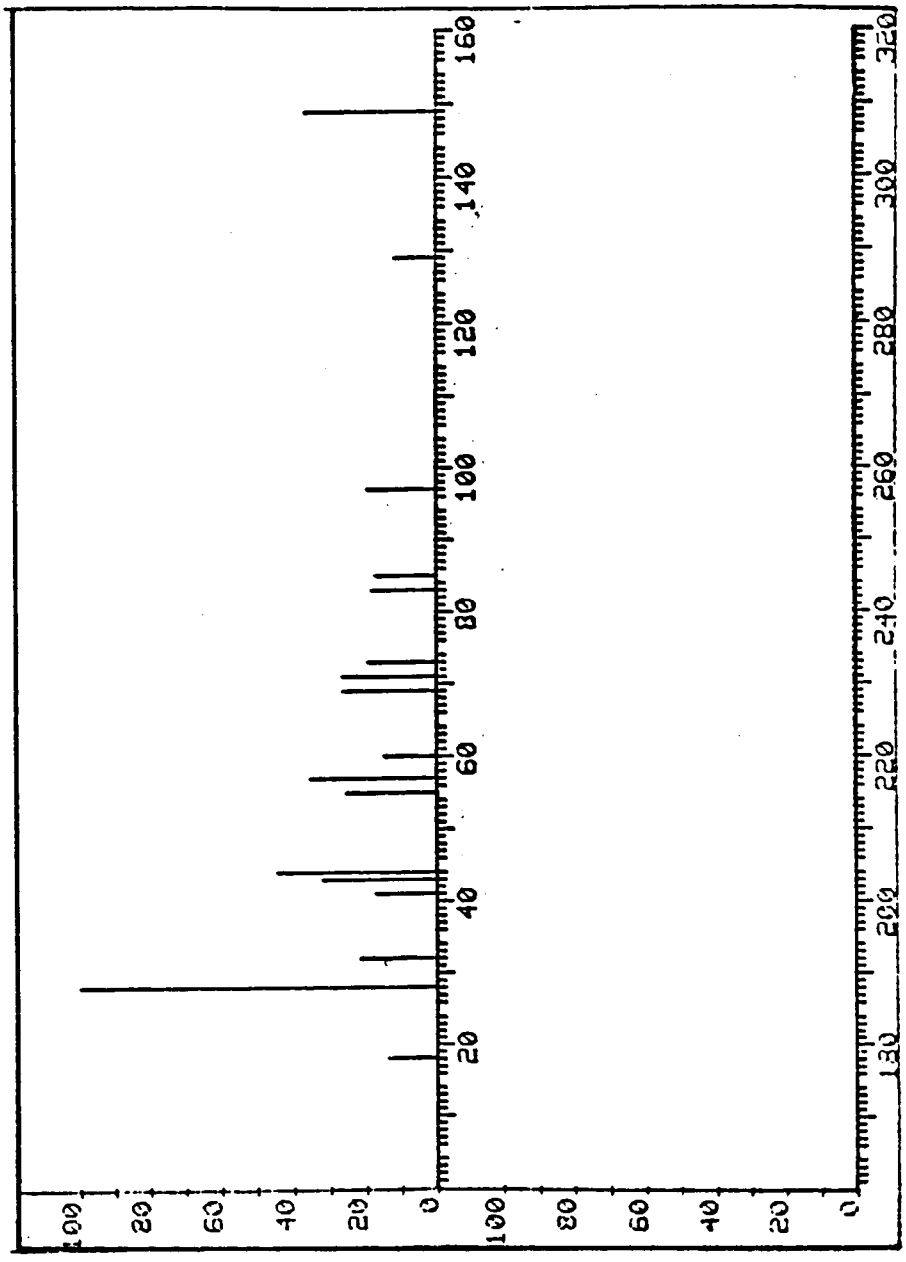

Figure B.6. Mass spectra of unexposed Nylon 66/CuCl film (2.0 min).

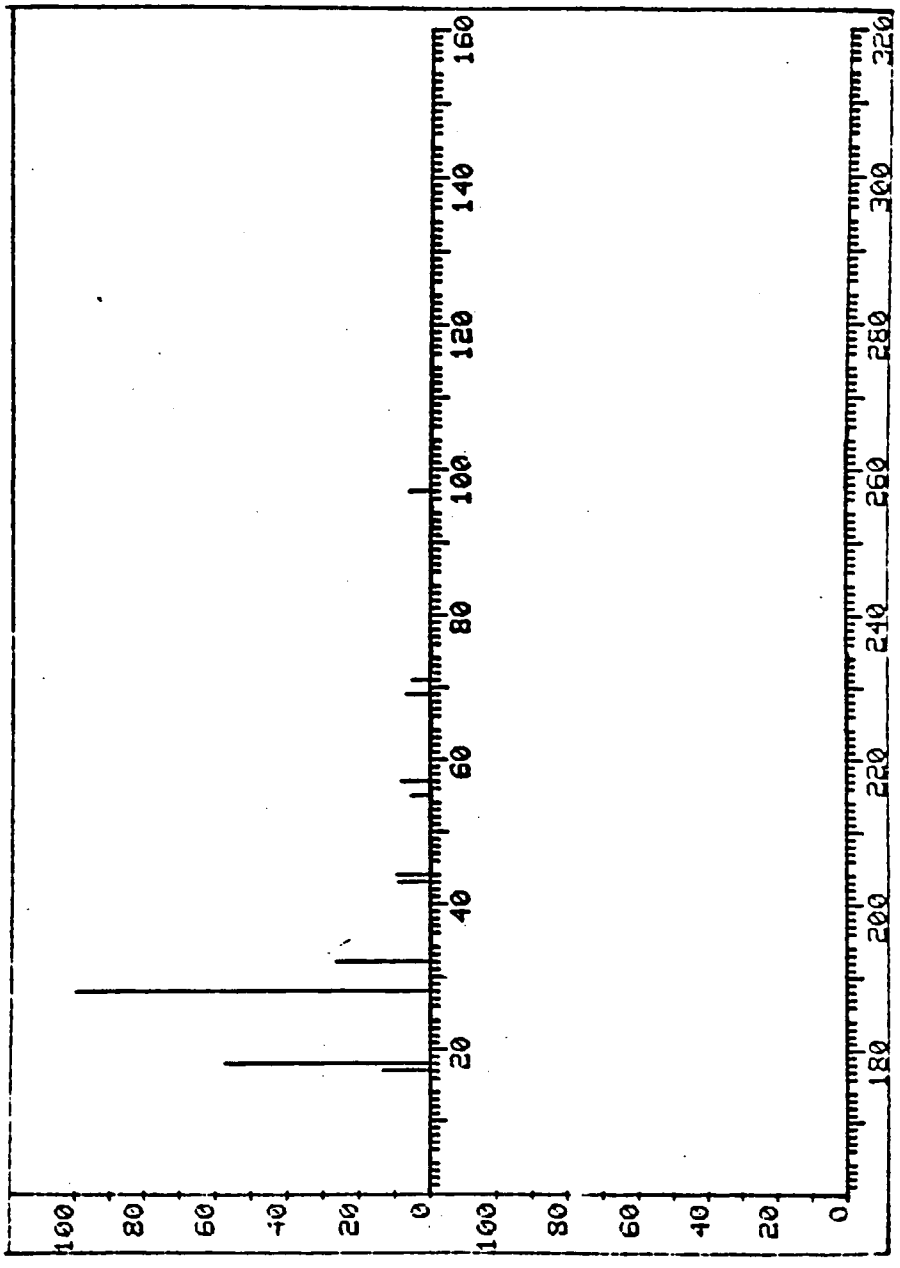

Figure B.7. Mass spectra of unexposed Nylon 66 fiber (2.0 min).

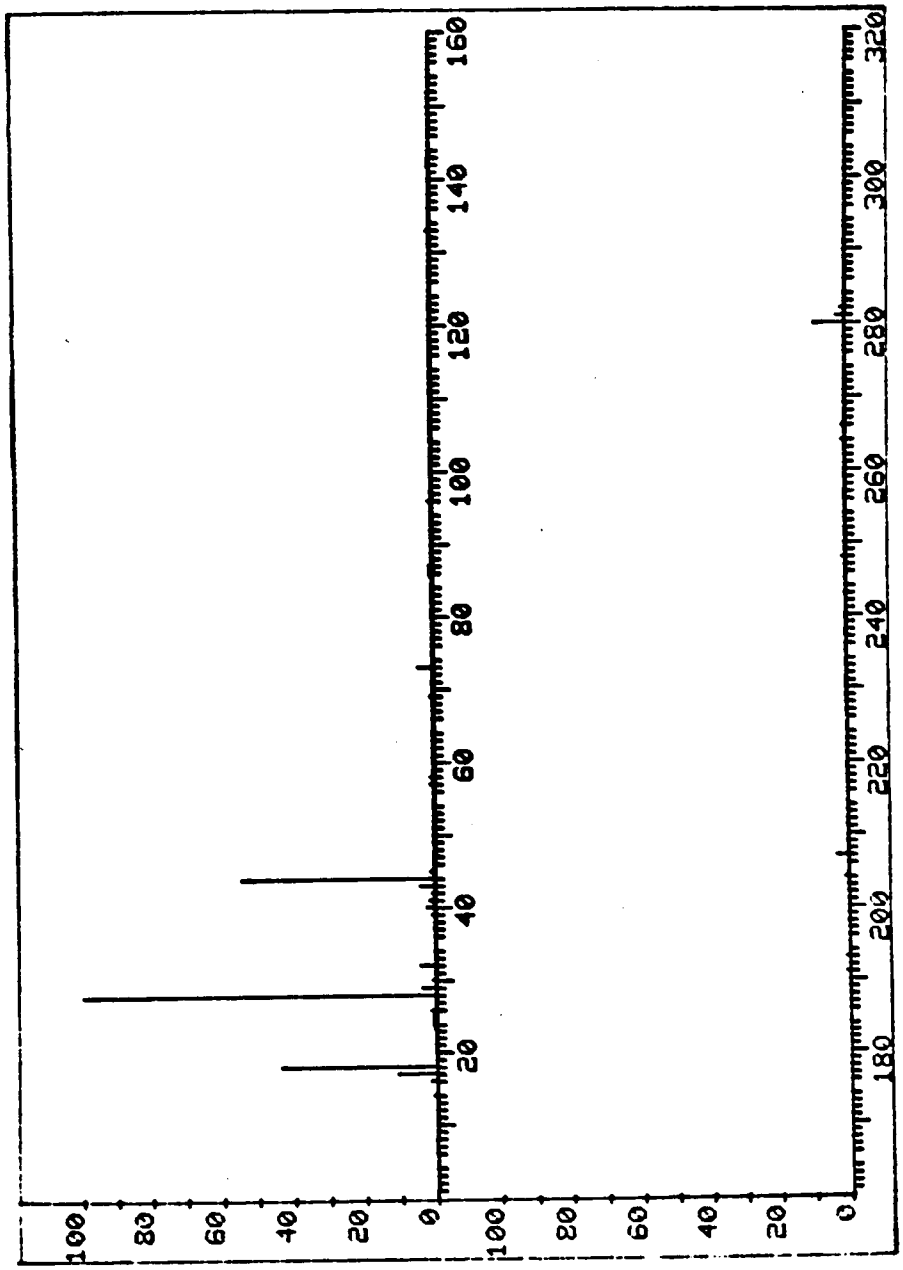

Figure B.8. Mass spectra of volatile products formed during the 24 hour photolysis of Nylon 66 film.

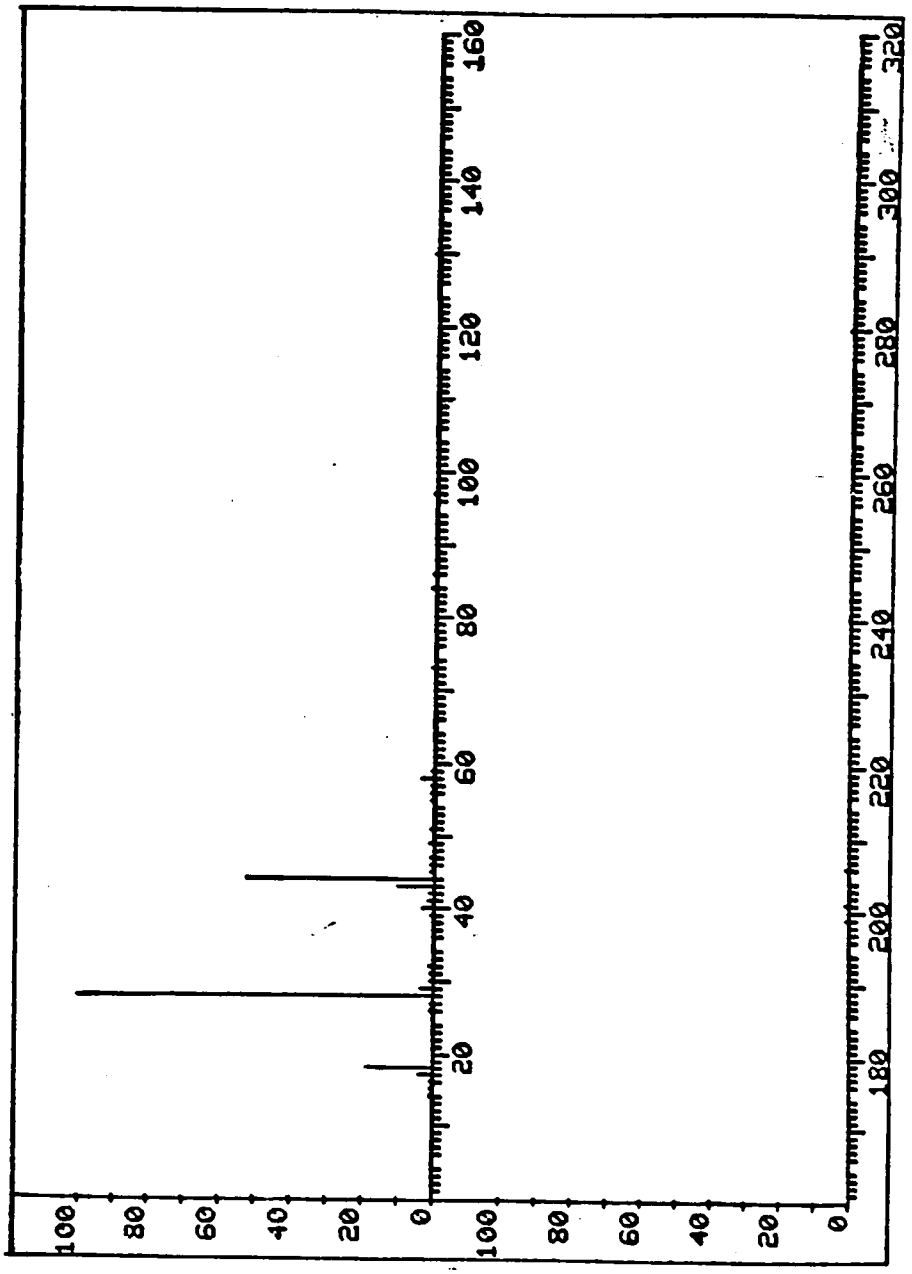

Figure B.9. Mass spectra of volatile products formed during the 48 hour photolysis of Nylon 66 film.

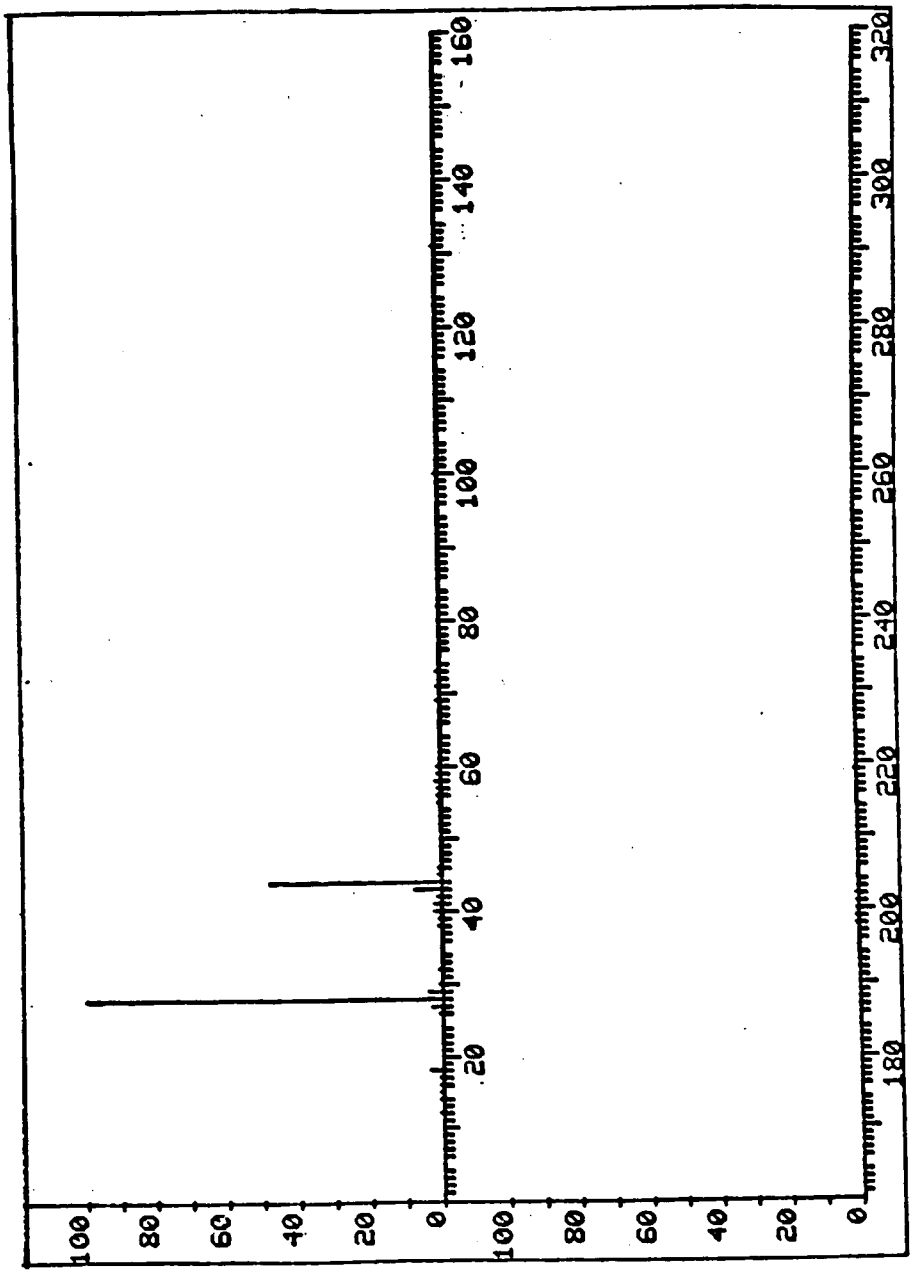

Figure B.10. Mass spectra of volatile products formed during the 24 hour photolysis of Nylon 66/$MnCl_2$ film.

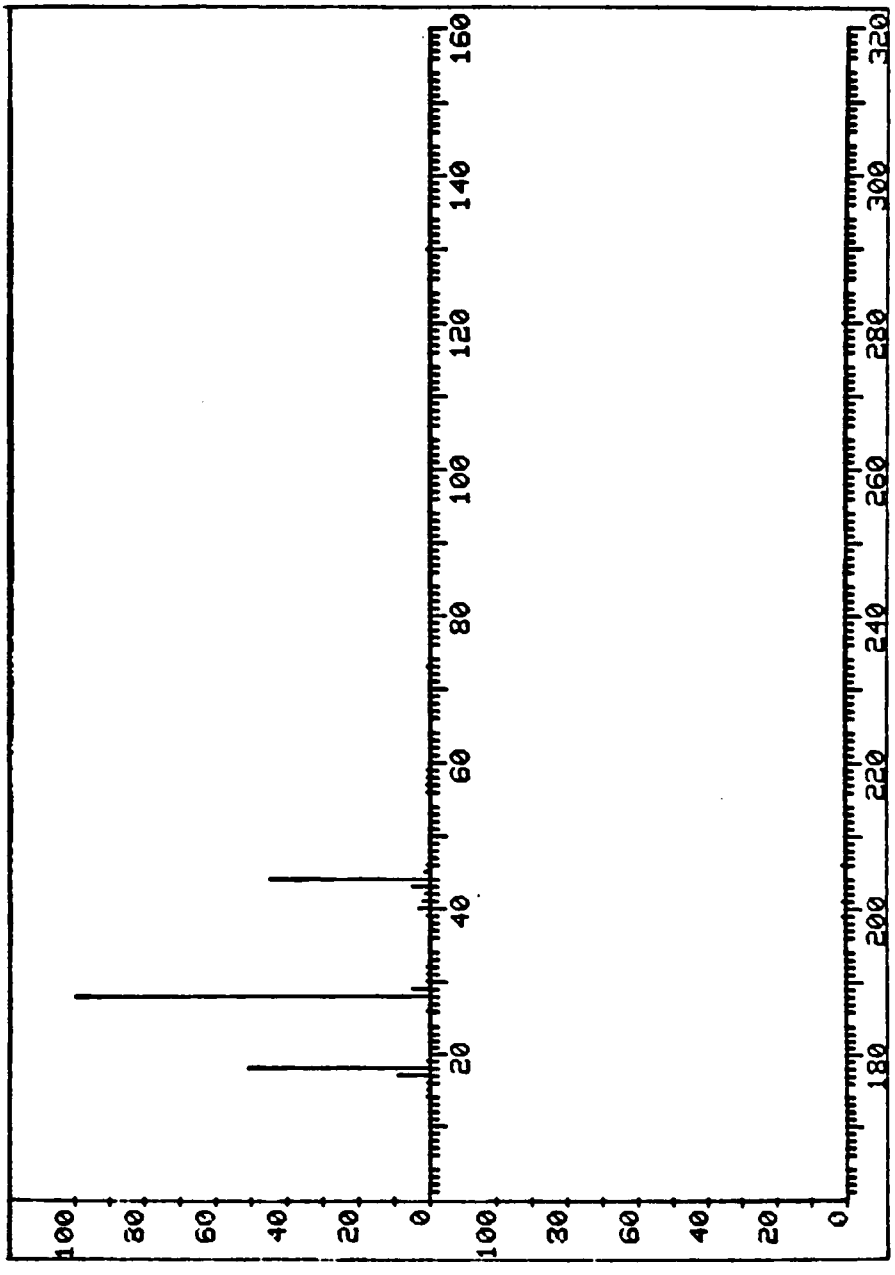

Figure B.11. Mass spectra of volatile products formed during the 48 hour photolysis of Nylon 66/$MnCl_2$ film.

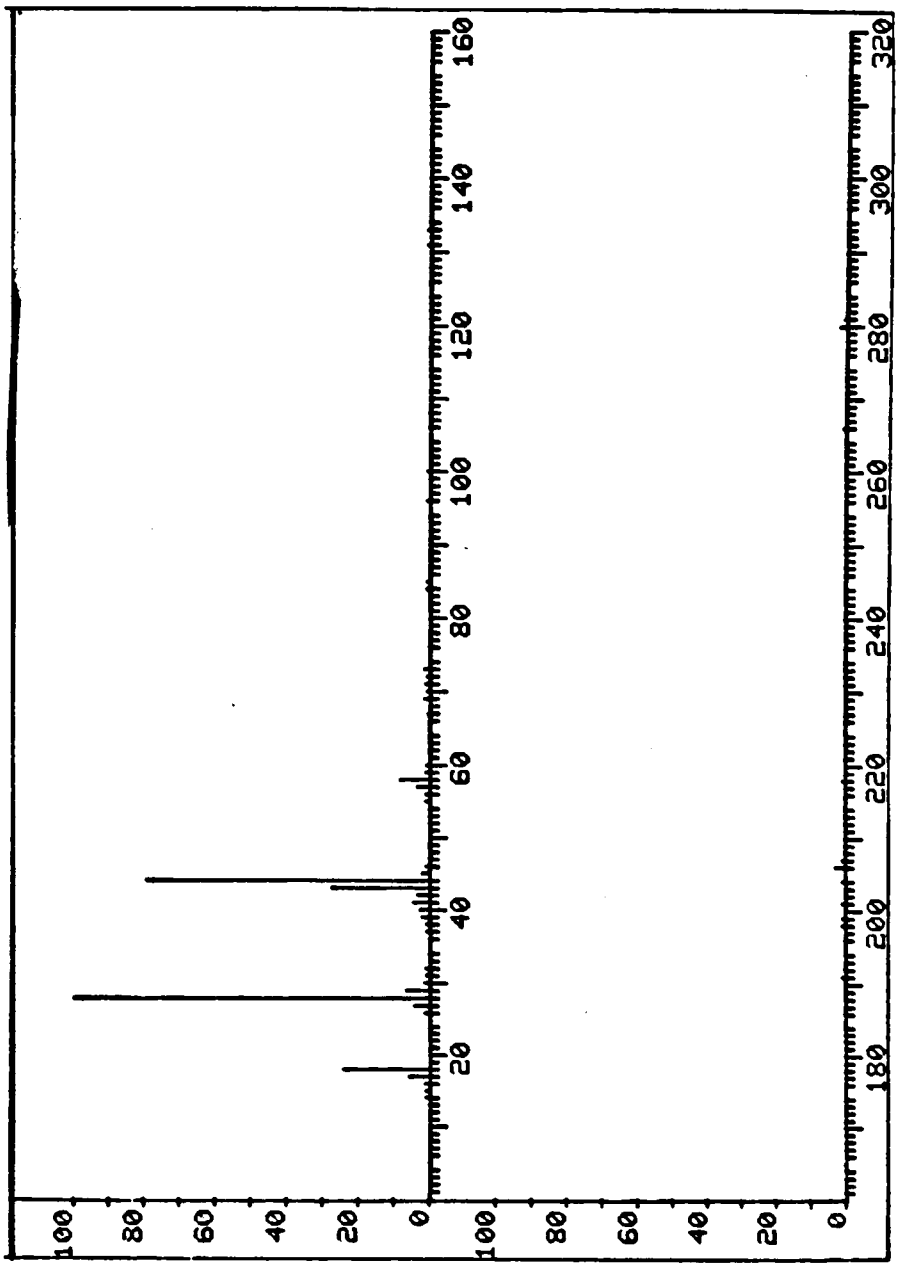

Figure B.12. Mass spectra of volatile products formed during the 24 hour photolysis of Nylon 66/CuCl film.

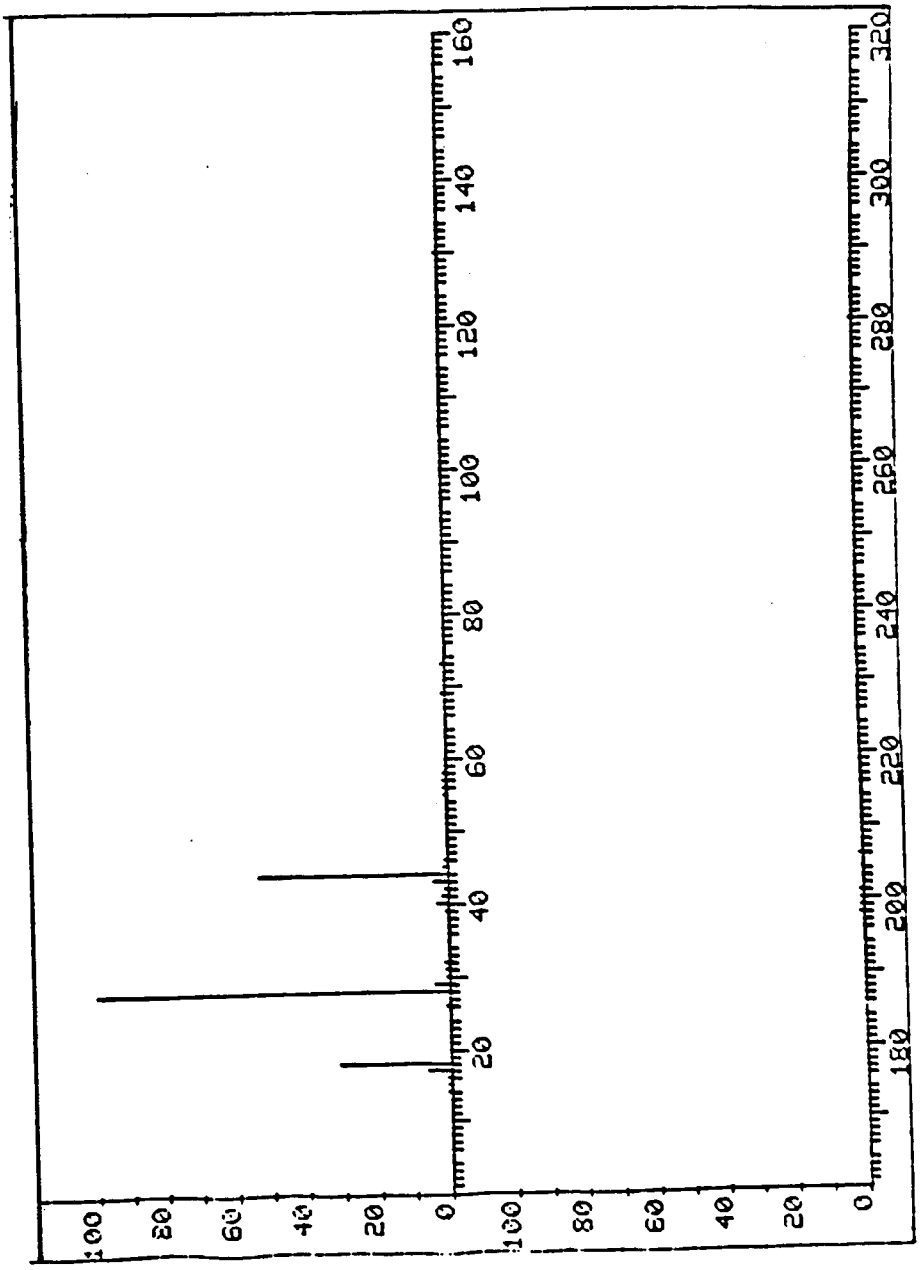

Figure B.13. Mass spectra of volatile products formed during the 48 hour photolysis of Nylon 66/CuCl film.

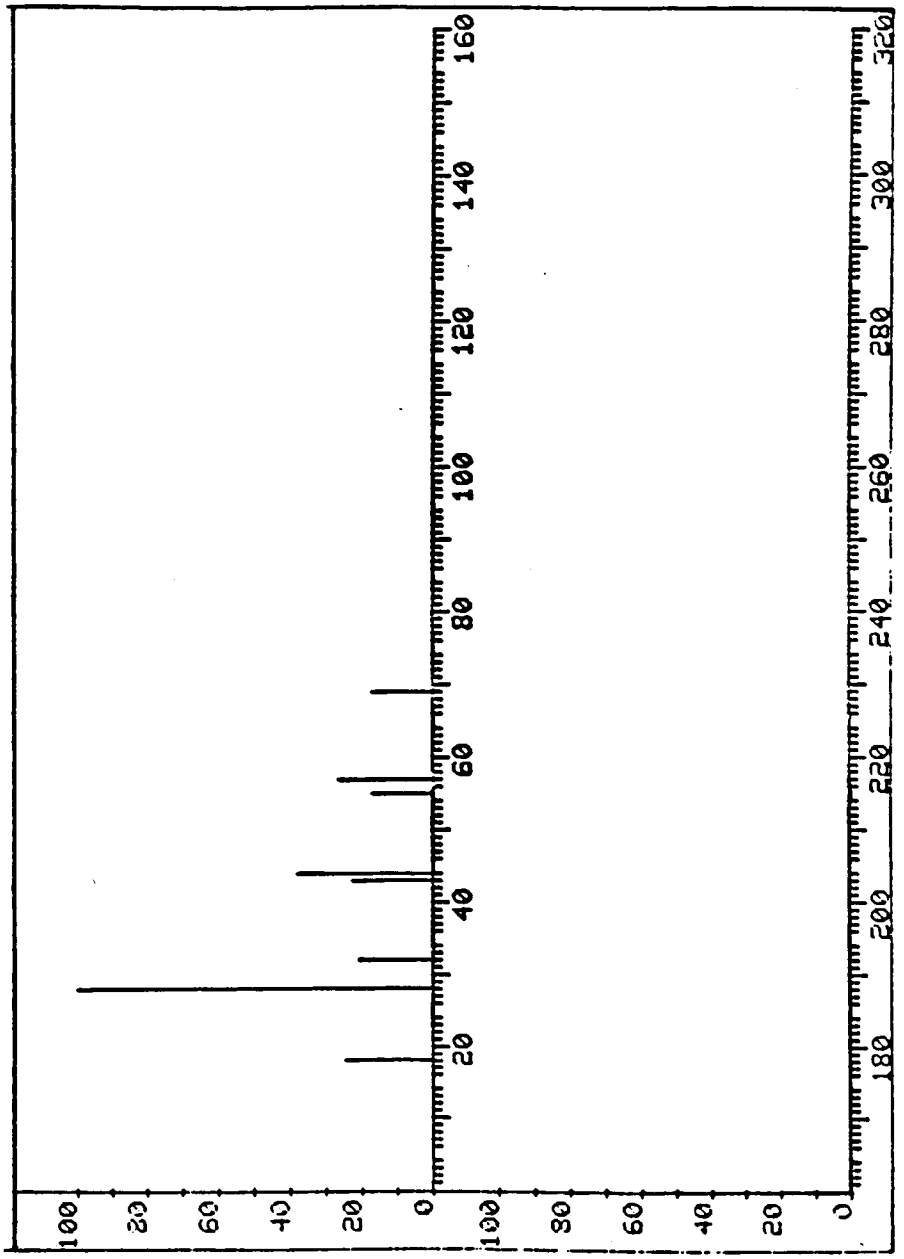

Figure B.14. Mass spectra of Nylon 66 film photolyzed for 24 hours (2.0 min).

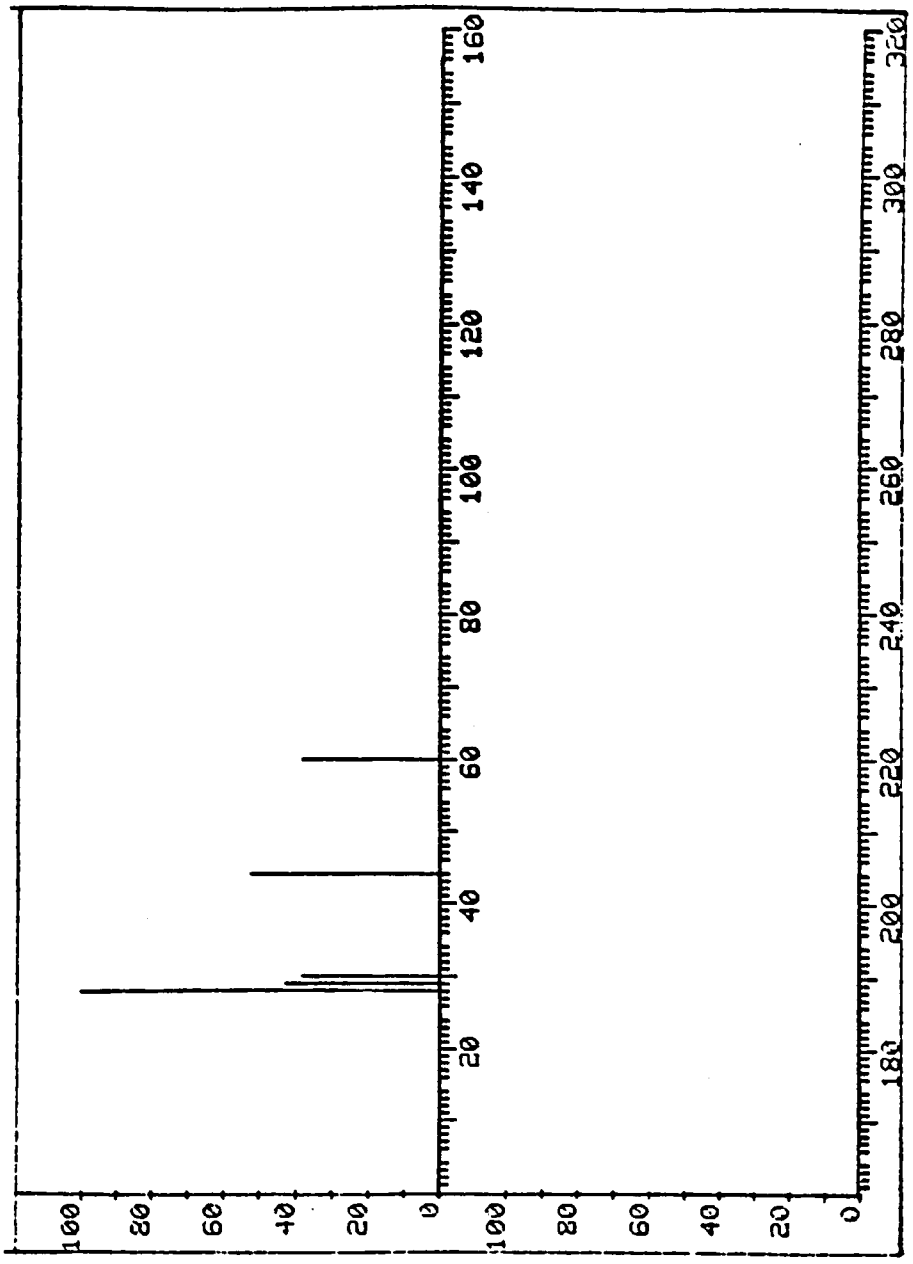

Figure B.15. Mass spectra of Nylon 66 film photolyzed for 48 hours (1.3 min).

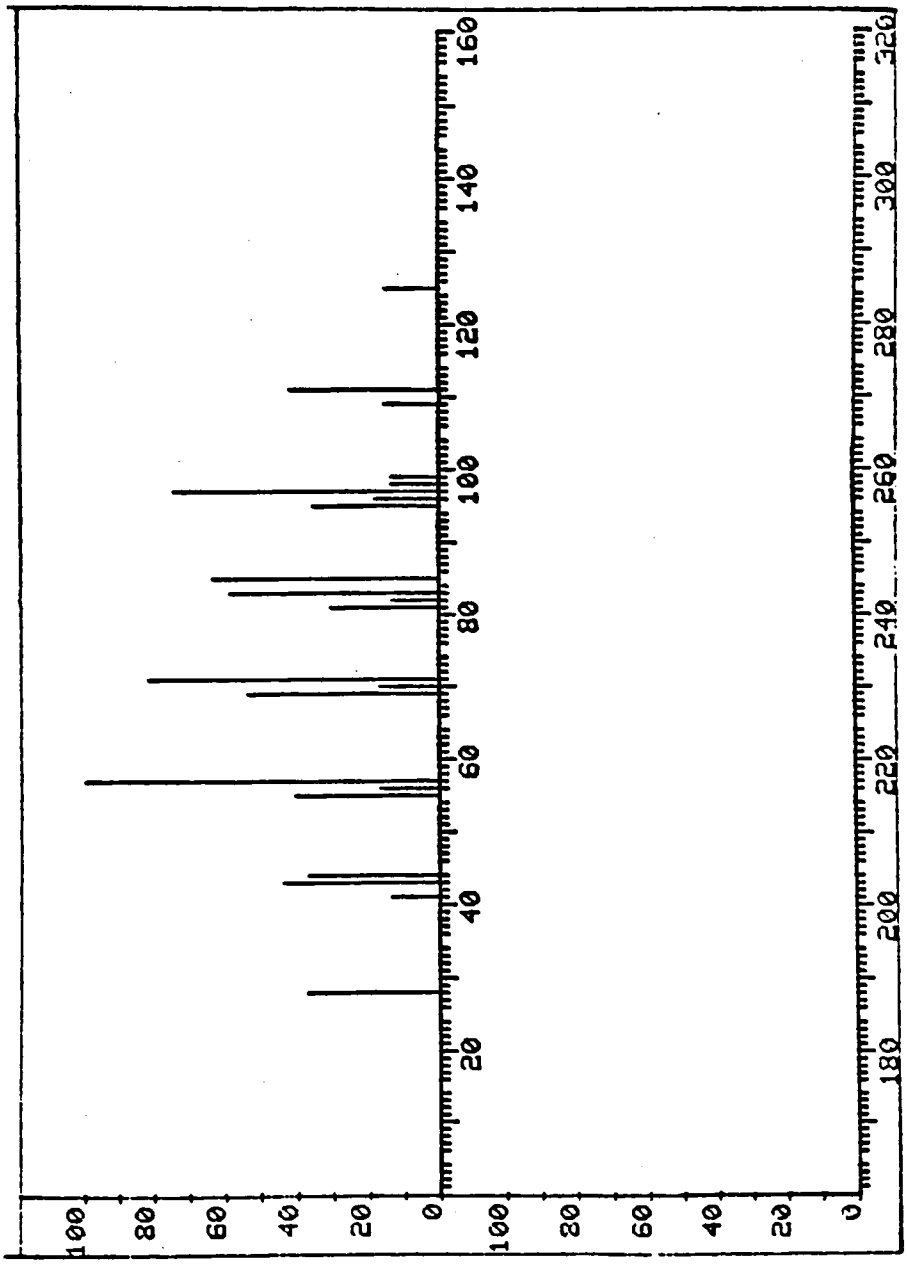

Figure B.16. Mass spectra of Nylon 66 film photolyzed for 48 hours (2.0 min).

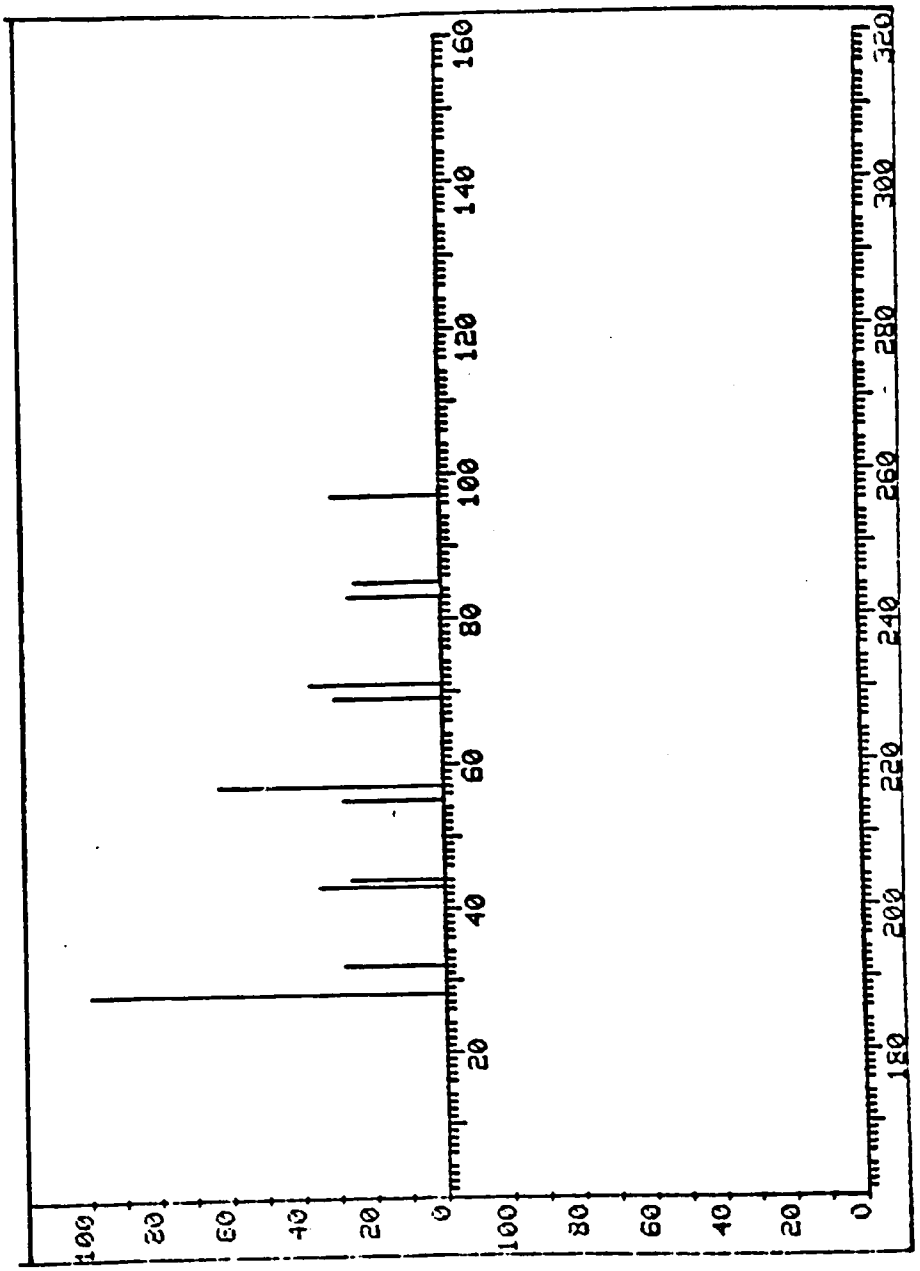

Figure B.17. Mass spectra of Nylon 66/$MnCl_2$ film photolyzed for 24 hours (2.0 min).

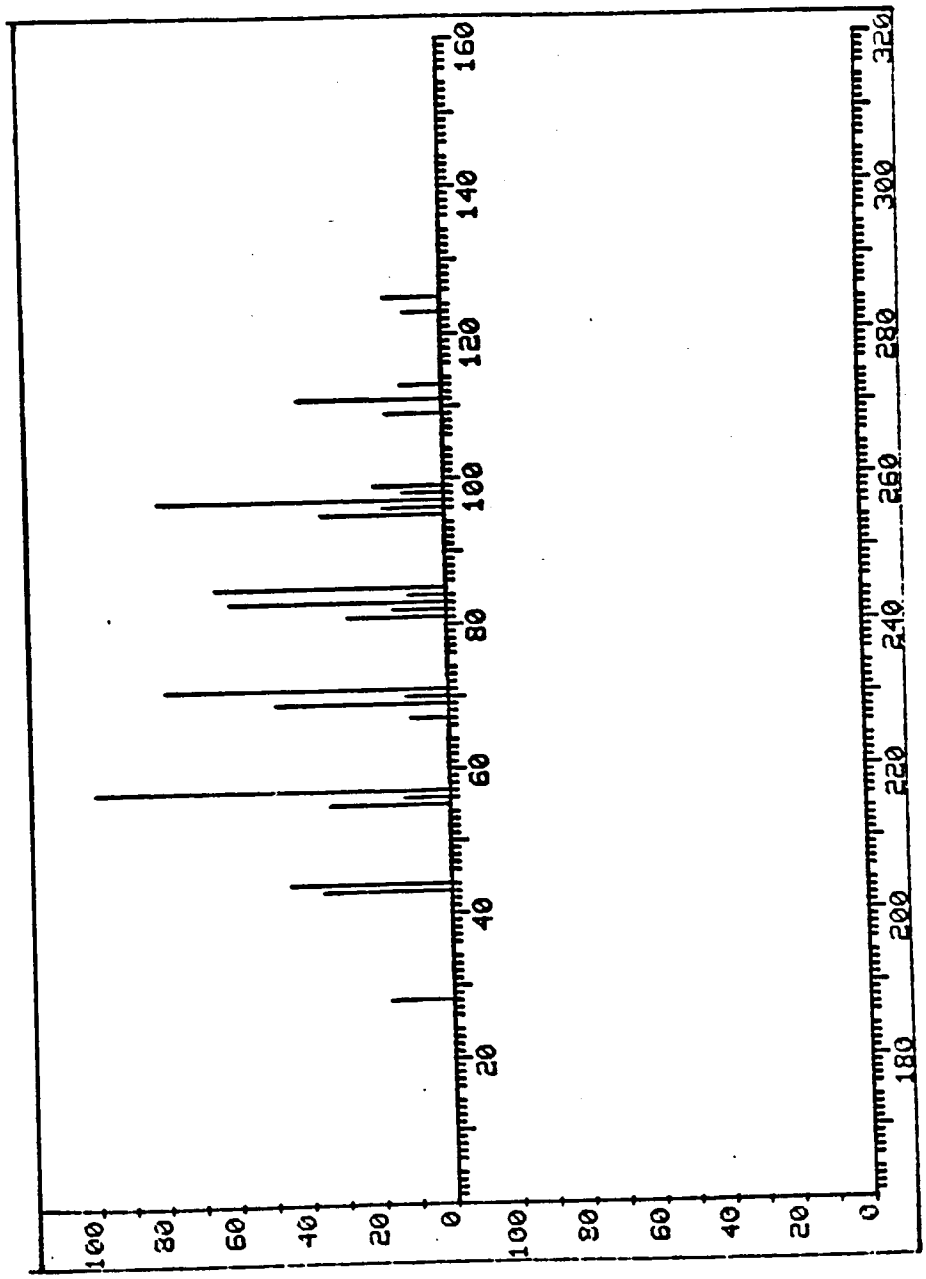

Figure B.18. Mass spectra of Nylon 66/$MnCl_2$ film photolyzed for 48 hours (2.0 min).

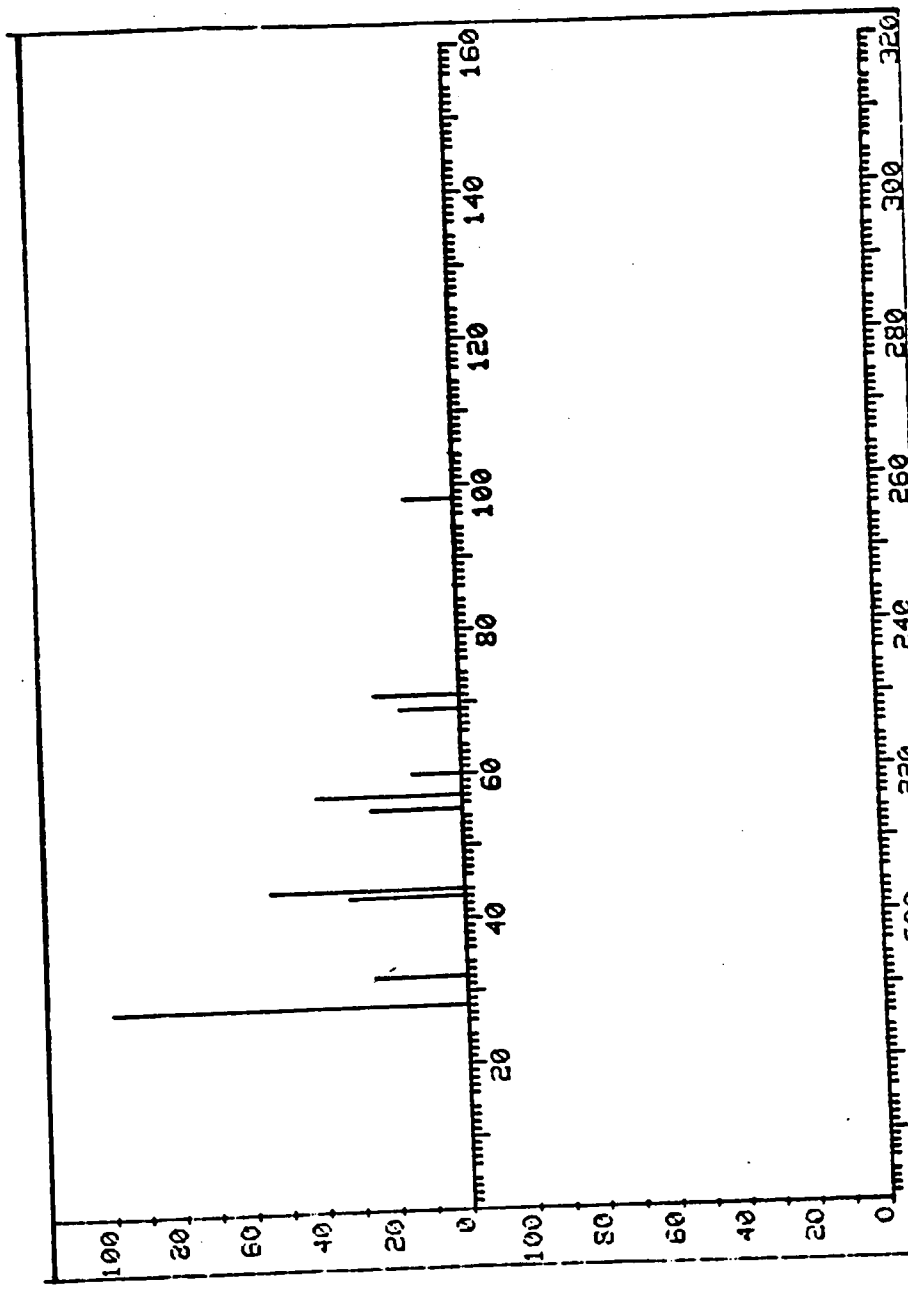

Figure B.19. Mass spectra of Nylon 66/CuCl film photolyzed for 24 hours (2.0 min).

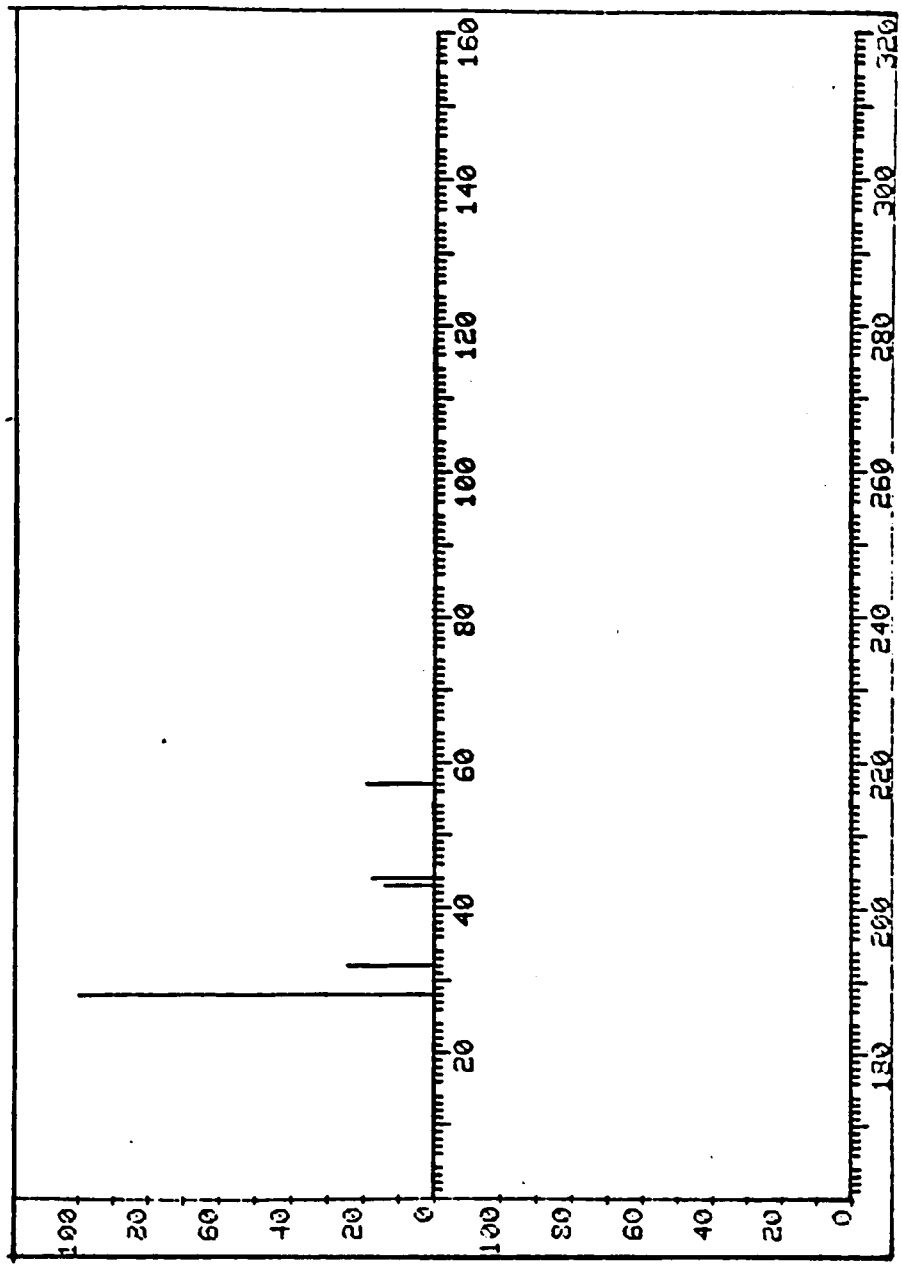

Figure B.20. Mass spectra of Nylon 66/CuCl film photolyzed for 48 hours (2.0 min).

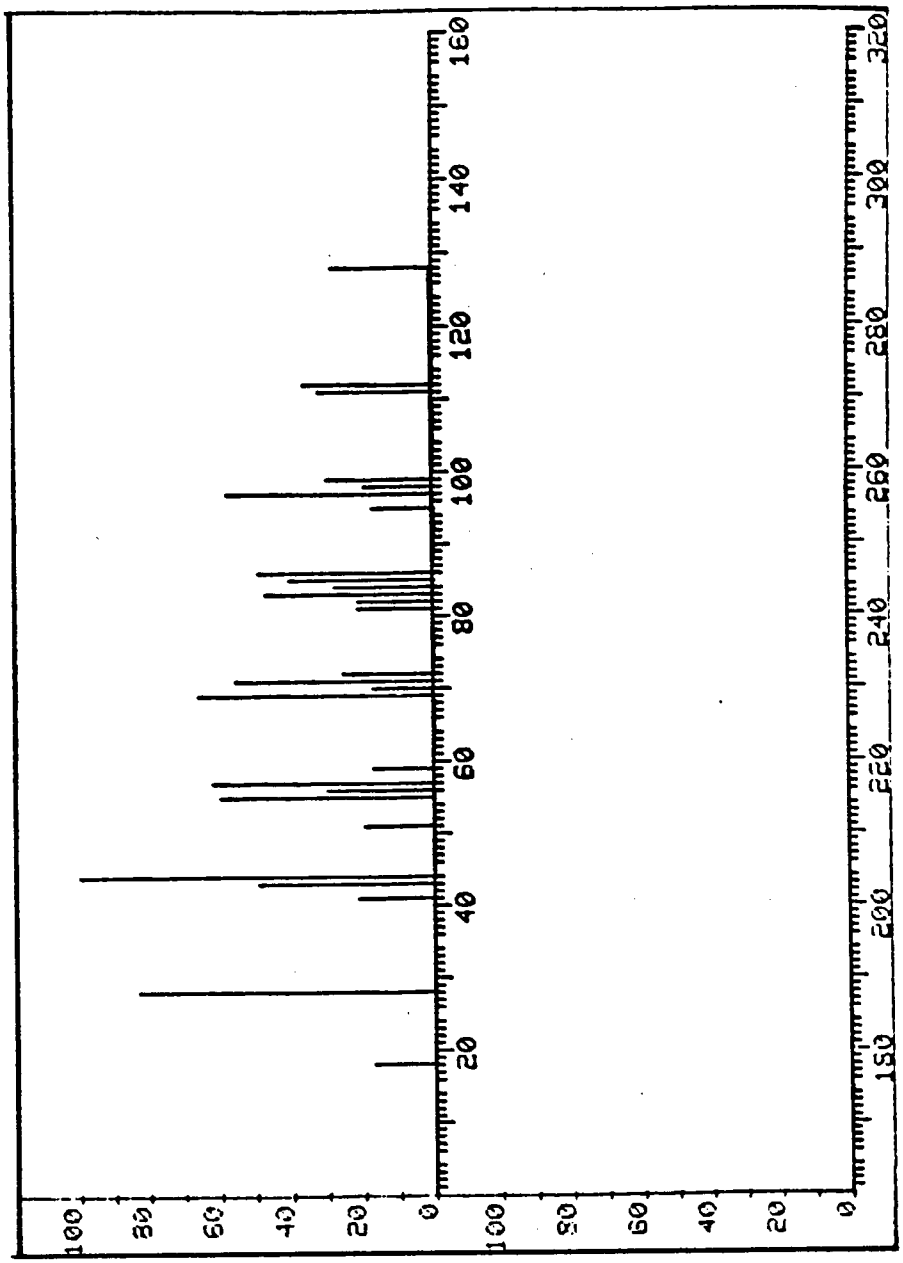

Figure B.21. Mass spectra of Nylon 66 films photooxidized in the UV chamber for 24 hours (2.1 min).

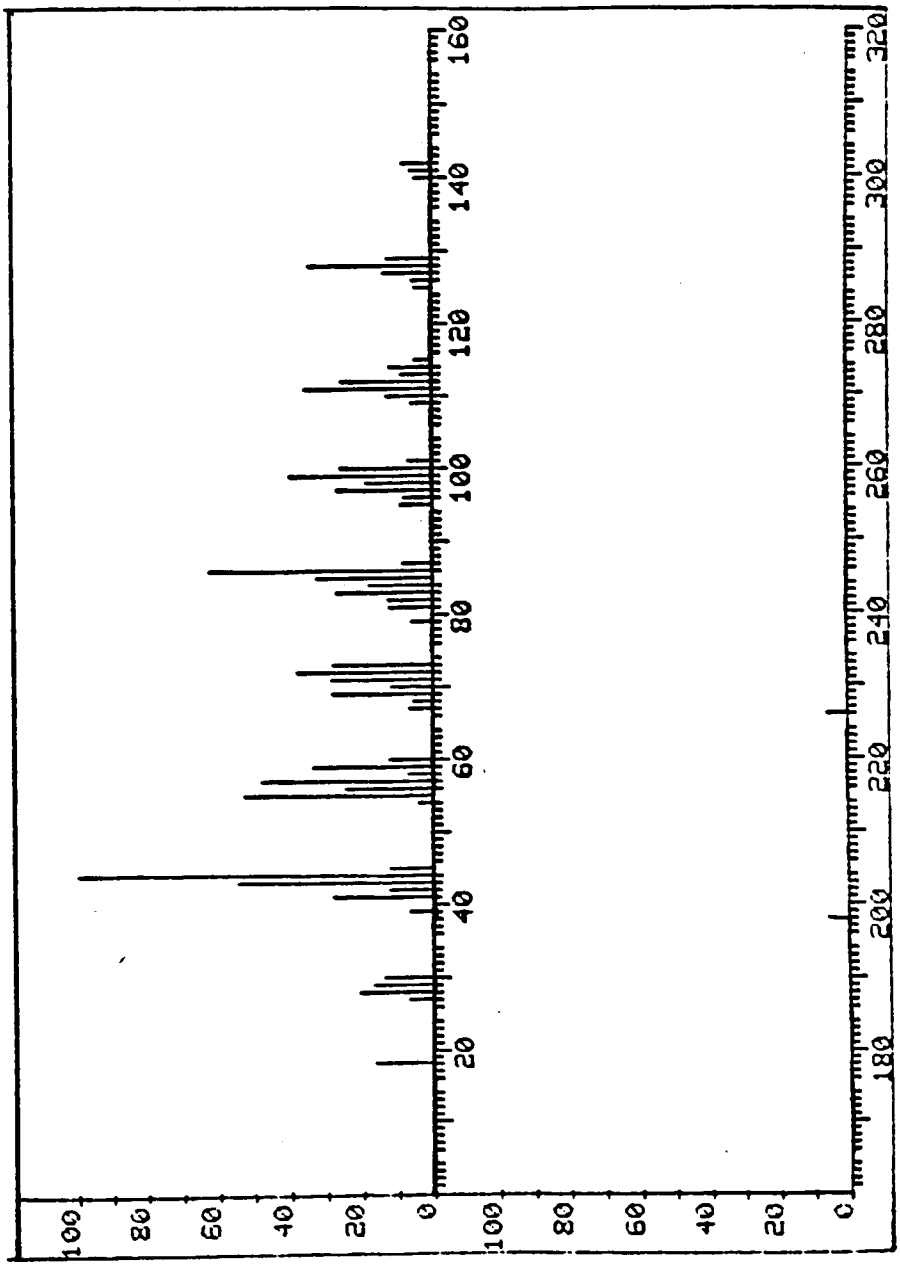

Figure B.22. Mass spectra of Nylon 66 films photooxidized in the UV chamber for 48 hours (2.3 min).

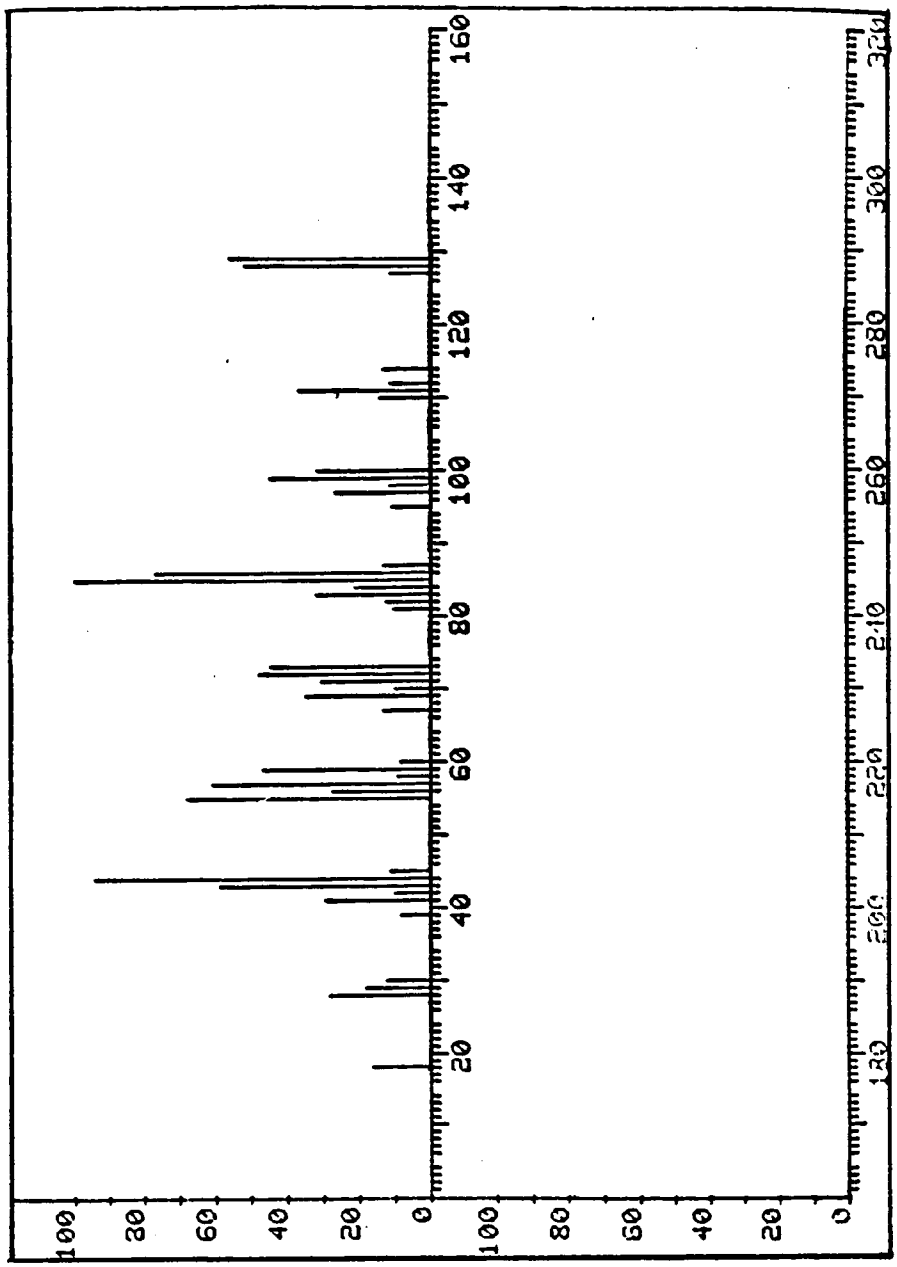

Figure B.23. Mass spectra of Nylon 66 films photooxidized in the UV chamber for 96 hours (2.1 min).

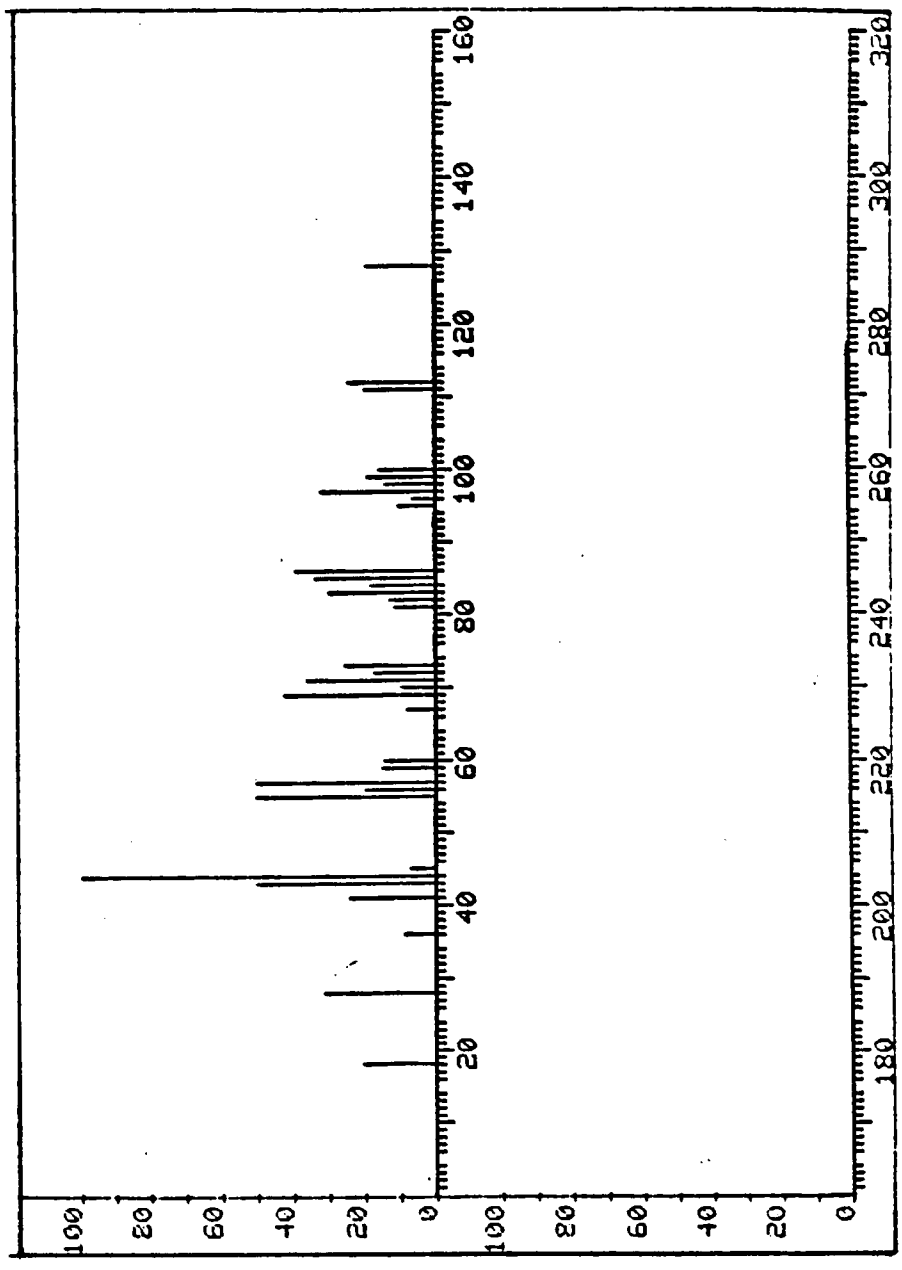

Figure B.24. Mass spectra of Nylon 66/$MnCl_2$ films photooxidized in the UV chamber for 24 hours (2.0 min).

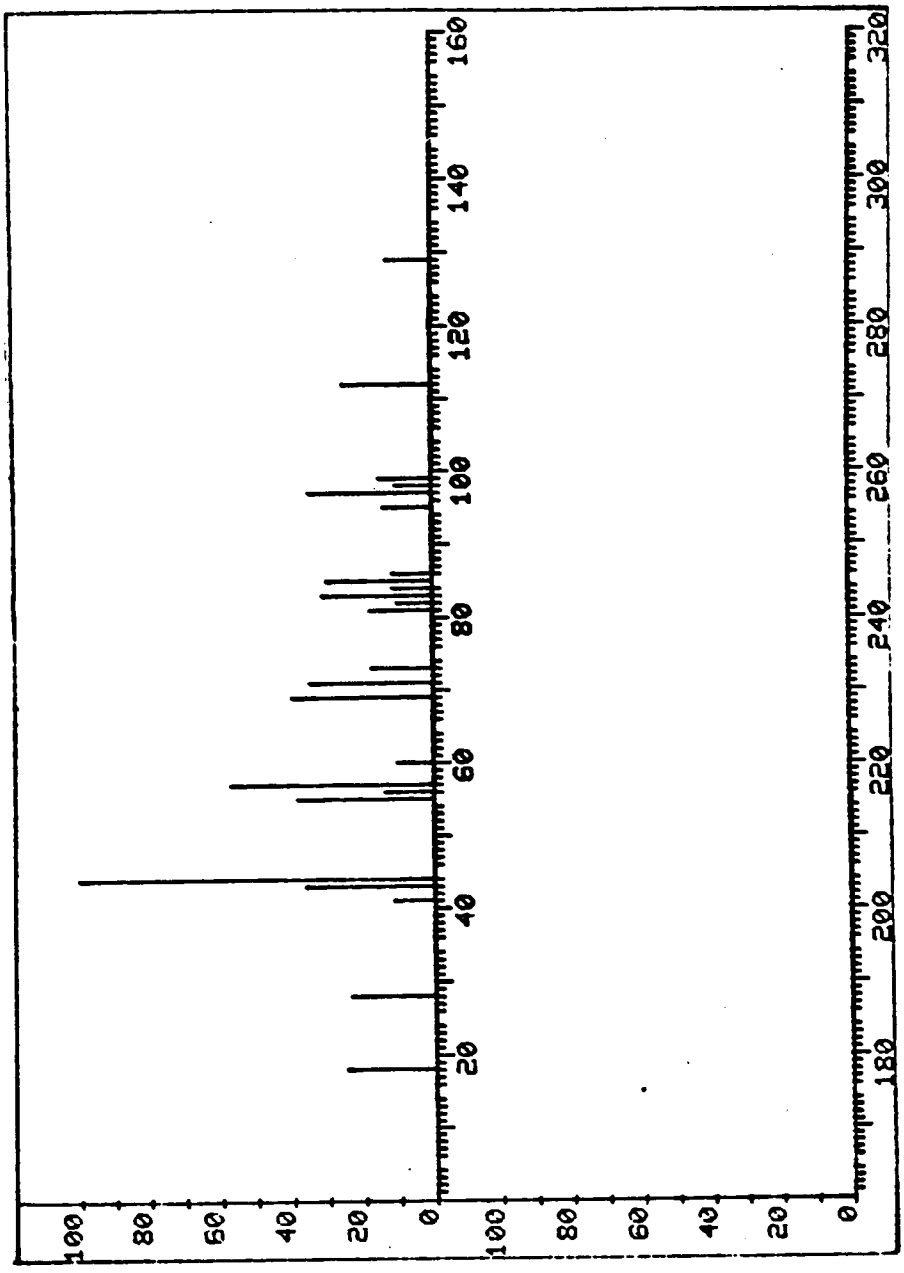

Figure B.25. Mass spectra of Nylon 66/$MnCl_2$ films photooxidized in the UV chamber for 48 hours (2.0 min).

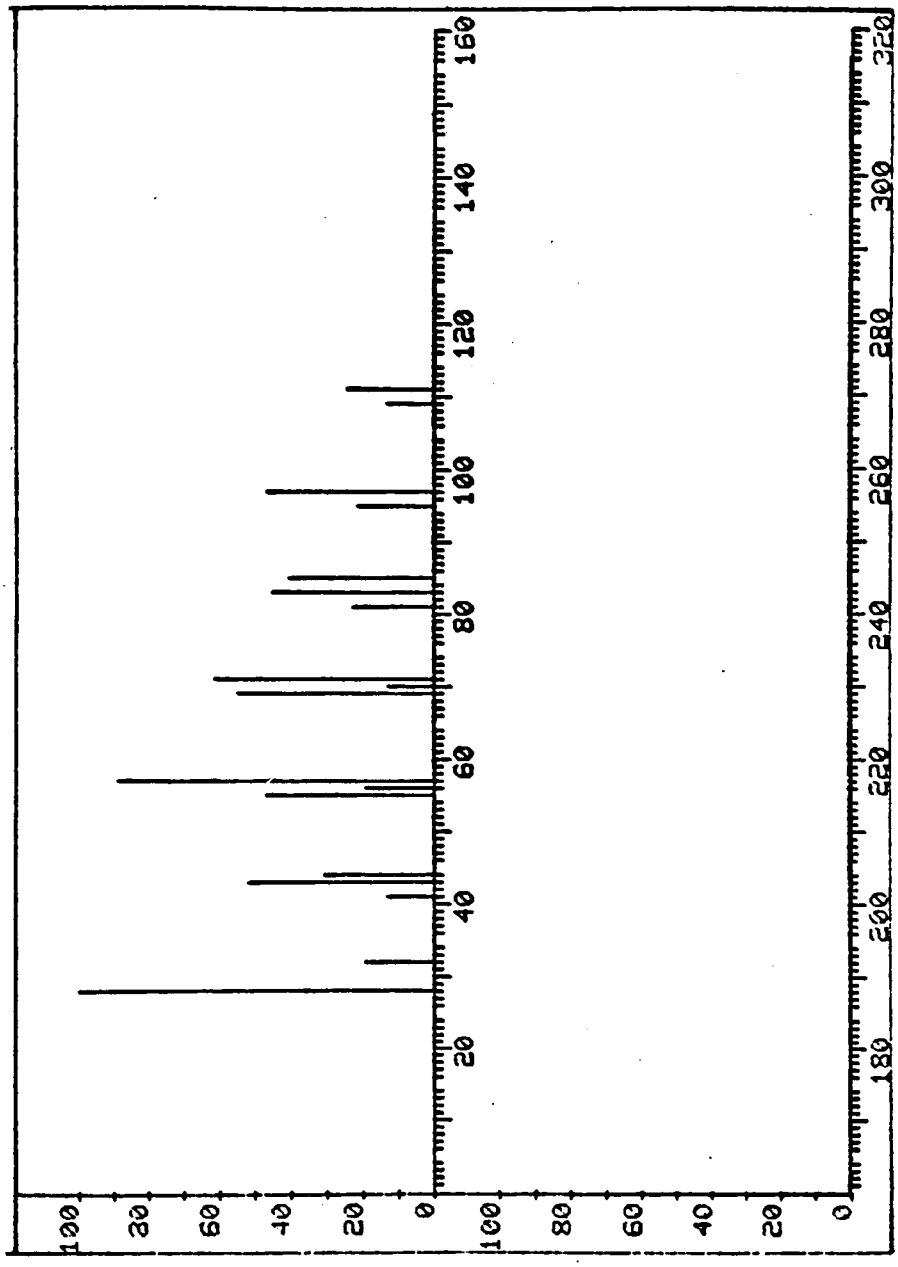

Figure B.26. Mass spectra of Nylon 66/CuCl films photooxidized in the UV chamber for 24 hours (2.0 min).

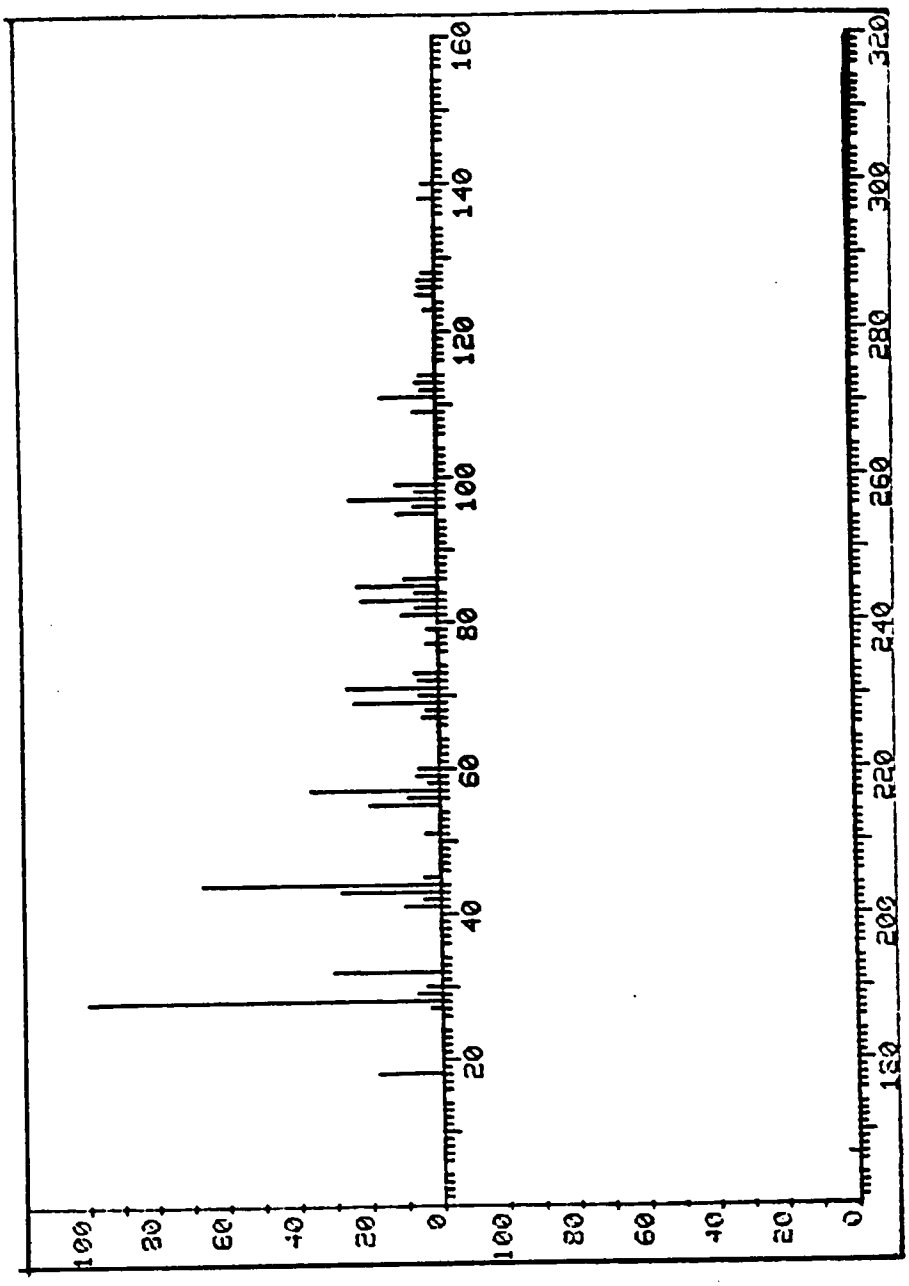

Figure B.27. Mass spectra of Nylon 66/CuCl films photooxidized in the UV chamber for 48 hours (2.0 min).

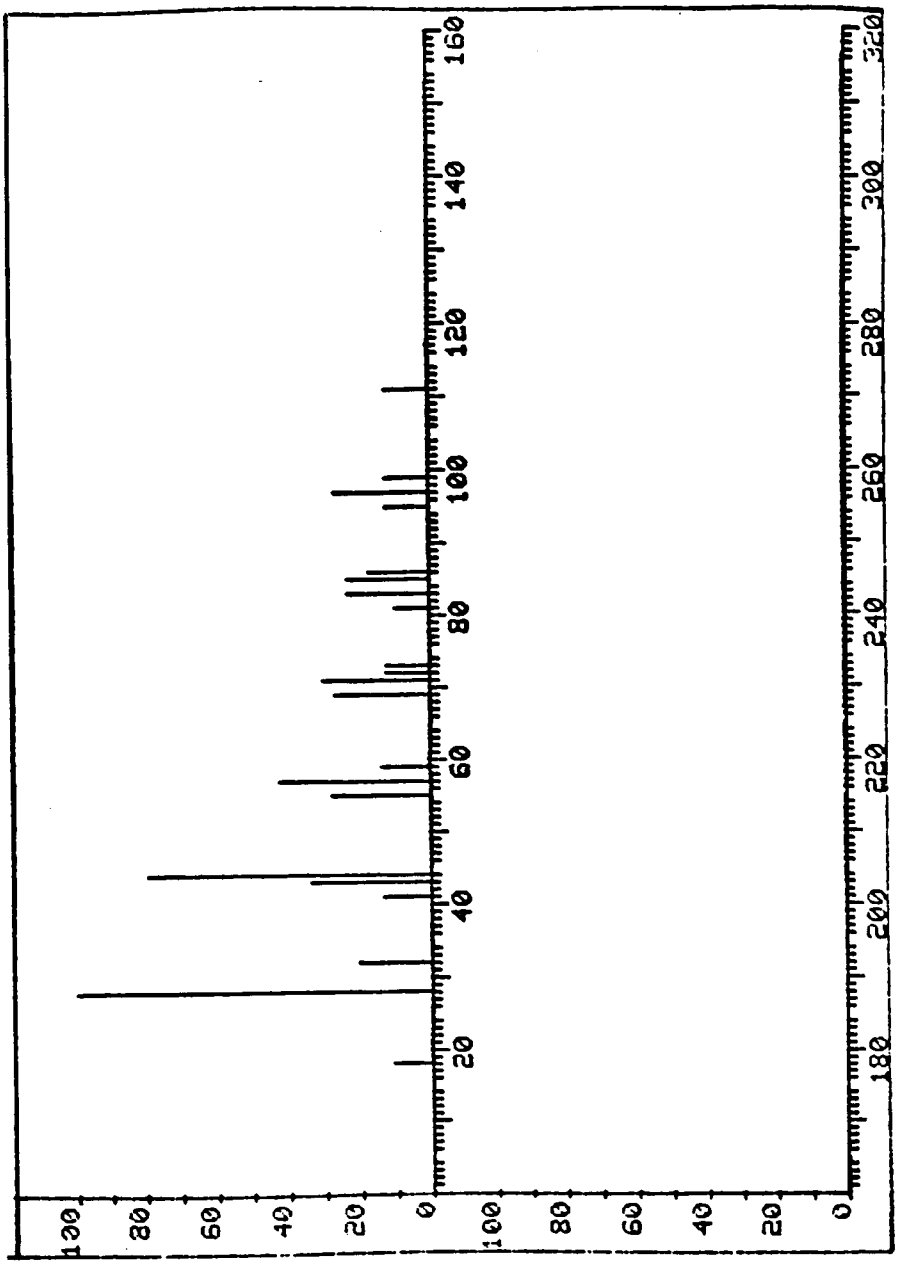

Figure B.28. Mass spectra of Nylon 66/CuCl films photooxidized in the UV chamber for 96 hours (2.0 min).

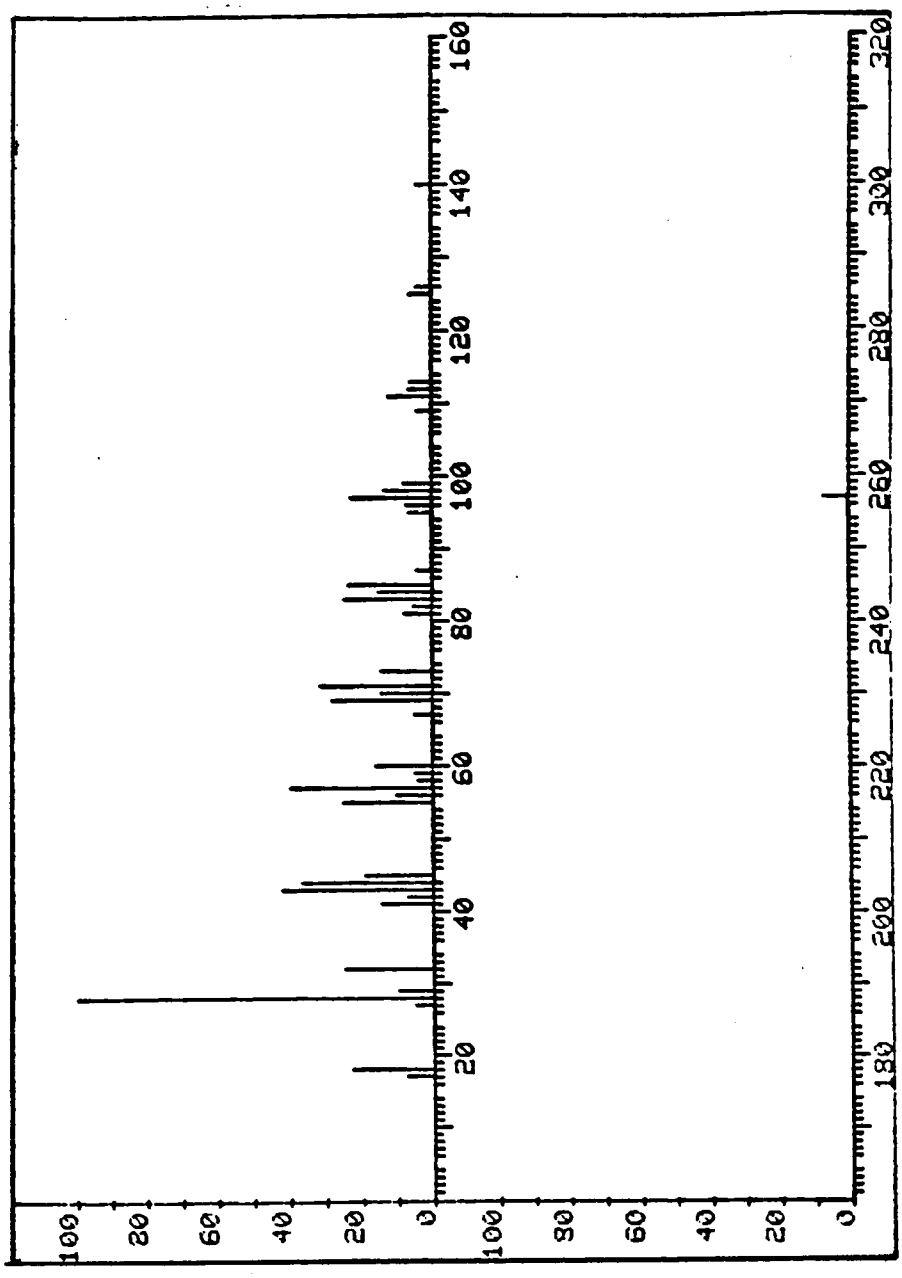

Figure B.29. Mass spectra of Nylon 66 fibers photooxidized in the UV chamber for 48 hours (2.0 min).

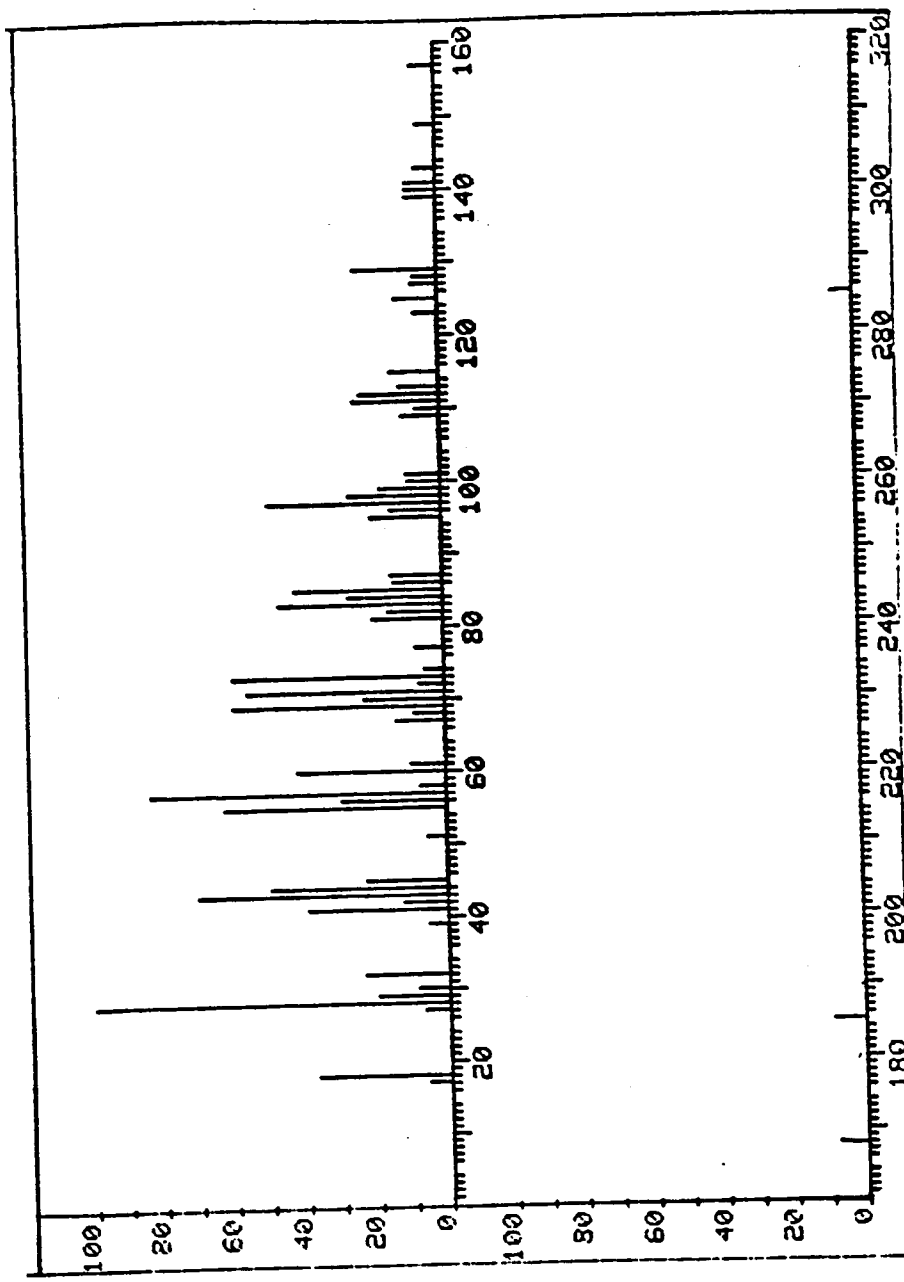

Figure B.30. Mass spectra of Nylon 66 fibers photooxidized in the UV chamber for 96 hours (2.0 min).

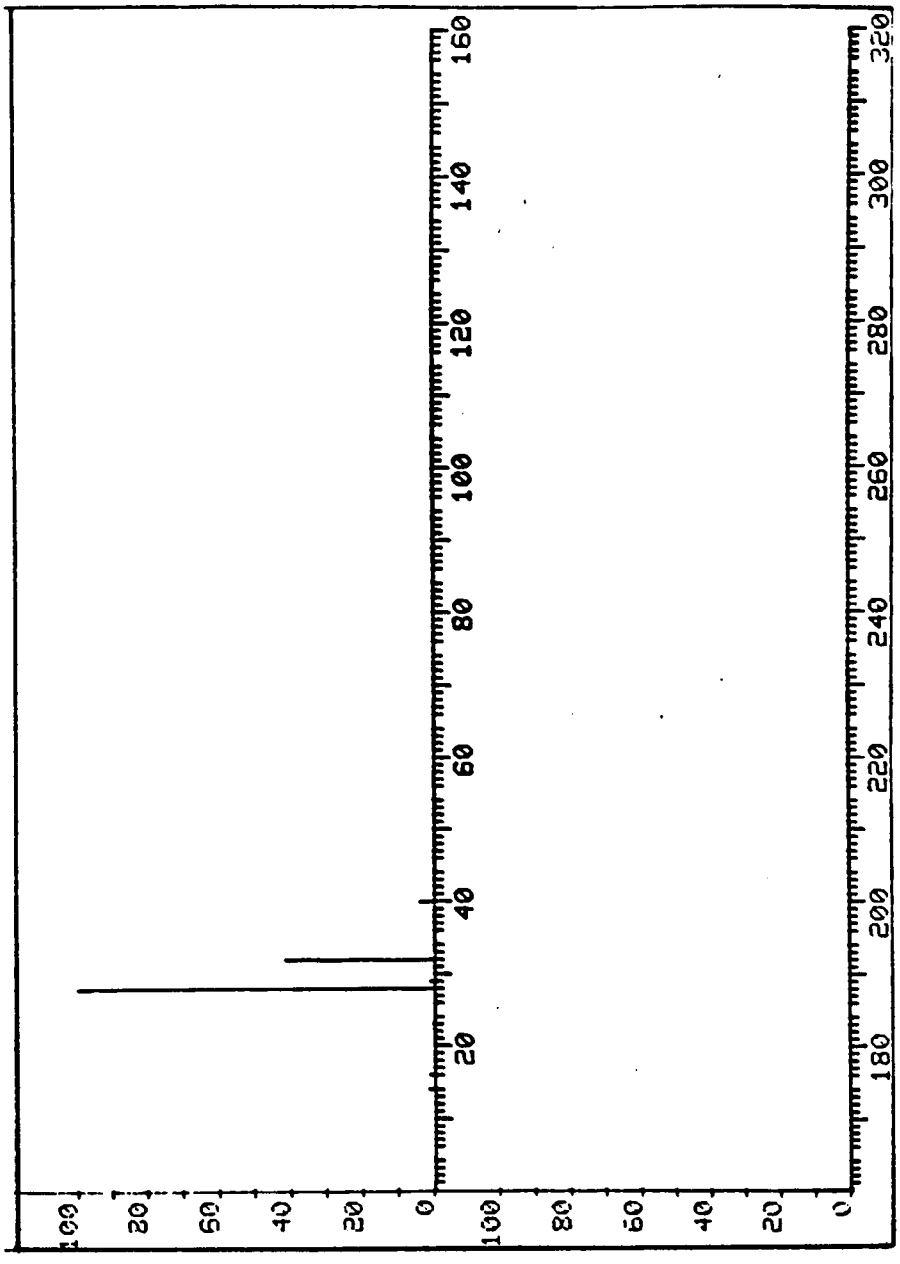

Figure B.31. Mass spectra of volatile products formed during the 24 hour photooxidation (UV chamber) of Nylon 66 film.

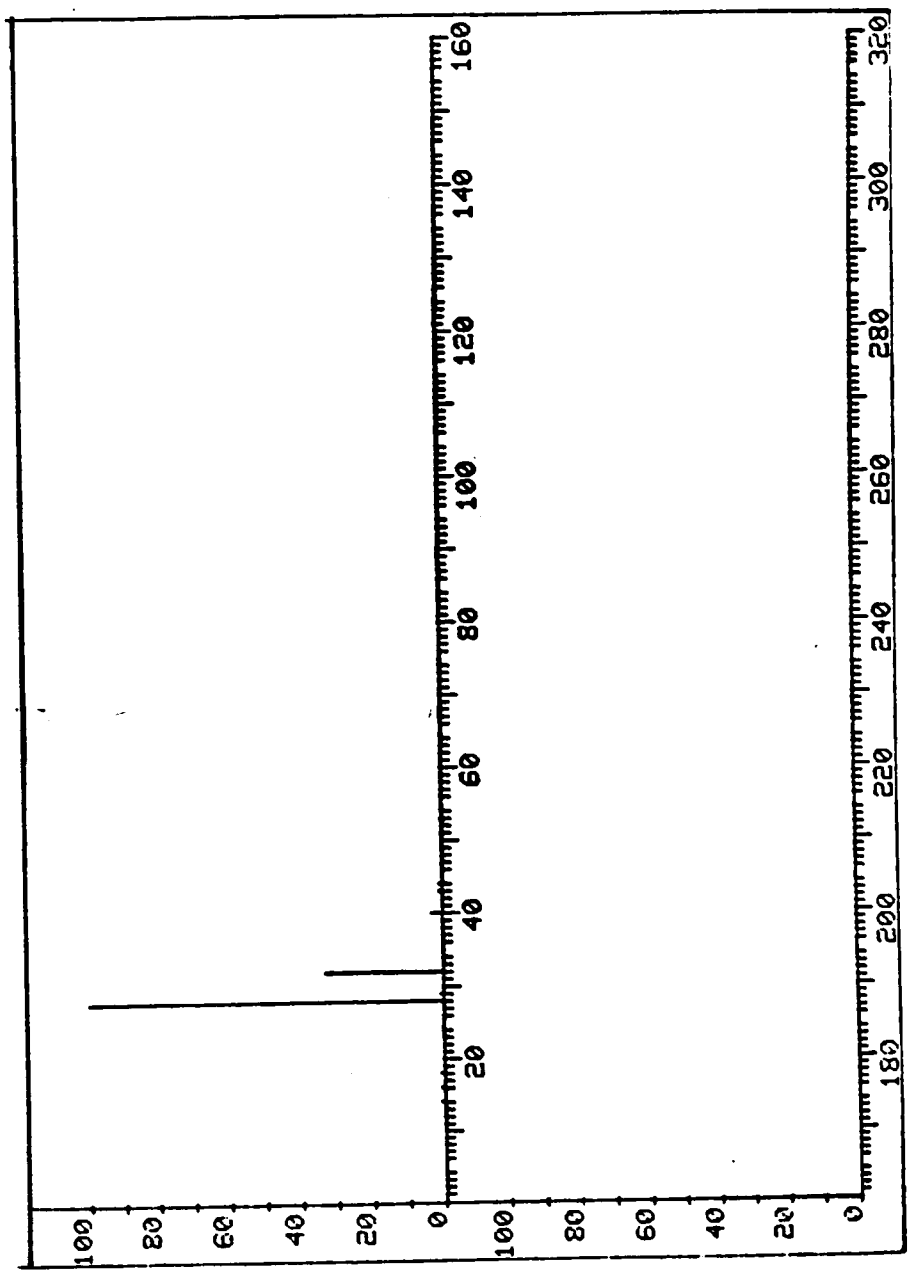

Figure B.32. Mass spectra of volatile products formed during the 48 hour photooxidation (UV chamber) of Nylon 66 film.

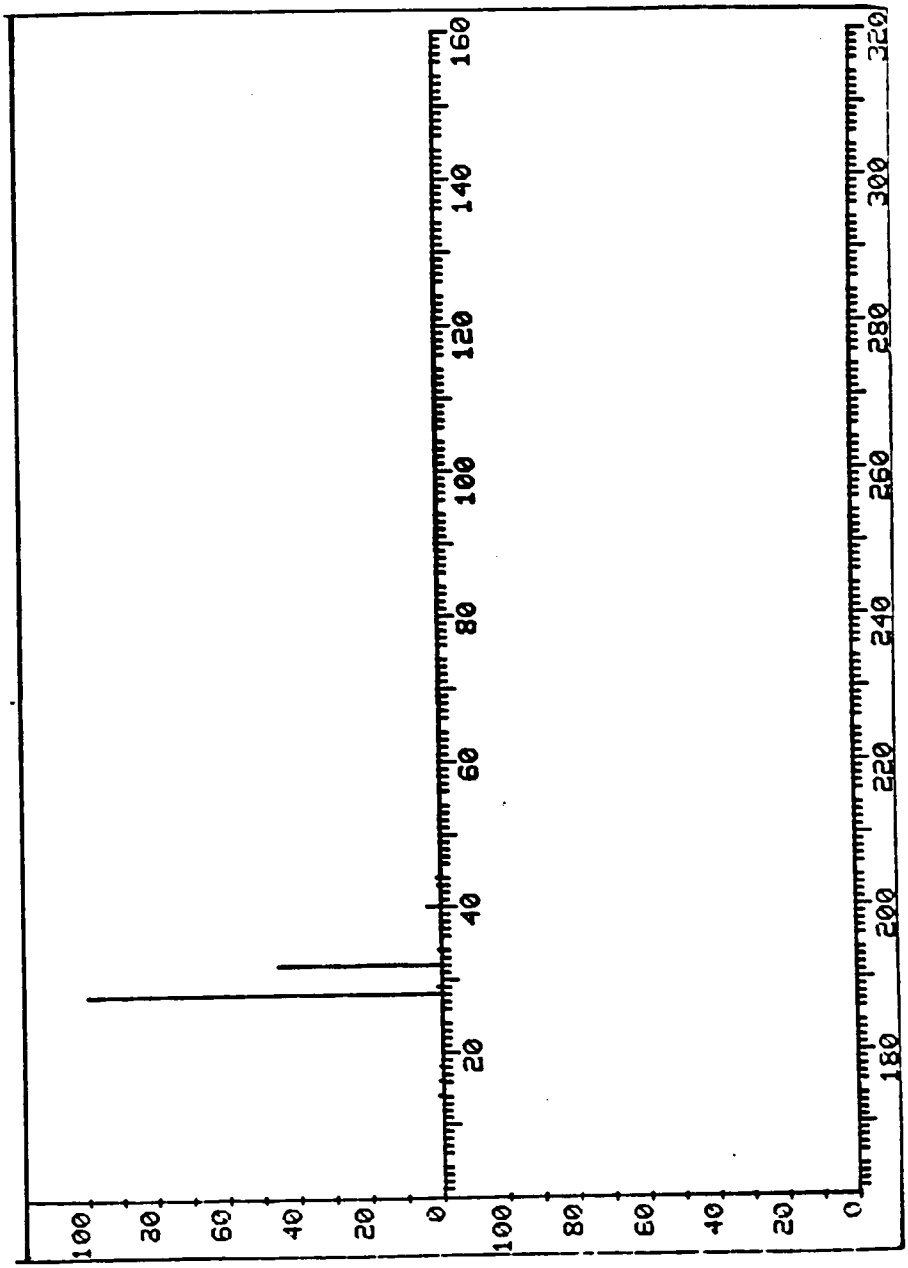

Figure B.33. Mass spectra of volatile products formed during the 96 hour photooxidation (UV chamber) of Nylon 66 film.

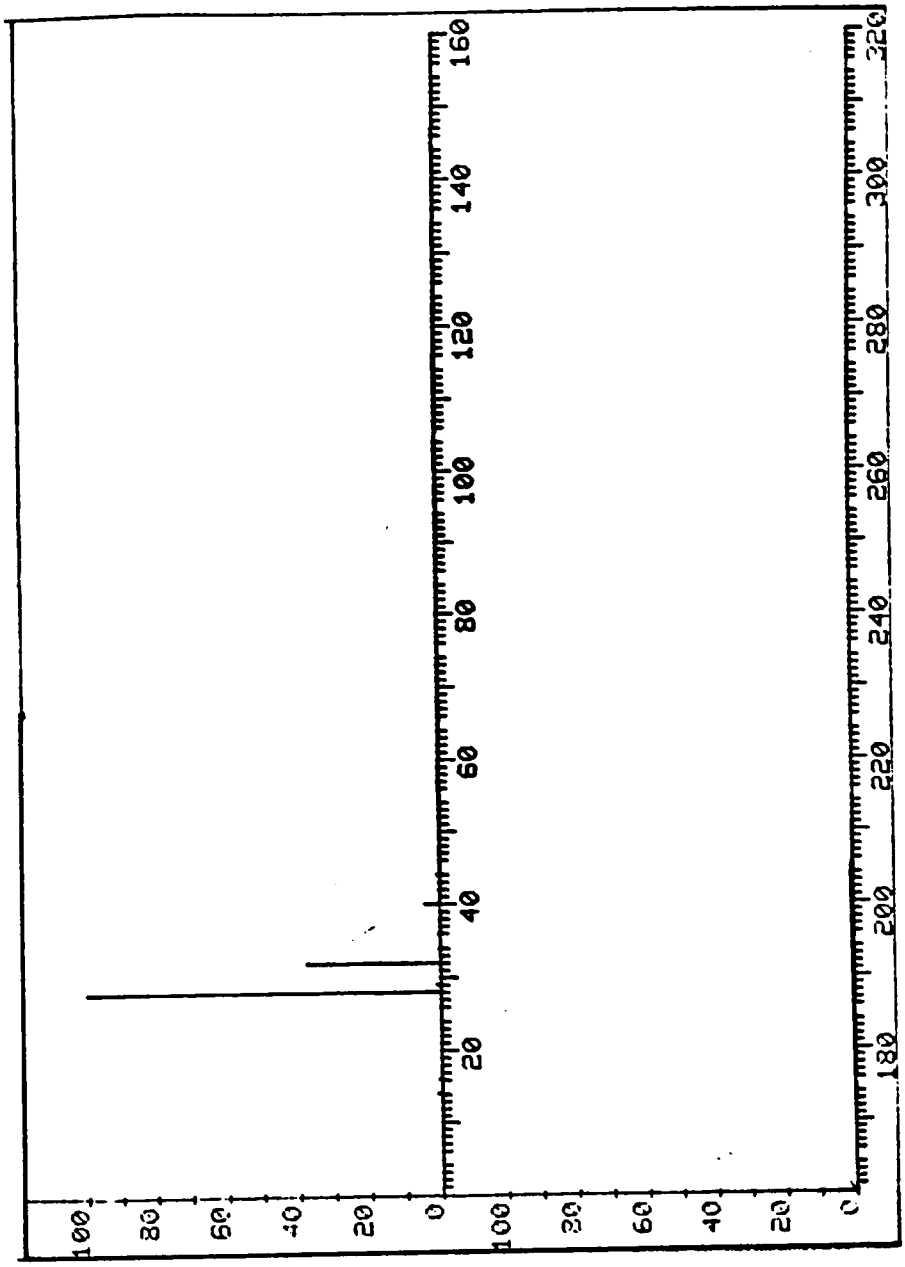

Figure B.34. Mass spectra of volatile products formed during the 24 hour photooxidation (UV chamber) of Nylon 66/$MnCl_2$ film.

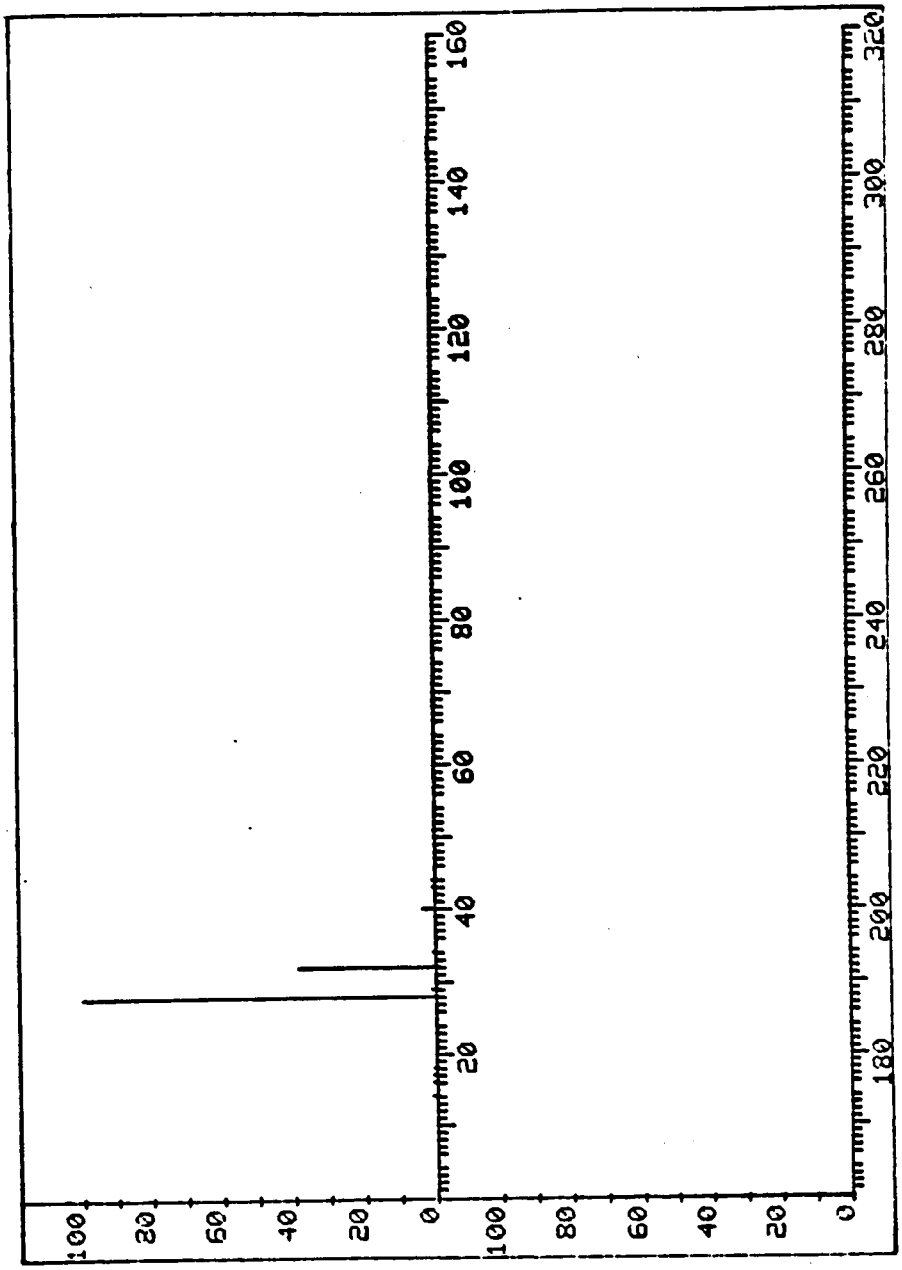

Figure B.35. Mass spectra of volatile products formed during the 48 hour photooxidation (UV chamber) of Nylon 66/$MnCl_2$ film.

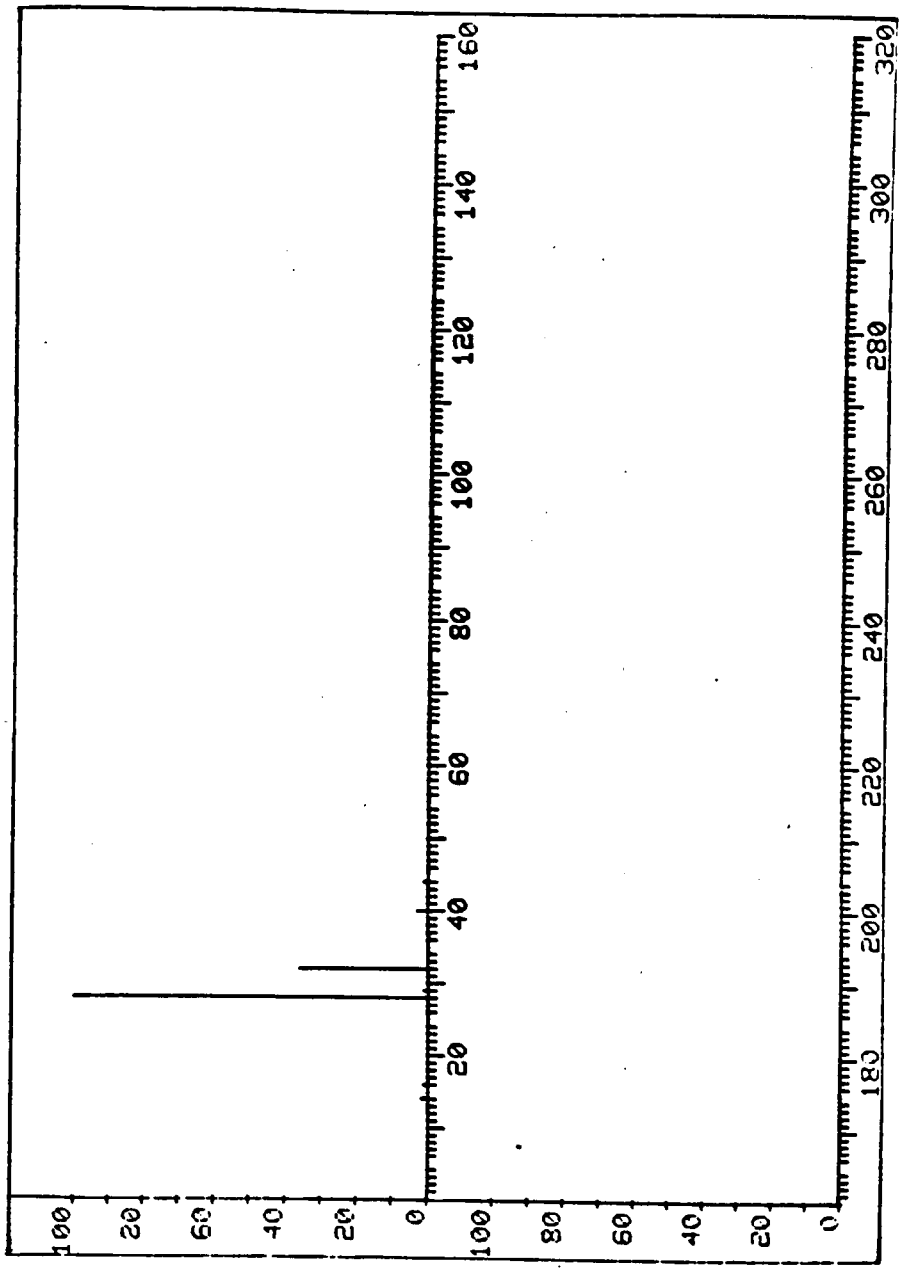

Figure B.36. Mass spectra of volatile products formed during the 96 hour photooxidation (UV chamber) of Nylon 66/$MnCl_2$ film.

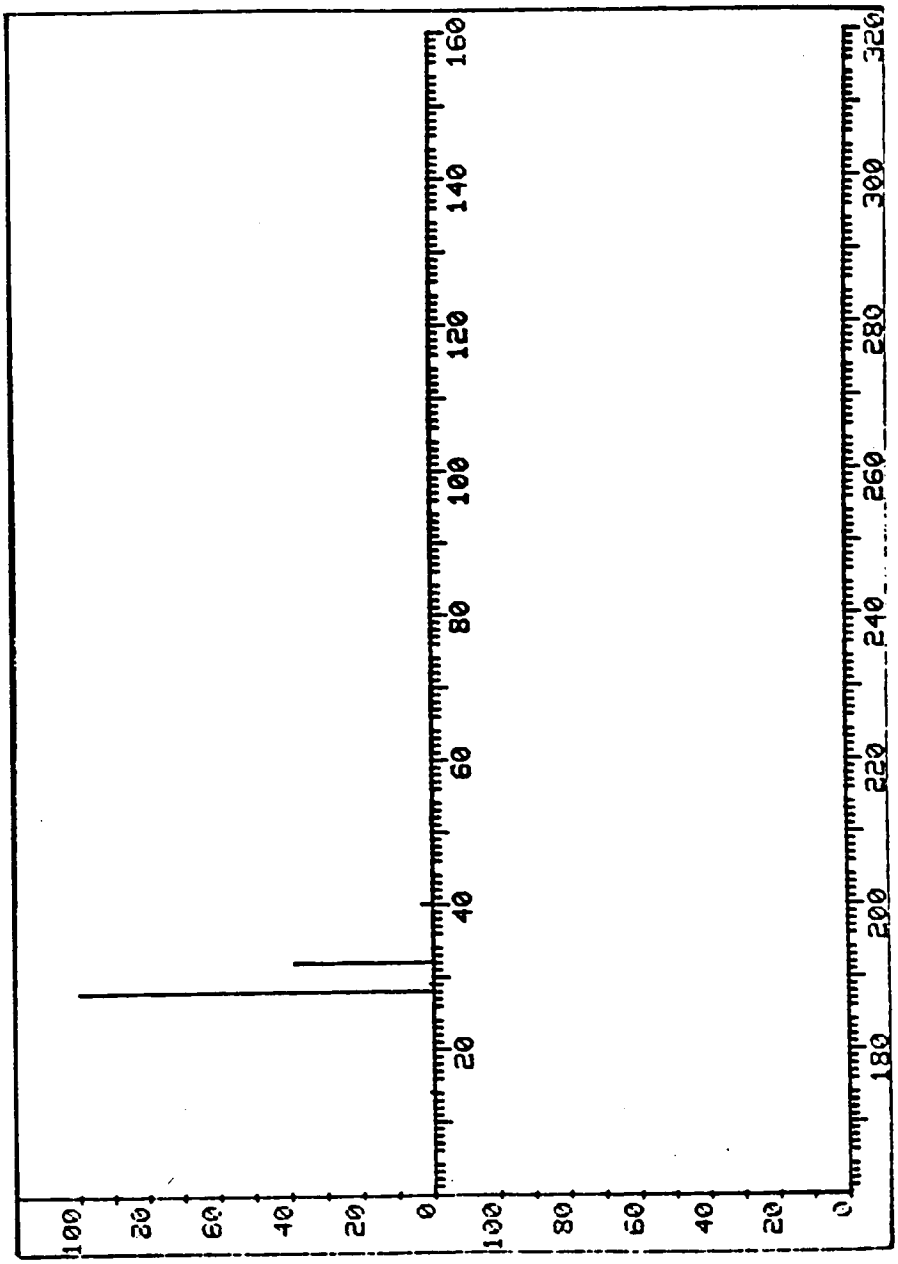

Figure B.37. Mass spectra of volatile products formed during the 24 hour photooxidation (UV chamber) of Nylon 66/CuCl.

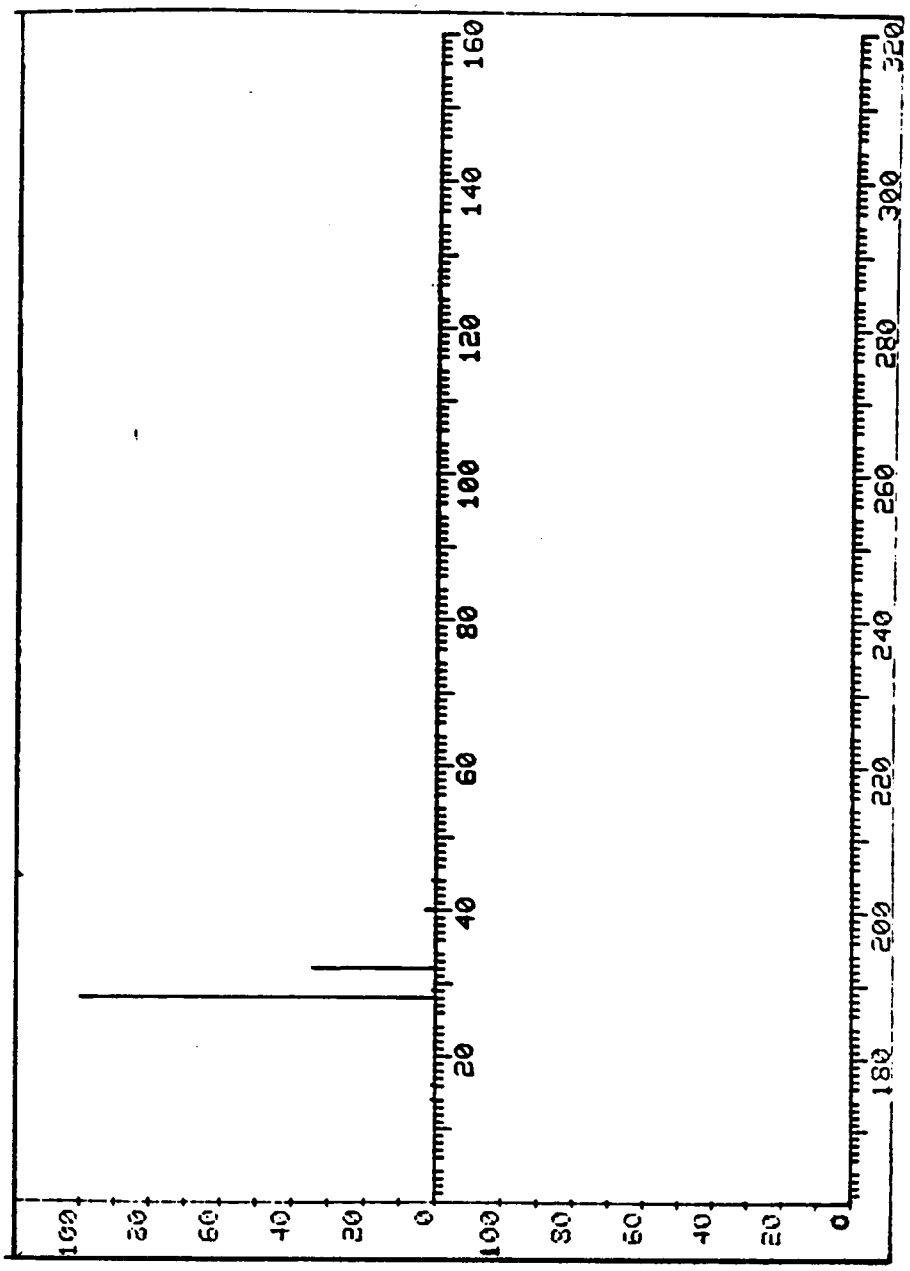

Figure B.38. Mass spectra of volatile products formed during the 48 hour photooxidation (UV chamber) of Nylon 66/CuCl.

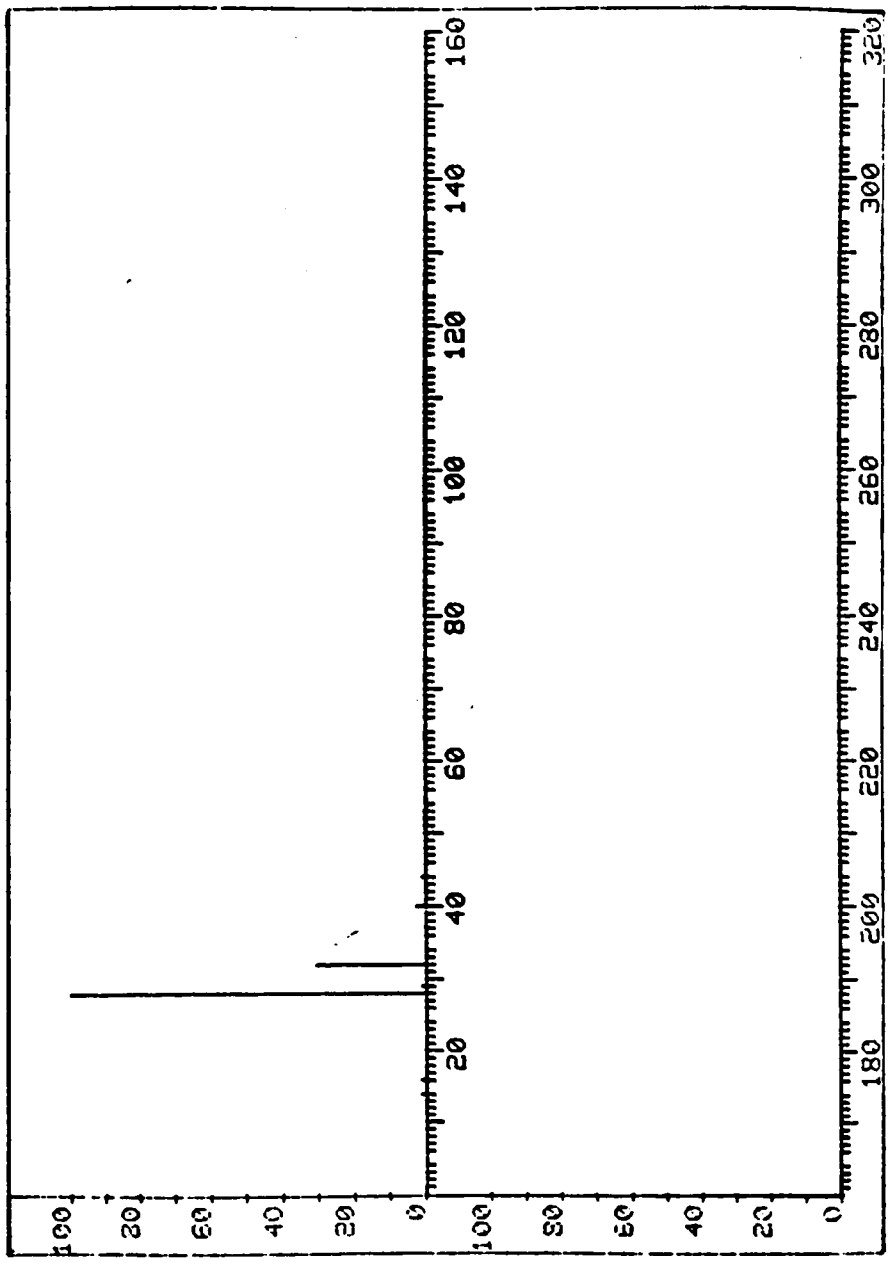

Figure B.39. Mass spectra of volatile products formed during the 96 hour photooxidation (UV chamber) of Nylon 66/CuCl.

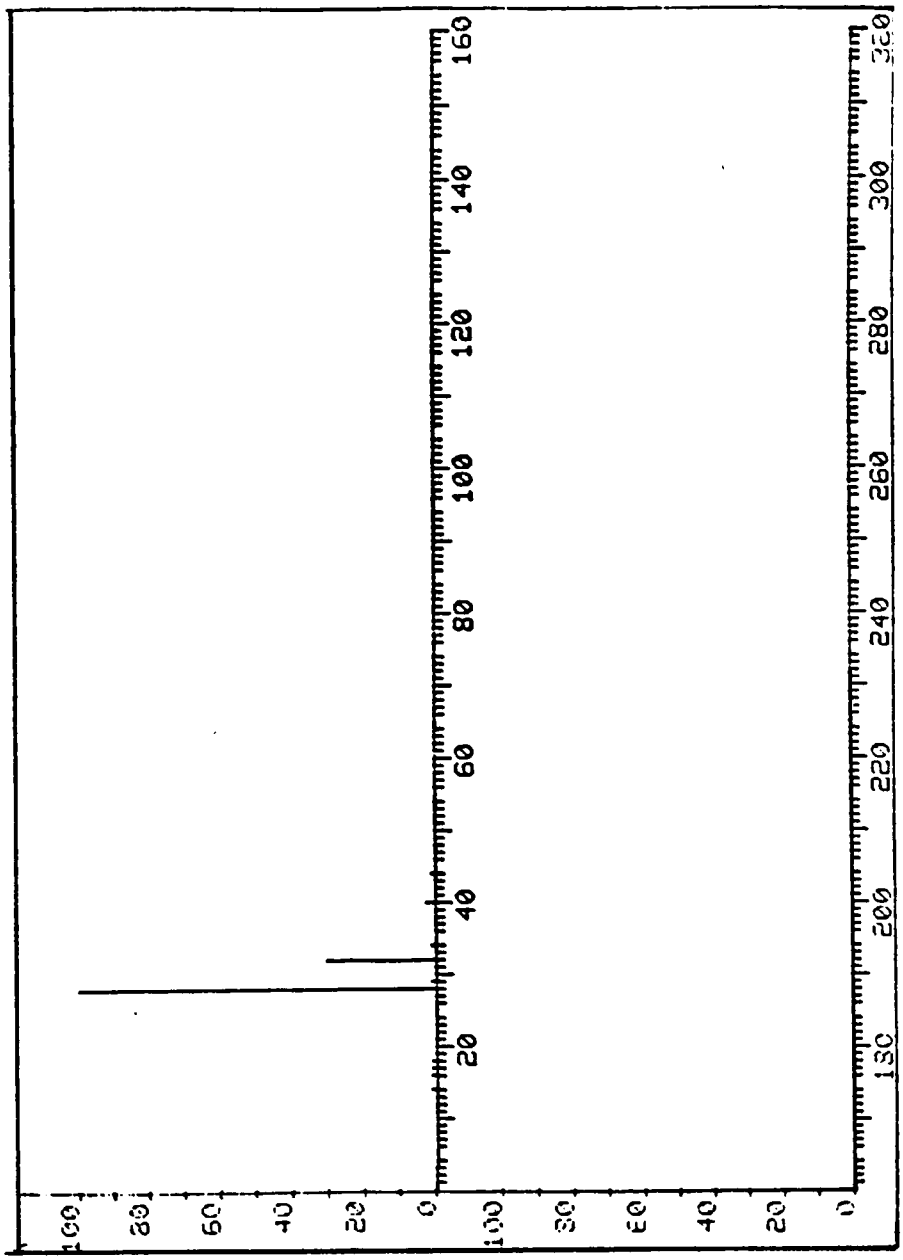

Figure B.40. Mass spectra of volatile products formed during the 48 hour photooxidation (UV chamber) of Nylon 66 fiber.

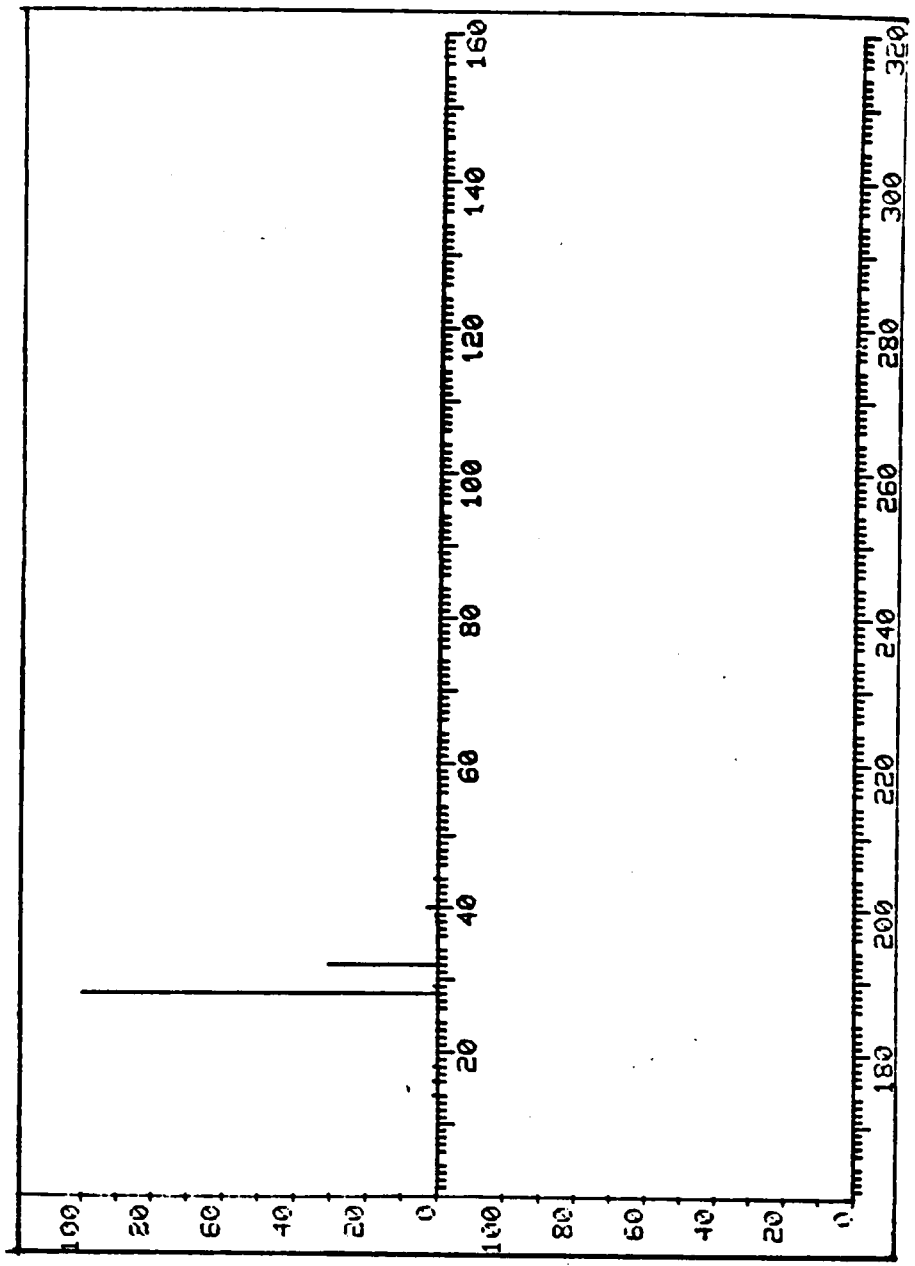

Figure B.41. Mass spectra of volatile products formed during the 96 hour photooxidation (UV chamber) of Nylon 66 fiber.

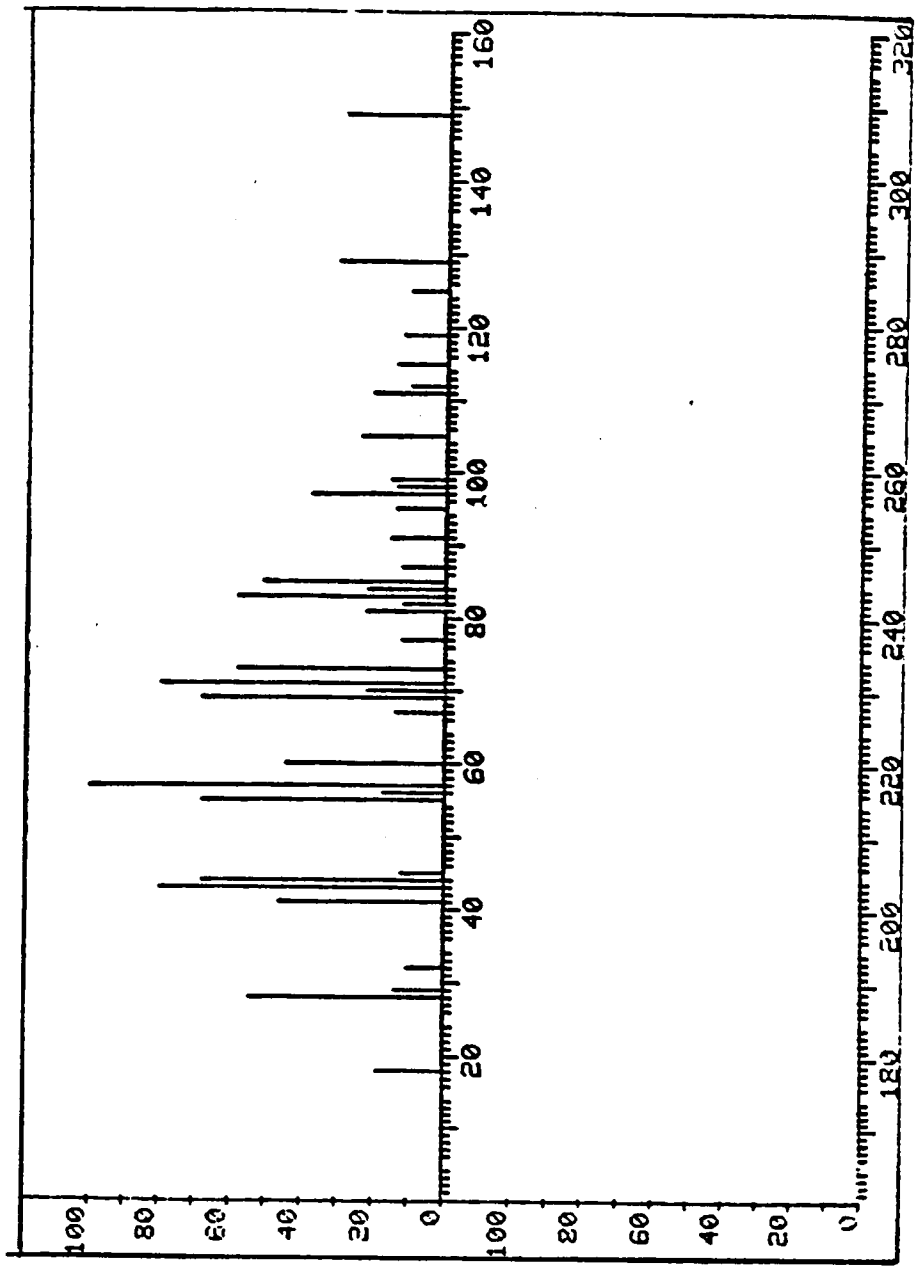

Figure B.42. Mass spectra of Nylon 66 fiber photooxidized in the Weatherometer for 48 hours (2.0 min).

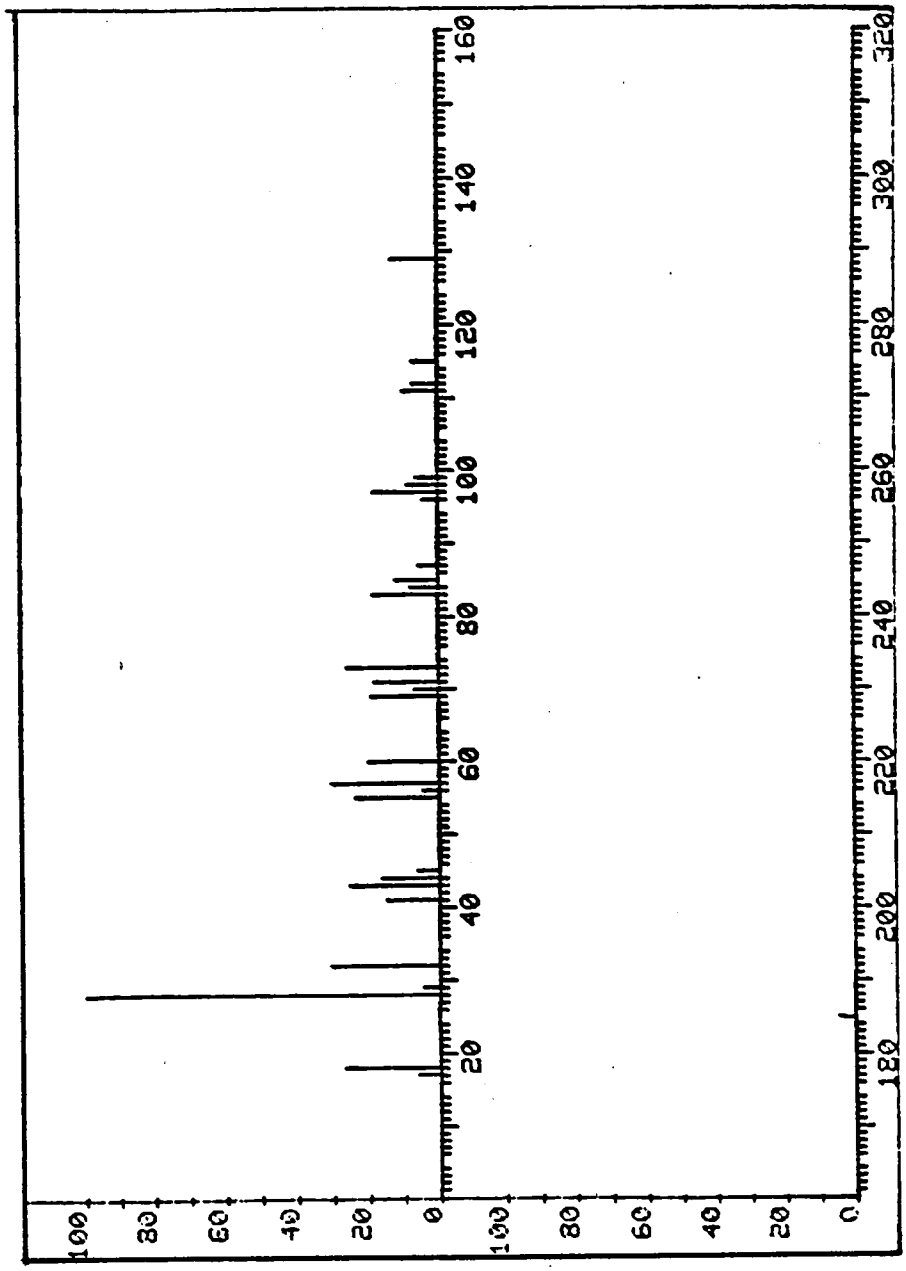

Figure B.43. Mass spectra of Nylon 66 fiber photooxidized in the Weatherometer for 96 hours (2.0 min).

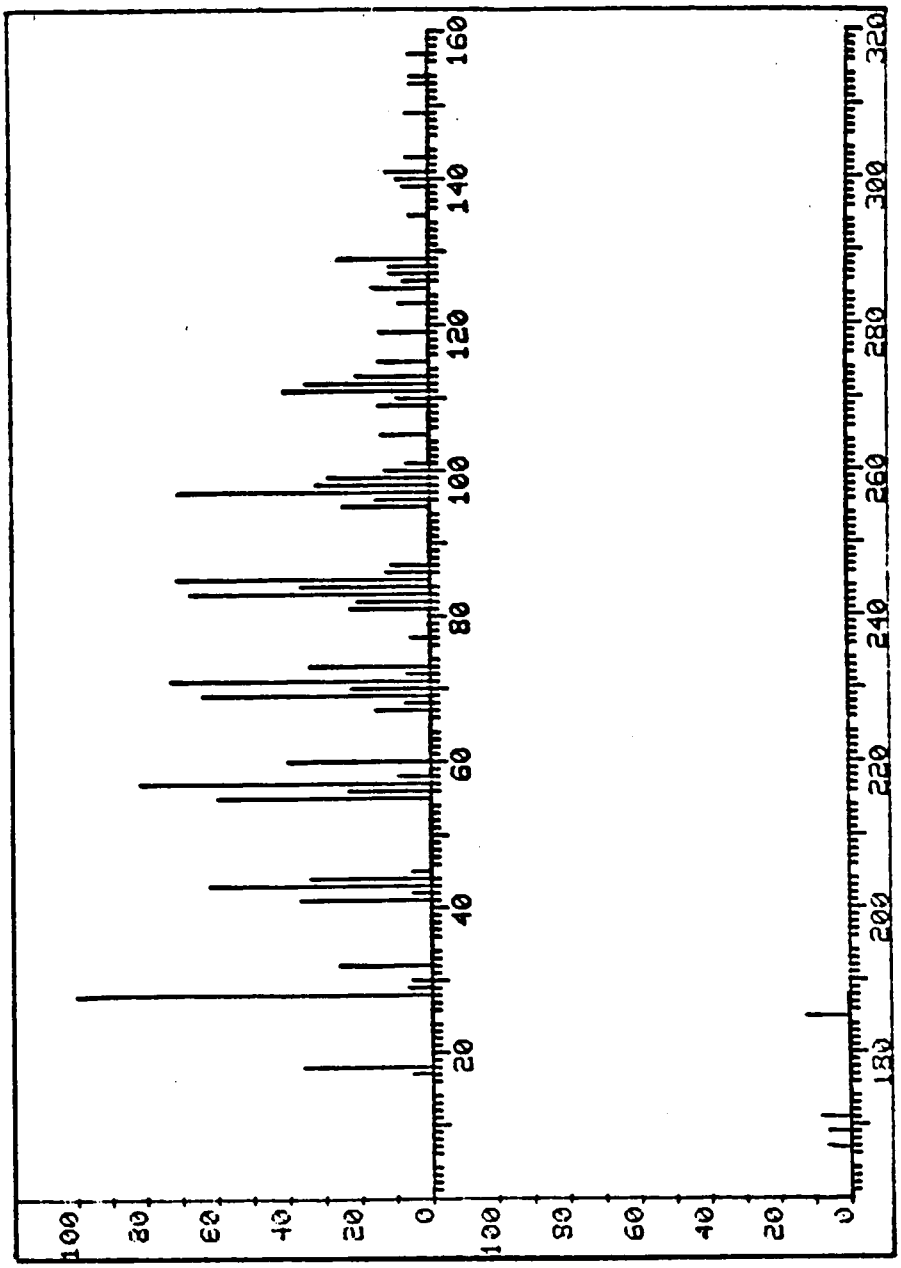

Figure B.44. Mass spectra of Nylon 66 fiber photooxidized in the Weatherometer for 147 hours (2.0 min).

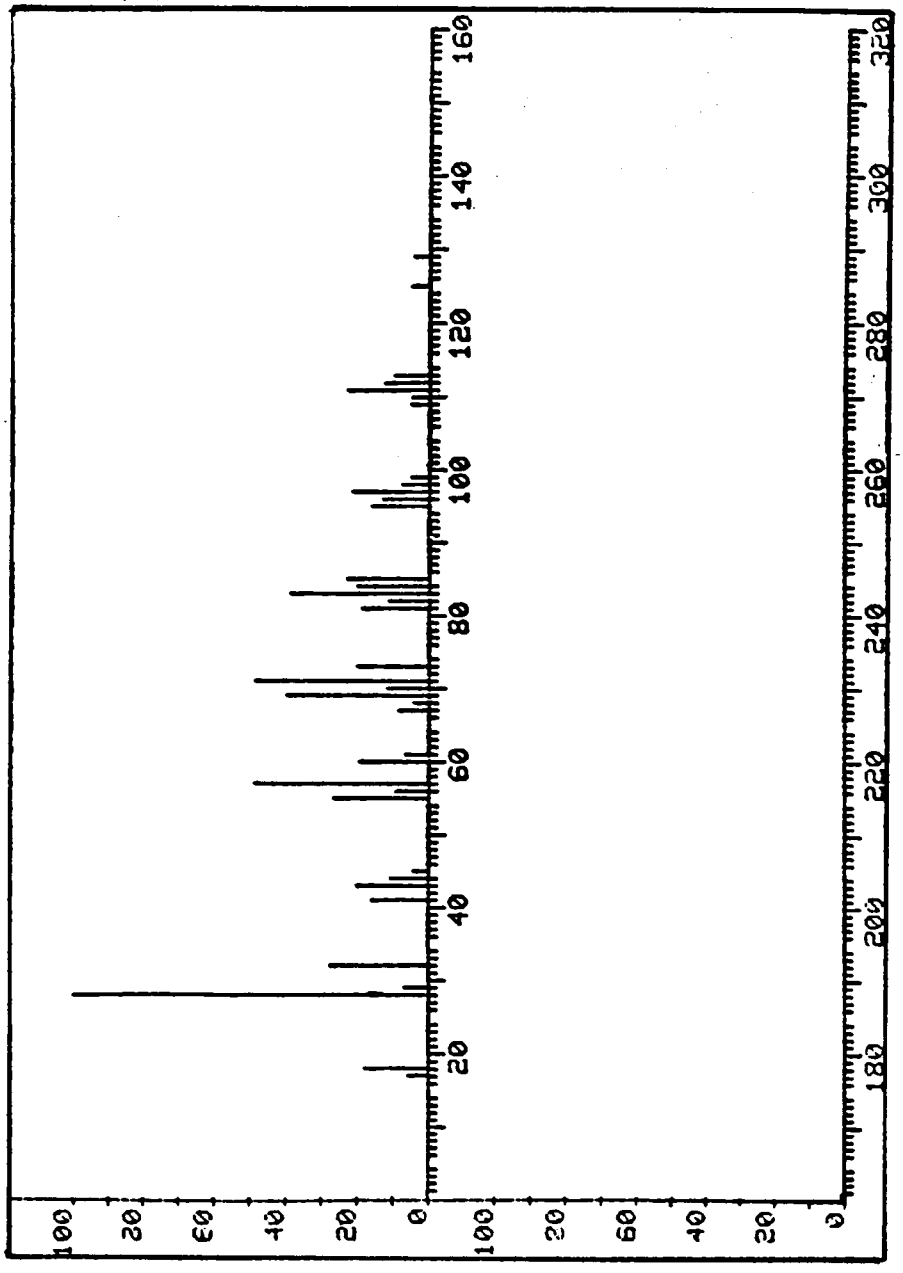

Figure B.45. Mass spectra of Nylon 66 fiber photooxidized in the Weatherometer for 195 hours (2.0 min).

VITA

The author was born in Baton Rouge, Louisiana on October 14, 1956. She attended elementary school in Birmingham, Alabama and graduated from Shades Valley High School in June 1975. The following September, she entered The University of Alabama in Birmingham, and in August of 1978 received a Bachelor of Science in Chemistry. In the fall of 1978, she accepted a Research Assistantship under the direction of Drs. Lerena Yielding and Robert L. Settine, and began study towards the Master's degree in Chemistry. The degree was awarded in June 1981.

Upon graduation from UAB, the author accepted a teaching assistantship in the Chemistry Department at the University of Tennessee, Knoxville. In January of 1983, she accepted a Research Assistantship under the direction of Drs. Tyrone L. Vigo of the U. S. D. A. and James F. Kinstle of the Chemistry Department. Due to the nature of the appointment, the author switched to the Textiles, Merchandising and Design Department, where she received a Doctor of Philosophy degree with a major in Textile Chemistry in June of 1985.

It was during her course of studies at UAB when the author met Kenneth Muschelewicz, and they were married in November of 1980. They have one daughter, Aliya, born July 16, 1984.

The author is a member of the American Association of Textile Chemists and Colorists, Alpha Lambda Delta Honor Society, the American Chemical Society, and is a Charter Member of the Alpha Epsilon Delta Honor Society.